Performance Evaluation and Enhancement of MIMO Broadcast Channels

by

Peng Lu
B.E., Beijing Institute of Technology, Beijing, China, 1999
M.E., Institute of Electronics, Chinese Academy of Sciences, Beijing, China, 2003

A Dissertation Submitted in Partial Fulfillment of the
Requirements for the Degree of

DOCTOR OF PHILOSOPHY

in the Department of Electrical and Computer Engineering

Performance Evaluation and Enhancement of MIMO Broadcast Channels

by

Peng Lu
B.E., Beijing Institute of Technology, Beijing, China, 1999
M.E., Institute of Electronics, Chinese Academy of Sciences, Beijing, China, 2003

Supervisory Committee

Dr. Hong-Chuan Yang, Supervisor
(Department of Electrical and Computer Engineering, University of Victoria)

Dr. Xiaodai Dong, Departmental Member
(Department of Electrical and Computer Engineering, University of Victoria)

Dr. Aaron Gulliver, Departmental Member
(Department of Electrical and Computer Engineering, University of Victoria)

Dr. Kui Wu, Outside Member
(Department of Computer Science, University of Victoria)

Supervisory Committee

Dr. Hong-Chuan Yang, Supervisor
(Department of Electrical and Computer Engineering, University of Victoria)

Dr. Xiaodai Dong, Departmental Member
(Department of Electrical and Computer Engineering, University of Victoria)

Dr. Aaron Gulliver, Departmental Member
(Department of Electrical and Computer Engineering, University of Victoria)

Dr. Kui Wu, Outside Member
(Department of Computer Science, University of Victoria)

ABSTRACT

In Multiple-Input Multiple-Output (MIMO) broadcast channels, the multi-antenna basestation transmits information to multiple non-cooperative mobile users simultaneously. Among various transmission schemes, zero-forcing beamforming (ZFBF) and random unitary beamforming (RUB) are of particular interest due to their low implementation complexity and ability to explore the multiplexing gain provided by multiple transmit antennas.

To investigate the effects of multiuser diversity on sum-rate performance, previous studies of beamforming schemes in multiuser MIMO systems usually employ asymptotical analysis. In this work, while assuming channel gain follows Rayleigh flat fading, we study the sum-rate performance of ZFBF and RUB through exact mathematic analysis. For this purpose, we derive the statistics of selected users's effective channel gain, which enable us to calculate the sum rate accurately and efficiently. With derived sum-rate expressions, we evaluate and compare the sum-rate performance of MIMO broadcast channels with RUB and dual-transmit-antenna ZFBF. In

addition, we apply this analytical method to study strategies that mitigate multiuser interference for RUB-based multiuser MIMO systems. The strategies we consider in the thesis include

- Reducing the number of served users at a time. We present a new user scheduling scheme, which imposes a threshold on user's SINR for feedback load reduction and only activates those beams that are requested by feedback users.
- Exploiting receive diversity. When receivers use more than one antennas, we evaluate the sum-rate performance gain offered by selection combining (SC) and optimum combining (OC) schemes, respectively.

In addition to beamforming techniques, we study the symbol error rate (SER) performance of MIMO broadcast channels with vector perturbation (VP) precoding and quantized channel feedback. Based on the established equivalent relations in terms of minimum mean square error (MMSE) and SER between quantized and perfect channel feedback cases, we investigate the tradeoff between feedback load and achievable diversity gain.

Contents

List of Tables

List of Figures

ACKNOWLEDGEMENTS

I would like to thank:

Dr. Hong-Chuan Yang, for his support and guidance during my PhD study, which have made this dissertation possible. I thank him for his insights and suggestions that helped to shape my research skills. His valuable feedback contributed greatly to this dissertation.

Dr. Xiaodai Dong, Dr. Aaron Gulliver, Dr. Kui Wu, and Dr.

Robert Schober for their valuable feedback which helped me to improve the dissertation in many ways.

My friends, for their presences and fun-loving spirits that made the otherwise grueling experience enjoyable. They are Sanal Sasankan, Pengfei Zhang, Araya Chaowalit, Rooholah Hasanizadeh, Yihai Zhang, and Xiaodong Li.

My grandmother, parents, and wife, for always being there when I needed them most, and for supporting me through all these years.

Chapter 1

Introduction

Recent research and industry activities have brought the fourth-generation (4G) wireless communications systems closer to implementation and standardization. The expected data rate requirements will be an order of magnitude higher than 3G. Current technologies based on TDMA/CDMA are not capable of handling the wideband signals required to reach the 4G target data rates. Multiple-Input Multiple-Output (MIMO) techniques, with the potential to increase both the data throughput and transmission reliability, are considered to be one of the enabling technologies in the 4G wireless communications systems.

Currently, MIMO is the key physical layer technology for two future mobile communications systems: Long Term Evolution (LTE) and Worldwide Interoperability for Microwave Access (WiMax). LTE is the 4G evolution of cellular systems and is expected to provide true mobile broadband experience beyond the capability of existing high-speed packet access (HSPA)-based 3G systems, while WiMax is a technology that is expected to deliver last mile wireless broadband access.

In this work, we study MIMO technology under a practical scenario, where multiple antennas are used at the basestation while mobile receivers, due to size, power, and cost limits, have less or only a single antenna. We investigate how to achieve maximum benefits promised by MIMO technology under the constraint of processing complexity and feedback load. For this purpose, we firstly provide some background information on this research topic and elaborate the challenges we are facing.

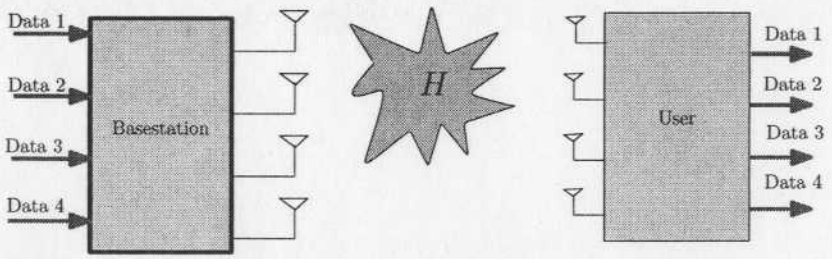

Figure 1.1: Point-to-point MIMO systems.

1.1 MIMO Broadcast Channels

In point-to-point MIMO communications systems, as illustrated in Fig. 1.1, multiple antennas are used at both the transmitter and receiver. The capacity of MIMO channels increases linearly with $\min(M, N)$, where M and N denote the number of antennas at the transmitter and mobile receiver, respectively [1,2]. In practice, however, it is difficult to implement as many antennas at mobile users as the basestation due to the size, cost and complexity limitations, which implies $N < M$. In the meantime, the number of users in the system K is usually larger than M. In the downlink of multiuser MIMO systems, if the basestation adopts time division multiple access (TDMA), where only one user is served at a time, the spatial degrees of freedom offered by additional transmit antennas at the basestation can not be fully exploited for capacity benefit [7], [8]. Considering there are $K > M$ users in the system, the basestation may choose to transmit information to multiple non-cooperative mobile users simultaneously to increase the system throughput, resulting in so-called *MIMO broadcast channels.*

The structure of multiuser MIMO systems is illustrated in Fig. 1.2, where the basestation employed with four antennas transmits information to four single-antenna users at the same time. Whereas, simultaneously transmitting independent data streams for non-cooperative users will incur *inter-user (multiuser) interference.* This is because one user is unable to distinguish between its desired signal and interference signal resulting from simultaneous transmission to other users. In such a circumstance, the job of interference mitigation has to be done at the basestation using preprocessing techniques (precoding). Studies have shown that to what extent the multiuser interference can be mitigated depends on how much channel state information (CSI) of mobile users the basestation has.

Under the assumption that perfect CSI is available at the transmitter, information-

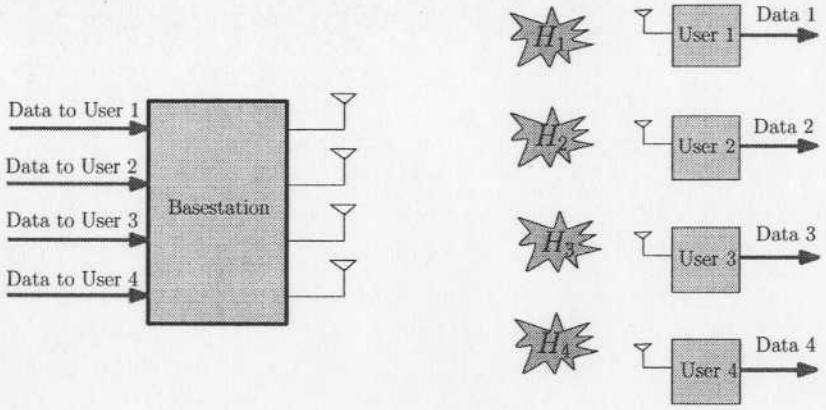

Figure 1.2: Multiuser MIMO systems.

theoretic results dated back to the beginning of this century show that serving multiple mobile users at the same time can fully explore the multiplexing gain provided by the multiple transmit antennas.

Capacity of MIMO Broadcast Channels For signal-antenna broadcast channel, the channel is degraded and its capacity region is known and achieved by supposition coding [3], [4]. MIMO broadcast channel, however, is generally not degraded and its capacity region is unknown.

Pioneering work by Caire and Shamai [5] obtains the sum capacity of the MIMO broadcast channel for the special case of $K = 2$ users. They propose a transmission scheme which uses Costa's dirty paper coding (DPC) [9]. By maximizing the dirty paper lower bound and minimizing Sato's upper bound [6], Caire and Shamai show that they are equal and thus the proposed scheme is optimal in achieving the sum capacity for the case of two users. The computation is complex and hard to extend to more general cases [12].

Some following works generalize Caire and Shamai's results on the optimality of dirty paper region for the sum capacity of the broadcast channel. In [13], Yu and Cioffi use a Generalized Decision Feedback Equalizer structure for precoding at the transmitter. The sum capacity for general cases under power constraint is found to be the saddle-point of the mutual information expression maximizing over signal covariance and minimizing over noise covariance. The results only hold for those channels for which the worst case correlation of the noise in the Sato upper bound is non-singular.

In [12], Viswanath and Tse handle channels with multiple transmit antennas but

only one antennas at each user. The tightness of the Marton inner bound and Sato's upper bound is proven by showing the intimate uplink-downlink duality and point-to-point reciprocity. In [14], Vishwanath, Jindal and Goldsmith establish a duality between dirty paper region for the MIMO broadcast channel and capacity region of the MIMO multiple-access channel, which simplifies the calculation of the achievable region of the MIMO broadcast channel.

1.2 Beamforming Techniques

When perfect CSI of mobile users is available at the transmitter, DPC is the optimal transmission scheme since it achieves sum capacity of MIMO broadcast channels. However, heavy computational complexity involved with such non-linear precoding scheme prohibits its implementation in practical communications systems [10]. As such, there is a growing interest in low-complexity transmission schemes that can effectively explore the spatial multiplexing gain of MIMO broadcast channels. Transmit beamforming is one of the suboptimal strategies that can serve multiple users at the same time [15–17, 19]. Interestingly, the data throughput achieved with beamforming is shown to scale at the same rate of $M \log\log(K)$ as DPC, when K is sufficiently large.

With transmit beamforming, the data stream of each selected user is coded independently and multiplied by a beamforming vector. The transmit vector is generated as the superposition of all selected users' data streams. Since the number of active users is usually larger than the number of transmit antennas, namely $K > M$. The basestation may select a subset of users ($\leq M$) out of K users for simultaneous transmission. When users' channels experience independent fading, there is likely to be a subset of users with very good channel quality, which is characterized by more closeness to orthogonality between users's channel vectors and larger power gain. The *sum rate*, defined as the sum of data rates of all users, can be enhanced by transmitting to those carefully chosen users. The system-wide performance improvement brought by the freedom to select users is called *multiuser diversity gain.*

To appropriately select the users and design the beamforming vectors, the basestation requires some form of CSI of mobile users. For communications systems with Time-Division Duplex (TDD), using the reciprocity of radio propagation channels, CSI can be obtained by measuring the uplink channels. For Frequency-Division Duplex (FDD), the acquisition of CSI is usually realized through feedback mecha-

nism. Since feedback decreases spectral efficiency of wireless communications systems, there exists a tradeoff between feedback load and sum-rate performance of multiuser MIMO systems. Current research interests focus on two low-complexity beamforming schemes, zero-forcing beamforming (ZFBF) [19–22] and random unitary beamforming (RUB) [15, 28–31]. Both beamforming schemes are shown to achieve the same scaling law as DPC when there are asymptotically large number of users in the system.

1.2.1 Zero-forcing Beamforming

ZFBF is an appealing beamforming scheme in that ZFBF can completely eliminate the multiuser interference with the knowledge of perfect CSI. This is achieved by designing one user's beamforming vector to be orthogonal to other selected users' channel vectors [18]. As a result, ZFBF realizes interference free multiuser transmission at the cost of a certain loss of power gain due to the projection of channel vectors onto the beamforming direction. Consequently, to maximize the spatial multiplexing gain of ZFBF, the base station needs to select users, whose channel vectors have relative large power gain and, at the same time, are near orthogonal to one another to minimize the projection power loss. While most previous work on ZFBF have been based on either simulation study or asymptotical analysis, we adopt a different approach in this work and perform exact analysis of the sum rate of two low-complexity user selection schemes for ZFBF transmission with two antennas.

1.2.2 Random Unitary Beamforming

RUB is a low-complexity solution for exploring multiplexing gain over MIMO broadcast channels. With RUB, a set of M orthonormal beams (beamforming vectors) are used, which is generated randomly and known to both the basestation and mobile users. To explore multiuser diversity gain, each user will feedback certain signal to interference and noise ratio (SINR) information of available beams, based on which the basestation carries out proper user selection. In this thesis, we focus on the following three research topics associated with RUB-based multiuser MIMO systems.

Exact sum-rate analysis We attack the exact sum-rate analysis of the RUB scheme presented in [15]. The major difficulty in performing exact sum-rate analysis is to obtain the statistics of the ordered beam SINRs for a particular user, which involves the order statistics of correlated random variables. Fortunately, with the help of some recent results of order statistics [32], we derive the accurate statistical

characterization of ordered beam SINRs for a user [33], which are then applied to obtain the analytical expression of the average sum rate. In addition, we also derive an approximate expression for the sum rate over high signal to noise ration (SNR) region.

Efficient user scheduling strategy Feedback thresholding is a commonly adopted mechanism to reduce the feedback load [47]. Wang *et. al.* [30] suggested to only allow those users with their largest SINR above a threshold to feed back their best beam indexes and the corresponding SINR. More interesting, it is shown in [36] that the optimal sum rate scaling law is still achievable even if the qualified users just feed back the indexes of their best beams. In this work, we present a new user scheduling strategy with low feedback load. Similar to the strategy proposed in [36], only those users with their largest SINR above a threshold will feed back their best beam indexes. When the threshold is high and/or the number of users is moderate, it may happen that a beam is not requested by any user. When this happens, [36] suggests to randomly select a user for such a beam. Since random user selection for an unrequested beam can not guarantee high SINR for the selected users and will introduce more inter-user interference, we propose to keep only beams being requested by at least one user active for transmission. Our proposed strategy, which is termed as adaptive beam activation based on conditional best beam index feedback (ABA-CBBI) in this thesis, can effectively explore multiuser diversity and control inter-user interference for sum-rate capacity benefit.

We carry out a theoretical sum-rate analysis of the proposed ABA-CBBI strategy and accurately quantify the resulting average feedback load. Based on these analytical results, we study the effects of the feedback threshold on sum-rate performance and its optimization. We show that the proposed scheduling strategy with optimal threshold values can offer great sum-rate performance, especially over high SNR region.

Receiver combining techniques When there are $N>1$ receive antennas at mobile users, a conventional approach is to treat those antennas independently and carry out user selection on a per-antenna basis. In this work, we apply selection combining (SC) and optimum combining (OC) [44, 60–63] at the receiver. The basic idea is to perform linear combining on the signals from N receive antennas for all M available beams and determine the beam that leads to the largest combined SINR. After that, each user feeds back its best beam index and corresponding combined SINR to the basestation for user selection. The resulting systems only require the same feedback load as single-antenna-per-user case and each receiver just needs to implement a lin-

ear combiner. We show in the work that the SC based scheme has nearly the same performance as the conventional approach while the OC based scheme can achieve much better performance.

1.3 Vector Perturbation Precoding

In terms of symbol error rate (SER) performance, beamforming as a linear precoding technique generally suffer from a performance loss comparing to non-linear techniques including BLAST [67], vector perturbation (VP) precoding [72], Tomlinson-Harashima (TH) precoding [69,71] and lattice-basis reduction precoding [73,74]. Non-linear techniques employ Tomlinson-Harashima (TH) coding [75, 76] to reshape the data vector by adding a perturbation vector to it. The transmit vector is generated by multiplying the perturbed data vector with a precoding matrix.

In this work, we study SER performance of VP with quantized channel feedback. The channel quantization is modeled by following the rate-distortion theory. Based on minimum mean square error (MMSE) criterion, we study the optimal design of precoding matrix and perturbation vector. Equivalent relations in terms of both MMSE and SER between quantized and perfect channel feedback cases are established, based on which we investigate the relation between feedback load and SER performance.

1.4 Significance of Research

Previous studies of beamforming schemes focus on the effects of multiuser diversity on the sum-rate performance. Therefore, asymptotical analysis is usually adopted, where the number of users is assumed to be very large. In this thesis, we study the beamforming schemes through accurate theoretical analysis. This approach serves two purposes. The first is to provide an exact expression of the sum rate, based on which we can study the relation between sum rate and various system parameters including the number of transmit and receive antennas, the number of users, feedback load, and SNR. The second is to optimize design parameters in user selection/scheduling to maximize sum rate.

Based on the analytical results, we propose methods to mitigate multiuser interference resulting from imperfect CSI at the basestation. The contributions of this work include 1) A new user scheduling strategy for multiuser MIMO system with RUB. The proposed strategy can not only benefit from the multiuser diversity but

also reduce multiuser interference. As a result, the proposed strategy achieves better sum-rate performance than existing strategies while requiring lower feedback load. 2) Sum-rate performance improvement for RUB-based multiuser MIMO system with SC and OC. For SC scheme, we carry out accurate sum-rate performance analysis. For OC scheme, we adopt an novel geometric approach to derive the statistics of its output SIR, which provides insight into the role of receive diversity in multiuser interference suppression. Please note that we assume the channel is Rayleigh fading throughout the thesis, the issue of users having different path loss shall also be taken in consideration in the design of practical user scheduling schemes. For fairness, the users already being selected using the methods described in this work may be removed from the following scheduling.

For VP with quantized channel feedback, we consider a joint optimal design of precoding matrix and perturbation vector based on the MMSE criterion. We investigate the tradeoff between SER performance and feedback load. We show that feedback load per user should scale at $M \log_2(\text{SNR})$ to achieve full diversity order.

1.4.1 Thesis Outline

The remainder of the thesis is organized as follows. Chapter 2 analyzes the sum rate of ZFBF-based multiuser MIMO systems with two low-complexity user selection schemes. In Chapter 3, we present the sum-rate analysis of RUB-based multiuser MIMO systems. Based on the achieved analytical results, we propose a simple and efficient user scheduling strategy for RUB-based multiuser MIMO systems and analyze its sum-rate performance in Chapter 4. In Chapter 5, we propose to enhance the sum-rate performance for RUB-based multiuser MIMO systems with receiver combining techniques. We present our results related to VP precoding with quantized channel feedback in Chapter 6. Some conclusions drawn from the work are discussed in Chapter 7.

Chapter 2

Sum-rate Analysis for Zero-forcing Beamforming

With Zero-forcing Beamforming (ZFBF), one user's beamforming vector is designed to be orthogonal to other selected users' channel vectors. With knowledge of perfect CSI at the basestation, ZFBF can completely eliminate the multiuser interference. However, the channel power gain with ZFBF is reduced because of the projection of channel vectors onto the beamforming direction. To minimize the projection power loss, it is desirable that the base station selectively serve those users, whose channel vectors have relative large power gain and, at the same time, are near orthogonal to one another.

The optimum ZFBF user selection strategy involves the exhaustive search of all possible user subsets, which becomes prohibitive to implement when the number of users is large. The upper bound of sum rate achieved with ZFBF is given by simulations in [19]. Several low-complexity user selection strategies have been proposed in [19–24]. Among them, two greedy search algorithms, the successive projection ZFBF (SUP-ZFBF) [19] [21] and greedy weight clique ZFBF (GWC-ZFBF) [20] are attractive for implementation simplicity and their ability to achieve the same scaling law as the DPC scheme.

Most previous work on multiuser MIMO schemes with ZFBF have been based on either simulation study or asymptotic analysis, which have limited applicability to accurate tradeoff analysis and design parameter optimization. In this chapter, we adopt a different approach and study the multiuser ZFBF transmission schemes through mathematic analysis. Specifically, we derive the exact analytical expressions

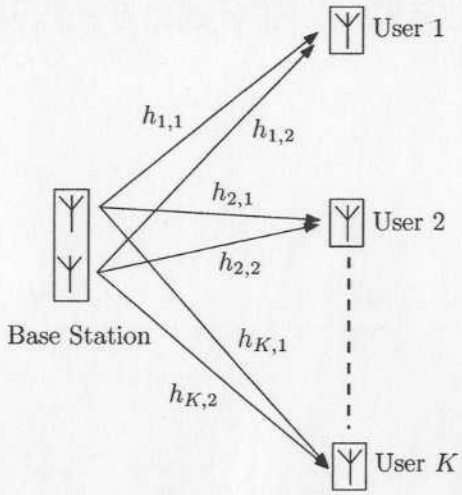

Figure 2.1: Structure of the multiuser MIMO system under consideration.

for the sum rate of the SUP-ZFBF and GWC-ZFBF user selection strategies for the important dual-transmit-antenna scenario.

This chapter is organized as follows. In section 2.1, we describe the system and channel model used in this chapter. After detailing the modes of operation of the two user selection schemes under consideration in section 2.2, we develop their exact sum-rate expressions in section 2.3. In section 2.4, we present some selected numerical examples and discussions.

2.1 System and Channel Models

The multiuser MIMO broadcast system under consideration is shown in Fig. 2.1. Specifically, the base station is equipped with two transmit antennas. There are totally K users in the system, where $K \geq 2$, and each user has one receive antenna. We assume all users experience Rayleigh flat fading. The channel gain from the ith transmit antenna to the kth user h_{ki} is assumed to be independent and identically distributed (i.i.d.) zero mean complex Gaussian random variable with unitary variance. As such, the instantaneous MISO channel from the base station to the kth mobile user can be characterized by a zero-mean complex Gaussian channel vector, denoted by $\mathbf{h}_k = [h_{k1}\ h_{k2}]^T,\ k = 1, 2, \cdots, K$. Accordingly, the norm square of user channel vectors $\|\mathbf{h}_k\|^2$, termed as *channel power gain* in this thesis, are independent identical distributed (i.i.d.) Chi-square random variables with four degrees of free-

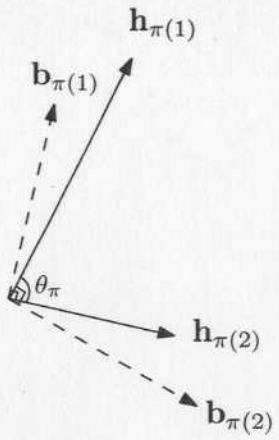

Figure 2.2: Zero-forcing beamforming for two-user case.

dom, with probability density function (PDF) and cumulative distribution function (CDF) given by

$$f_{\|\mathbf{h}\|^2}(x) = xe^{-x}, \quad x \geq 0, \tag{2.1}$$

and

$$F_{\|\mathbf{h}\|^2}(x) = \gamma(2, x), \quad x \geq 0, \tag{2.2}$$

respectively, where $\gamma(2, x)$ is the lower incomplete gamma function, defined as $\gamma(2, x) = \int_0^x te^{-t}\mathrm{d}t$.

For the purpose of user selection and subsequent zero-forcing beamforming transmission, every user in the system feeds back its channel vector to the base station, based on which the base station will select two users to serve simultaneously. The user selection strategy will be explained in details in the next section. Let $\pi(1)$ and $\pi(2)$ denote the indexes of the selected users. As shown in Fig. 2.2, $\mathbf{b}_{\pi(1)}$ and $\mathbf{b}_{\pi(2)}$, which have unit norm, denote the beamforming vectors for the two selected users. The beamforming vector of one user is chosen to be orthogonal to the channel vector of the other user, resulting in so called zero-forcing beamforming. The transmitted signal vector from two antennas over one symbol period can then be written as

$$\mathbf{x} = \sum_{i=1}^{2} \sqrt{P_{\pi(i)}}\mathbf{b}_{\pi(i)}s_{\pi(i)}, \tag{2.3}$$

where $s_{\pi(i)}$ and $P_{\pi(i)}$ are the data symbol and transmit power scaling factor, respectively, for user $\pi(i)$. The power constraint imposed on the transmitted signal is $E[\|\mathbf{x}\|^2] \leq P$. Because of the orthogonality between beamforming vectors and channel

vectors, the received symbol at user $\pi(i)$ is consequently given by

$$r_{\pi(i)} = \mathbf{h}_{\pi(i)}^T \mathbf{x} + n_{\pi(i)} = \sqrt{P_{\pi(i)}} \mathbf{h}_{\pi(i)}^T \mathbf{b}_{\pi(i)} s_{\pi(i)} + n_{\pi(i)} \tag{2.4}$$

where $n_{\pi(i)}$ is the additive zero-mean Gaussian noise with variance N_0. Note that the interference between two user transmission is completely eliminated, whereas, the effective channel power gain for user $\pi(i)$ becomes the norm square of the projection of its channel vector $\mathbf{h}_{\pi(i)}$ onto the corresponding beamforming vector $\mathbf{b}_{\pi(i)}$, which is termed as *projection power* in this thesis. Let θ_π, as illustrated in Fig. 2.2, denote the angle between $\mathbf{h}_{\pi(1)}$ and $\mathbf{h}_{\pi(2)}$. The effective power gain $\gamma_{\pi(i)}$ can be written as

$$\gamma_{\pi(i)} = \|\mathbf{h}_{\pi(i)}\|^2 |\sin(\theta_\pi)|^2. \tag{2.5}$$

Note that $|\sin(\theta_\pi)|^2$ can be viewed as projection power loss factor due to ZFBF. Assuming the total transmit power P is equally divided between two selected users, then the instantaneous sum rate of the syatem is given by

$$R = \sum_{i=1}^{2} \log(1 + \frac{\rho}{2} \gamma_{\pi(i)}) \tag{2.6}$$

where $\rho = \frac{P}{N_0}$ denote the total transmit SNR. We next analyze the sum rate of ZFBF based multiuser MIMO system with two different user selection strategies.

2.2 User Selection Strategies

In this section, we briefly discuss the low-complexity user selection methods for ZFBF under consideration, SUP-ZFBF [19] and GWC-ZFBF [20]. Basically, both schemes sequentially perform user selection from a user subset, which contains users whose channel vectors are near orthogonal to the channel vectors of already selected users. In this work, two channel vectors are claimed to be near orthogonal if θ, the angle between the two channel vectors, satisfies $|\sin(\theta)|^2 \geq \lambda_d$, where $0 < \lambda_d < 1$ is a constant value. With GWC-ZFBF, the next selected user is the one with the largest channel power gain, whereas, with SUP-ZFBF, the next user is the one with the largest projection power of its channel vector onto the complement space of the space spanned by the channel vectors of already selected users. The modes of operation of GWC-ZFBF and SUP-ZFBF for two transmit antenna case are summarized as

follows.

2.2.1 GWC-ZFBF

1. Order all K users based on their channel power gain $\|\mathbf{h}_k\|^2$ as $\|\mathbf{h}_{(1)}\|^2 > \|\mathbf{h}_{(2)}\|^2 > \cdots > \|\mathbf{h}_{(K)}\|^2$.

2. Select the one with the largest channel power gain as the first user, i.e., $\pi(1) = (1)$.

3. Examine sequentially the angle between $\mathbf{h}_{\pi(1)}$ and $\mathbf{h}_{(k)}$, $k = 2, 3, \ldots, K$ and select the first user whose channel vector is near orthogonal to $\mathbf{h}_{\pi(1)}$. Equivalently, the second selected user will be the one with the largest channel power gain among all users in the set

$$\mathcal{U} = \{i | |\sin(\theta_i)|^2 = 1 - \frac{|<\mathbf{h}_i, \mathbf{h}_{\pi(1)}>|^2}{\|\mathbf{h}_i\|^2 \|\mathbf{h}_{\pi(1)}\|^2} \geq \lambda_d\}, \tag{2.7}$$

   where θ_i is the angle between $\mathbf{h}_i$ and $\mathbf{h}_{\pi(1)}$.

2.2.2 SUP-ZFBF

1. Select the user with the largest channel power gain as the first user.

2. Calculate and rank the projection power onto the complementary space of $\mathbf{h}_{\pi(1)}$ for all users in $\mathcal{U}$, which is defined in (2.7).

3. Select the user with the largest projection power as the second user, i.e.,

$$\pi(2) = \max_{i \in \mathcal{U}} \{\|\mathbf{h}_i\|^2 |\sin(\theta_i)|^2\} \tag{2.8}$$

As SUP-ZFBF needs to calculate the projection power of all users in $\mathcal{U}$ while GWC-ZFBF stops searching when it encounters the first user that is near orthogonal to $\mathbf{h}_{\pi(1)}$, SUP-ZFBF exhibits higher computational complexity than GWC-ZFBF [20].

2.3 Sum-Rate Analysis

In this section, we derive the analytical expressions of the sum rate for ZFBF-based multiuser MIMO system with afromentioned user selection strategies. Specifically,

we need to calculate the statistical average of (2.6), which necessitates the statistics of channel power gains of selected users $\|\mathbf{h}_{\pi(i)}\|^2$, $i = 1, 2$ and projection power loss factor $|\sin(\theta_\pi)|^2$ [1].

2.3.1 Common analysis for both schemes

For both user selection schemes, the first selected user has the largest channel power gain among K users. Since the power gains of K users are i.i.d. random variables with PDF and CDF given by (2.1) and (2.2), respectively, the PDF of $\|\mathbf{h}_{\pi(1)}\|^2$ for both schemes is expressed as [25]

$$f_{\|\mathbf{h}_{\pi(1)}\|^2}(x) = K f_{\|\mathbf{h}\|^2}(x)(F_{\|\mathbf{h}\|^2}(x))^{K-1}. \tag{2.9}$$

Note that (2.9) remains the same no matter whether the second can be selected or not. If no user's channel vector is near orthogonal to the channel vector of the first selected user, i.e., $\mathcal{U} = \emptyset$, the basestation could not find the second user and thus transmits to the first selected user using traditional beamforming approach. In this case, the sum rate for both user selection schemes is expressed as

$$E[R|\mathcal{U} = \emptyset] = \int_0^\infty \log(1 + \frac{\rho}{2}x) f_{\|\mathbf{h}_{\pi(1)}\|^2}(x)\mathrm{d}x. \tag{2.10}$$

It is shown in [19] that $|\sin(\theta)|^2$, where θ is the angle between a random channel vector and $\mathbf{h}_{\pi(1)}$, follows the standard uniform distribution over the interval $[0, 1]$. Therefore, after the selection of the first user, the probability that a remaining user belongs to $\mathcal{U}$ is

$$\Pr[|\sin(\theta)|^2 \geq \lambda_d] = 1 - \lambda_d. \tag{2.11}$$

It follows that

$$\Pr[\mathcal{U} = \emptyset] = \lambda_d^{K-1} \quad \text{and} \quad \Pr[\mathcal{U} \neq \emptyset] = 1 - \lambda_d^{K-1}. \tag{2.12}$$

where $\emptyset$ denotes empty set and therefore $\Pr[\mathcal{U} \neq \emptyset]$ is the probability of $\mathcal{U} \neq \emptyset$ and as such the second user can be selected. Considering these two mutually exclusive cases

[1] The major challenge in extending this analysis to multiple antenna scenario is to determine the corresponding statistics of $|\sin(\theta_\pi)|^2$.

of $\mathcal{U} = \emptyset$ and $\mathcal{U} \neq \emptyset$, the average sum rate of both schemes can be calculated as

$$E[R] = \Pr[\mathcal{U} = \emptyset]E[R|\mathcal{U} = \emptyset] + \Pr[\mathcal{U} \neq \emptyset]E[R|\mathcal{U} \neq \emptyset] \tag{2.13}$$

As the first term can be obtained using (2.10) and (2.12), we now need to determine the average sum rate when $\mathcal{U}$ is not empty. This analysis requires the PDF of $\|\mathbf{h}_{\pi(2)}\|^2$ and $|\sin(\theta_\pi)|^2$, which will be derived separately for GWC-ZFBF and SUP-ZFBF in the following.

2.3.2 GWC-ZFBF specific analysis

With GWC-ZFBF, the second selected user is the one with the ith largest channel power gain, i.e. $\pi(2) = (i)$, if and only if user (i) belongs to $\mathcal{U}$ and none of users from (2) to $(i-1)$ does. Therefore, the probability of $\pi(2) = (i)$, given that $\mathcal{U}$ is not empty, can be calculated as

$$\Pr\left[\pi(2) = (i)|\mathcal{U} \neq \emptyset\right] = \frac{(1-\lambda_d)}{1-\lambda_d^{K-1}}\lambda_d^{i-2}, \quad i = 2, 3, \ldots, K. \tag{2.14}$$

By applying the total probability theorem, the PDF of the channel power gain of the second selected user is obtained as

$$f_{\|\mathbf{h}_{\pi(2)}\|^2}(x|\mathcal{U} \neq \emptyset) = \sum_{i=2}^{K} \Pr\left[\pi(2) = (i)|\mathcal{U} \neq \emptyset\right] f_{\|\mathbf{h}_{(i)}\|^2}(x|\pi(2) = (i)), \tag{2.15}$$

where $f_{\|\mathbf{h}_{(i)}\|^2}(\cdot)$ is the PDF of the ith largest channel power gain among K users, given by [25]

$$f_{\|\mathbf{h}_{(i)}\|^2}(x) = K\binom{K-1}{i-1} f_{\|\mathbf{h}\|^2}(x)\left(1 - F_{\|\mathbf{h}\|^2}(x)\right)^{i-1} F_{\|\mathbf{h}\|^2}^{K-i}(x). \tag{2.16}$$

After some mathematical manipulation, (2.15) can be rewritten as

$$\begin{aligned} f_{\|\mathbf{h}_{\pi(2)}\|^2}(x|\mathcal{U} \neq \emptyset) &= \frac{K(1-\lambda_d)}{\lambda_d(1-\lambda_d^{K-1})} f_{\|\mathbf{h}\|^2}(x) \\ &\cdot\Big(\left(\lambda_d + (1-\lambda_d)F_{\|\mathbf{h}\|^2}(x)\right)^{K-1} - F_{\|\mathbf{h}\|^2}^{K-1}(x)\Big). \end{aligned} \tag{2.17}$$

As the second user is selected from user subset $\mathcal{U}$, the projection power loss factor, $|\sin(\theta_\pi)|^2$, follows a uniform distribution with PDF given by

$$f_{|\sin(\theta_\pi)|^2}(y|\mathcal{U}\neq\emptyset)=\frac{1}{1-\lambda_d},\quad \lambda_d\leq y\leq 1. \tag{2.18}$$

Therefore, the sum rate for GWC-ZFBF scheme conditioned on $\mathcal{U}\neq\emptyset$ can be calculated as

$$\begin{aligned}E[R|\mathcal{U}\neq\emptyset]=\sum_{i=1}^{2}\int_0^\infty\int_{\lambda_d}^1\log(1+\frac{\rho}{2}xy) \\ \cdot f_{|\sin(\theta_\pi)|^2}(y|\mathcal{U}\neq\emptyset)\mathrm{d}y f_{\|\mathbf{h}_{\pi(i)}\|^2}(x|\mathcal{U}\neq\emptyset)\mathrm{d}x,\end{aligned} \tag{2.19}$$

which can be further simplifies, with the application of (2.18), to

$$E[R|\mathcal{U}\neq\emptyset]=\sum_{i=1}^{2}\int_0^\infty\frac{g(x)}{1-\lambda_d}f_{\|\mathbf{h}_{\pi(i)}\|^2}(x|\mathcal{U}\neq\emptyset)\mathrm{d}x, \tag{2.20}$$

where

$$\begin{aligned}g(x) &= \frac{2}{\rho x}[(1+\frac{\rho x}{2})\log(1+\frac{\rho x}{2}) \\ &\quad -(1+\frac{\lambda_d\rho x}{2})\log(1+\frac{\lambda_d\rho x}{2})]-\frac{1}{\ln(2)},\end{aligned} \tag{2.21}$$

and $f_{\|\mathbf{h}_{\pi(i)}\|^2}(\cdot)$ for $i=1$ and 2 are given in (2.9) and (2.17), respectively. Note that the distribution of $\|\mathbf{h}_{\pi(1)}\|^2$ is independent of the condition $\mathcal{U}\neq\emptyset$.

Finally, the final expression of sum-rate capacity of the multiuser MIMO system with GWC-ZEBF strategy can be obtained by substituting (2.10), (2.12), and (2.20) into (2.13) as

$$\begin{aligned}E[R] &= \lambda_d^{K-1}\int_0^\infty\log(1+\frac{\rho}{2}x)f_{\|\mathbf{h}_{\pi(1)}\|^2}(x)\mathrm{d}x \\ &\quad +\frac{1-\lambda_d^{K-1}}{1-\lambda_d}\sum_{i=1}^{2}\int_0^\infty g(x)f_{\|\mathbf{h}_{\pi(i)}\|^2}(x|\mathcal{U}\neq\emptyset)\mathrm{d}x.\end{aligned} \tag{2.22}$$

2.3.3 SUP-ZFBF specific analysis

With SUP-ZFBF, the second selected user is the user in $\mathcal{U}$ that has the largest projection power onto the complementary space of the first selected user's channel

vector. From (2.5), the second selected user's projection power is also its effective power gain. As such, the capacity of the second selected user can be obtained using the PDF of the largest projection power among all users in $\mathcal{U}$.

To derive that PDF, we first need to find the PDF of the channel power gain for a user in $\mathcal{U}$, which is denoted as $\|\tilde{\mathbf{h}}\|^2$. Noting that users in $\mathcal{U}$ can not have the largest channel power gain, the PDF of $\|\tilde{\mathbf{h}}\|^2$ can be obtained as

$$f_{\|\tilde{\mathbf{h}}\|^2}(x) = \frac{1}{K-1}\sum_{i=2}^{K} f_{\|\mathbf{h}_{(i)}\|^2}(x) = \frac{K}{K-1} f_{\|\mathbf{h}\|^2}(x)(1 - F_{\|\mathbf{h}\|^2}^{K-1}(x)), \tag{2.23}$$

where $f_{\|\mathbf{h}_{(i)}\|^2}(x)$ is the PDF of the ith largest channel power gain, which is given by (2.16). Letting $\|\tilde{\mathbf{h}}_p\|^2$ represent the projection power of a user in $\mathcal{U}$, we have

$$\|\tilde{\mathbf{h}}_p\|^2 = \|\tilde{\mathbf{h}}\|^2 |\sin(\tilde{\theta})|^2, \tag{2.24}$$

where $\tilde{\theta}$ is the angle between channel vectors of that user and the first selected user. Since $|\sin(\tilde{\theta})|^2$ follows the uniform distribution over the interval $[\lambda_d, 1]$, the CDF of $\|\tilde{\mathbf{h}}_p\|^2$ can be obtained as

$$F_{\|\tilde{\mathbf{h}}_p\|^2}(z) = \Pr[\|\tilde{\mathbf{h}}\|^2 |\sin(\tilde{\theta})|^2 < z] = \frac{1}{1-\lambda_d}\int_{\lambda_d}^{1}\int_{0}^{\frac{z}{y}} f_{\|\tilde{\mathbf{h}}\|^2}(x)\mathrm{d}x\mathrm{d}y. \tag{2.25}$$

After taking derivative with respect to z, the corresponding PDF is given by

$$f_{\|\tilde{\mathbf{h}}_p\|^2}(z) = \frac{1}{1-\lambda_d}\int_{\lambda_d}^{1}\frac{1}{y} f_{\|\tilde{\mathbf{h}}\|^2}(\frac{z}{y})\mathrm{d}y. \tag{2.26}$$

Denote the cardinality of the set $\mathcal{U}$, i.e., the number of users in $\mathcal{U}$, as $|\mathcal{U}|$. As the channel directions of users are independent, the distribution of $|\mathcal{U}|$ conditioned on $\mathcal{U} \neq \emptyset$ can be shown to be given by

$$\Pr[|\mathcal{U}| = k | \mathcal{U} \neq \emptyset] = \frac{1}{1-\lambda_d^{K-1}}\binom{K-1}{k}(1-\lambda_d)^k \lambda_d^{K-1-k}, \tag{2.27}$$
$$k = 1, \cdots, K-1.$$

When $|\mathcal{U}| = k$, the effective channel gain of the second selected user, $\gamma_{\pi(2)}$, is equal

to the largest projection power among k users and its PDF is thus given by

$$f_{\gamma_{\pi(2)}}(g||\mathcal{U}|=k) = k f_{\|\tilde{\mathbf{h}}_p\|^2}(g) F^{k-1}_{\|\tilde{\mathbf{h}}_p\|^2}(g). \tag{2.28}$$

Combining (2.27) and (2.28) and averaging over $|\mathcal{U}|$, the PDF of $\gamma_{\pi(2)}$ given that $\mathcal{U} \neq \emptyset$ can be obtained as

$$\begin{aligned} & f_{\gamma_{\pi(2)}}(g|\mathcal{U} \neq \emptyset) \qquad (2.29) \\ &= \sum_{k=1}^{K-1} \Pr(|U|=k|\mathcal{U} \neq \emptyset) f_{\gamma_{\pi(2)}}(g||U|=k) \\ &= \frac{(K-1)(1-\lambda_d)\lambda_d^{K-2}}{1-\lambda_d^{K-1}} f_{\|\tilde{\mathbf{h}}_p\|^2}(g)\big(1+\frac{1-\lambda_d}{\lambda_d} F_{\|\tilde{\mathbf{h}}_p\|^2}(g)\big)^{K-2}. \end{aligned}$$

To derive the distribution of $|\sin(\theta_\pi)|^2$, we start with the joint PDF of a remaining user's channel power, $\|\tilde{\mathbf{h}}\|^2$, and its projection power loss factor, $|\sin(\tilde{\theta})|^2$. Since they are independent random variables, their joint PDF can be expressed as

$$f_{\|\tilde{\mathbf{h}}\|^2,|\sin(\tilde{\theta})|^2}(x,y) = \frac{1}{1-\lambda_d} f_{\|\tilde{\mathbf{h}}\|^2}(x), \quad x \geq 0, \lambda_d \leq y \leq 1. \tag{2.30}$$

With a change of variables using (2.24), the joint PDF of projection power $\|\tilde{\mathbf{h}}_p\|^2$ and $|\sin(\tilde{\theta})|^2$ of a remaining user is obtained from (2.30) as

$$f_{\|\tilde{\mathbf{h}}_p\|^2,|\sin(\tilde{\theta})|^2}(z,y) = \frac{1}{(1-\lambda_d)y} f_{\|\tilde{\mathbf{h}}\|^2}(\frac{z}{y}), \; z \geq 0, \lambda_d \leq y \leq 1. \tag{2.31}$$

It follows that the conditional PDF of $|\sin(\tilde{\theta})|^2$ given that $\|\tilde{\mathbf{h}}_p\|^2 = z$ is given by

$$\begin{aligned} & f_{|\sin(\tilde{\theta})|^2}(y|\|\tilde{\mathbf{h}}_p\|^2 = z) = \frac{1}{(1-\lambda_d)y} f_{\|\tilde{\mathbf{h}}\|^2}(\frac{z}{y}) / f_{\|\tilde{\mathbf{h}}_p\|^2}(z), \qquad (2.32) \\ & z \geq 0, \lambda_d \leq y \leq 1. \end{aligned}$$

Since the projection power of the second selected user is given by (2.29), we can

obtain the PDF of $|\sin(\theta_\pi)|^2$ conditioned on $\mathcal{U} \neq \emptyset$ by averaging (2.32) over (2.29) as

$$\begin{aligned} & f_{|\sin(\theta_\pi)|^2}(y|\mathcal{U} \neq \emptyset) \\ &= \int_0^\infty f_{|\sin(\tilde{\theta})|^2}(y|\|\tilde{\mathbf{h}}_p\|^2 = z) f_{\gamma_{\pi(2)}}(z|\mathcal{U} \neq \emptyset) dz \\ &= \frac{(K-1)\lambda_d^{K-2}}{(1-\lambda_d^{K-1})y} \int_0^\infty f_{\|\tilde{\mathbf{h}}\|^2}\left(\frac{z}{y}\right)\left(1 + \frac{1-\lambda_d}{\lambda_d} F_{\|\tilde{\mathbf{h}}_p\|^2}(z)\right)^{K-2} \mathrm{d}z, \\ & \quad \lambda_d \leq y \leq 1. \end{aligned} \tag{2.33}$$

The complexity of calculating the PDF can be reduced by integrating up to a large number instead of infinity.

Finally, we can calculate the average system sum rate for SUP-ZFBF scheme given that $\mathcal{U} \neq \emptyset$ as

$$\begin{aligned} E[R|\mathcal{U} \neq \emptyset] = & \int_0^\infty \log(1 + \frac{\rho}{2} g) f_{\gamma_{\pi(2)}}(g|\mathcal{U} \neq \emptyset) \mathrm{d}g + \\ & \int_0^\infty \int_{\lambda_d}^1 \log(1 + \frac{\rho}{2} xy) f_{\|\mathbf{h}_{\pi(1)}\|^2}(x) f_{|\sin(\theta_\pi)|^2}(y|\mathcal{U} \neq \emptyset) \mathrm{d}y \mathrm{d}x \end{aligned} \tag{2.34}$$

The first term in the right hand of (2.34) is the sum rate for $\pi(2)$, in which $f_{\gamma_{\pi(2)}}(\cdot)$ is given by (2.29). The second term is the sum rate for $\pi(1)$, in which $f_{\|\mathbf{h}_{\pi(1)}\|^2}(\cdot)$ and $f_{|\sin(\theta_\pi)|^2}(\cdot)$ are given by (2.9) and (2.33), respectively. Consequently, the expression of sum rate of the multiuser MIMO system with SUP-ZEBF strategy can be obtained by substituting (2.10), (2.12) and (2.34) into (2.13) as

$$\begin{aligned} E[R] \;=\; & \lambda_d^{K-1} \int_0^\infty \log(1 + \frac{\rho}{2} x) f_{\|\mathbf{h}_{\pi(1)}\|^2}(x) \mathrm{d}x \\ & + (1 - \lambda_d^{K-1}) \Big(\int_0^\infty \log(1 + \frac{\rho}{2} g) f_{\gamma_{\pi(2)}}(g|\mathcal{U} \neq \emptyset) \mathrm{d}g \\ & + \int_0^\infty \int_{\lambda_d}^1 \log(1 + \frac{\rho}{2} xy) f_{\|\mathbf{h}_{\pi(1)}\|^2}(x) f_{|\sin(\theta_\pi)|^2}(y|\mathcal{U} \neq \emptyset) \mathrm{d}y \mathrm{d}x \Big). \end{aligned} \tag{2.35}$$

2.4 Numerical examples

We now present several numerical examples based on the analytical results. In particular, we focus on the effects of channel direction parameter λ_d and the number of users K on the sum-rate performance of both schemes. As the effect of transmit power on sum rate capacity is straightforward, the total transmit SNR is fixed to

$\rho = 10$ dB. Note that all the numerical results in this proposal have been verified through Monte Carlo simulation.

Fig. 2.3 illustrates the PDF of projection power loss factor $|\sin(\theta_\pi)|^2$ for both GWC-ZFBF and SUP-ZFBF schemes with different λ_d and/or K values. As we can see, $|\sin(\theta_\pi)|^2$ with GWC-ZFBF scheme always follows a uniform distribution over the interval $[\lambda_d, 1]$. On the other hand, $|\sin(\theta_\pi)|^2$ with SUP-ZFBF scheme is not uniformly distributed due to the user selection based on ordered projection power, which is correlated to channel direction. We can also observe from Fig. 2.3 that the PDF of $|\sin(\theta_\pi)|^2$ with SUP-ZFBF is an monotonically increasing function and the mass of the PDF shifts to the right as K increases. From this behavior, we can conclude that SUP-ZFBF can better exploit multiuser directional diversity than GWC-ZFBF by selecting "more orthogonal" users.

In Fig. 2.4, we plot the sum rate of both GWC-ZFBF and SUP-ZFBF schemes as function of channel direction constraint λ_d. As we can see, the sum rate of SUP-ZFBF remains roughly constant for the small to medium values of λ_d and decreases when λ_d becomes very close to 1. This is because that SUP-ZFBF scheme tends to select "more orthogonal" users, on whom the channel direction constraint has little effect unless λ_d is large. Since a larger value of λ_d will lead to less computation for projection power calculation and ranking, the optimal λ_d for SUP-ZFBF is the largest value before its sum-rate starts to decrease. From Fig. 2.4, we can also observe that the sum rate with GWC-ZFBF is a unimodal function of λ_d. Note that when λ_d is small, the GWC-ZFBF may select less orthogonal users, which incurs larger projection power loss. On the other hand, when λ_d is very large, the candidate users for selection reduces, which leads to sum-rate performance degradation for both schemes. Optimal choices of λ_d values from the sum-rate performance perspective for GWC-ZFBF are indicated on the figure. As we can see, the optimal values of λ_d for both schemes increases as the number of users K increase, which shows we should trade channel power diversity for directional diversity when there are more users in the system.

As an additional example, Fig. 2.5 plots the sum rate with both GWC-ZFBF and SUP-ZFBF schemes as function of the number of users K. We fix the value of λ_d for SUP-ZFBF to 0.5. The sum rate of GWC-ZFBF with two fixed values of λ_d and optimal λ_d are given. As shown in this figure, SUP-ZFBF outperforms GWC-ZFBF in term of sum rate. When GWC-ZFBF adaptively uses the optimal λ_d values for different K, however, the performance gap is very small, especially for a larger value of K.

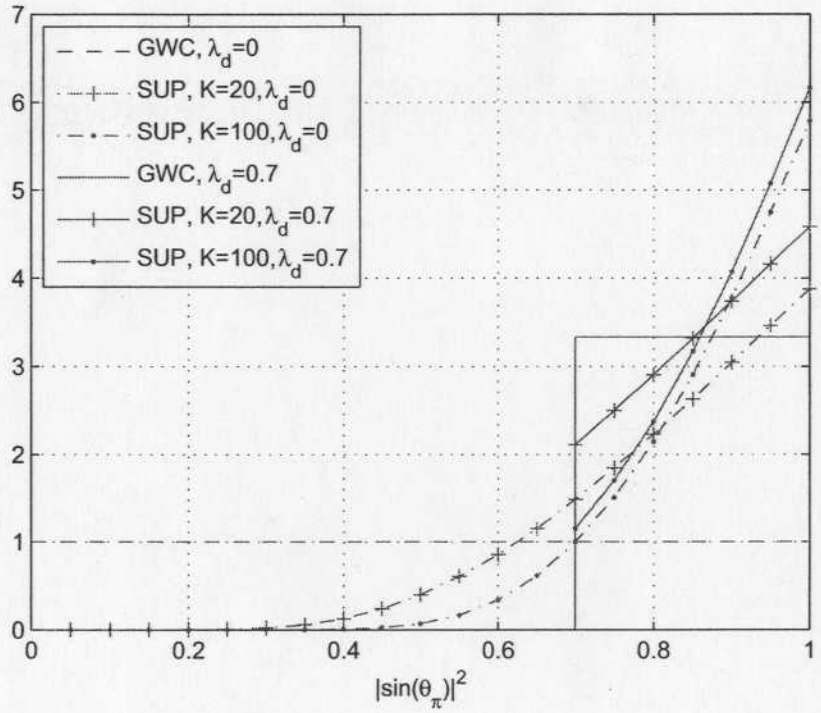

Figure 2.3: The PDF of $|\sin(\theta_\pi)|^2$ for GWC-ZFBF and SUP-ZFBF.

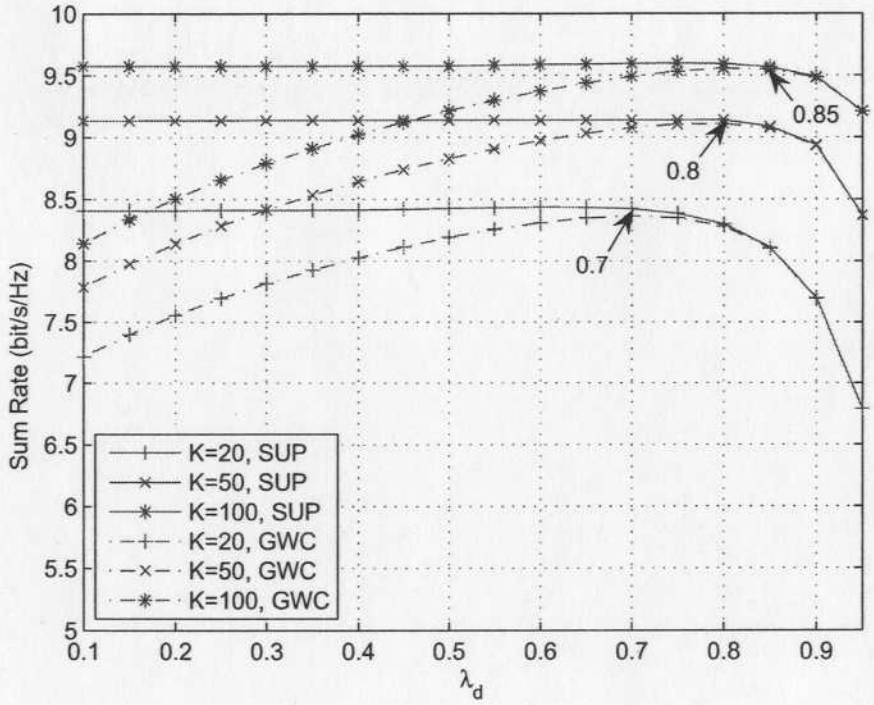

Figure 2.4: Effects of λ_d on the sum rate of GWC-ZFBF and SUP-ZFBF.

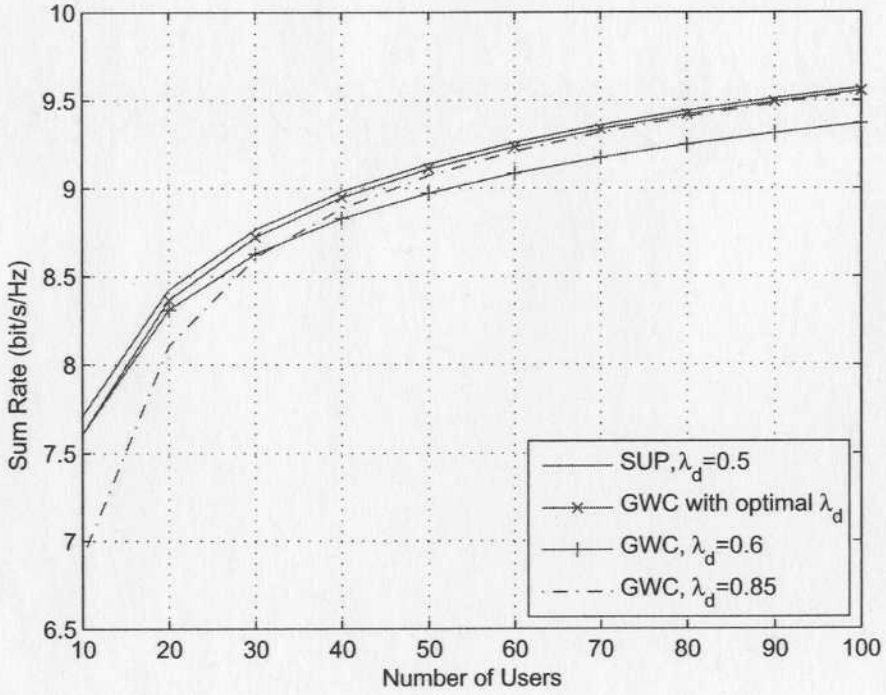

Figure 2.5: Sum rate of GWC-ZFBF and SUP-ZFBF schemes as the function of the number of users.

Chapter 3

Sum-rate Analysis for Random Unitary Beamforming

Random unitary beamforming (RUB) uses M randomly generated orthonormal vectors as beams (beamforming vectors), which are known to both the basestation and all mobile users. With these beams, the basestation communicates with as many as M selected users simultaneously. To explore multiuser diversity gain, each user feeds back some channel quality information, usually in terms of signal-to-interference-plus-noise ratio (SINR), of each beam. Based on feedback information, the basestation carries out proper user selection and beam assignment. In this chapter, we present the exact sum-rate analysis of the multiuser MIMO system with RUB.

This chapter is organized as follows. Section 3.1 presents the multiuser MIMO system and channel model adopted in this work. In section 3.2, we provide the statistics of the ordered beam SINR for a user, which are then applied to the sum-rate analysis of the RUB scheme in section 3.3. An approximate sum-rate analysis over high SNR region is given in section 3.4. Several selected numerical examples are discussed in section 3.5.

3.1 System and Channel Model

The basestation is equipped with M antennas and as such can generate a set of M random orthonormal beams from an isotropic distribution [28]. Let $\mathcal{U} = \{\mathbf{u}_1, \mathbf{u}_2, \cdots, \mathbf{u}_M\}$ denote the set of beamforming vectors, known to both the basestation and the mobile users. With these M beams, the basestation will transmit to as many as M differ-

ent users simultaneously. The transmitted signal vector from M antennas over one symbol period can be written as

$$\mathbf{x} = \sum_{m=1}^{M} \mathbf{u}_m s_m, \tag{3.1}$$

where s_m is the information symbol for the mth selected user. The transmitted signal vector $\mathbf{x}$ has an average power constraint of $\mathbf{E}(\mathbf{x}^H\mathbf{x}) \leq P$, where P is the maximum average transmitting power, $\mathbf{E}(\cdot)$ denotes the statistical expectation and $(\cdot)^H$ denotes the Hermitian transpose.

We assume that there are a total of K active users in the cell, where $K \geq M$. Each user is equipped with a single antenna. We further assume that with a certain slow power control mechanism, the users experience homogeneous flat fading. In particular, the channel gain from the ith antenna to the kth mobile users, denoted by h_{ik}, is assumed to be independent and identically distributed (i.i.d.) zero-mean unit-variance complex Gaussian random variable, i.e. $h_{ik} \sim \mathcal{CN}(0,1)$. As such, the instantaneous MISO channel from the basestation to the kth mobile user can be characterized by a zero-mean complex Gaussian channel vector, denoted by $\mathbf{h}_k = [h_{1k}, h_{2k}, \cdots, h_{Mk}]^T$.

During each symbol period, the basestation transmit simultaneously to a subset of M selected users using all M available beams. The received symbol at the ith chosen user, when the jth beam is assigned to it, can be written as

$$y_i = \mathbf{h}_i^T\mathbf{x} + n_i = \mathbf{h}_i^T\mathbf{u}_j s_j + \sum_{m=1, m\neq j}^{M} \mathbf{h}_i^T\mathbf{u}_m s_m + n_i, \tag{3.2}$$

where n_i is zero mean additive Gaussian noise with unit variance. When power are equally allocated among M beams, the signal to interference plus noise ratio (SINR) of user i while using the jth beam is given by

$$\gamma_{i,j} = \frac{\frac{P}{M}|\mathbf{h}_i^T\mathbf{u}_j|^2}{\frac{P}{M}\sum_{m=1,m\neq j}^{M}|\mathbf{h}_i^T\mathbf{u}_m|^2 + 1}, \quad j = 1, 2, \cdots, M. \tag{3.3}$$

We assume that each user can accurately estimate its own channel vector and determine the instantaneous SINR corresponding to different beams using Eq. (3.3) with the knowledge of beamforming vector set $\mathcal{U}$. The user will then feed back the index of its best beam and corresponding SINR. The basestation could assign the beam in

an ordered fashion. Basically, the basestation could rank the K best beam SINRs fed back by all users. If $\gamma_{k,m}$ is the largest SINR among all K ones, then the basestation assigns the mth beam to the kth user. After that, the basestation will rank the SINRs for the remaining beams. If now $\gamma_{n,l}$ is the largest, then the basestation assigns the lth beam to the nth user, where $l \neq m$ and $n \neq k$. This process is continued until either all beams have been assigned or there is no user requesting the remaining beams. In the later case, the basestation will allocate the remaining beams to randomly chosen users.

The sum rate of MIMO multiuser system based on RUB can be written as

$$R = \mathbf{E}\left(\sum_{m=1}^{M} \log_2(1+\gamma_m^B)\right), \tag{3.4}$$

where γ_m^B is the SINR of the mth beam. Hence, we need the statistical distribution of γ_m^B to evaluate the expectation in (3.4).

3.2 Statistics of Beam SINRs

It has been shown in [28], for a user i, the random variables $|\mathbf{h}_i^T \mathbf{u}_j|^2$, $j = 1, 2 \ldots, M$ are of independent χ^2 distribution with two degree of freedom. Note that even though SINRs for beams of different users, i.e. $\gamma_{i,j}$ with different i, are independent, the SINRs for the beams of the same user, i.e. $\gamma_{i,j}$ with the same i but different j, are correlated random variables as they involves the same channel gain vector $\mathbf{h}_i$. While noting the particular structure of (3.3), the cumulative distribution function (CDF) of the largest SINR for user i, denoted by $\gamma_{i,1:M}$, can be calculated in terms of the joint probability density function (PDF) of the largest one of M i.i.d. χ^2 random variables, $\alpha_{1:M}$, and the sum of the remaining $M-1$ ones, $z_1 = \sum_{m=2}^{M} \alpha_{m:M}$, ($\alpha_{m:M}$ denotes the mth largest χ^2 random variable among total M ones.) denoted by $f_{\alpha_{1:M},z_1}(y,z)$, as [33]

$$F_{\gamma_{i,1:M}}(x) = \Pr[\gamma_{i,1:M} < x] = \int_0^{\infty} \int_0^{x(M/P+z)} f_{\alpha_{1:M},z_1}(y,z)dydz. \tag{3.5}$$

After taking derivative with respect to x, the PDF of $\gamma_{i,1:M}$ is given by

$$f_{\gamma_{i,1:M}}(x) = \int_0^{\infty} (M/P+z) f_{\alpha_{1:M},z_1}(x(M/P+z),z)dz. \tag{3.6}$$

It was further shown in [33] that the joint PDF $f_{\alpha_{1:M},z_1}(y,z)$ is available in closed form, as given by

$$f_{\alpha_{1:M},z_1}(y,z) = \frac{M}{(M-2)!}e^{-y-z}\times\sum_{j=0}^{M-1}\binom{M-1}{j}(-1)^j(z-jy)^{M-2}\mathrm{U}(z-jy), \quad (3.7)$$

where $\mathrm{U}(\cdot)$ denotes unit step function. Similarly, the CDF and PDF of the lth largest SINR of user i, $\gamma_{i,l:M}$, can be written in terms of the joint PDF of $w_l = \sum_{m=1}^{l-1}\alpha_{m:M}$, $\alpha_{l:M}$, and $z_l = \sum_{m=l+1}^{M}\alpha_{m:M}$, denoted by $f_{w_l,\alpha_{l:M},z_l}(w,y,z)$, as

$$F_{\gamma_{i,l:M}}(x) = \int_0^{\infty}\int_0^{(M-l)w/(l-1)}\int_0^{x(M/P+z+w)} f_{w_l,\alpha_{l:M},z_l}(w,y,z)dydzdw, \quad (3.8)$$

and

$$f_{\gamma_{i,l:M}}(x) = \int_0^{\infty}\int_0^{(M-l)w/(l-1)}(M/P+z+w)\cdot \quad (3.9)$$
$$f_{w_l,\alpha_{l:M},z_l}(w,x(M/P+z+w),z)dzdw,$$

respectively. The closed-form expression of the joint PDF $f_{w_l,\alpha_{l:M},z_l}(w,y,z)$ can be obtained from [32, Eq. (28)] after some modifications as

$$p_{w_l,\alpha_{l:M},z_l}(w,y,z) = \quad (3.10)$$
$$M\binom{M-1}{l-1}\frac{[w-(l-1)y]^{l-2}}{(l-2)!(M-l-1)!}e^{-w-y-z}\mathrm{U}(w-(l-1)y)$$
$$\times\sum_{j=0}^{M-l}\binom{M-l}{j}(-1)^j(z-jy)^{M-l-1}\mathrm{U}(z-jy),$$
$$y>0, w>(l-1)y, z<(M-l)y. \quad (3.11)$$

3.3 Sum-rate Analysis

Based on the mode of operation of the RUB strategy with ordered beam assignment, we can see that the SINR of the first beam is always the largest one of all K best beam SINRs that are fed back, i.e. $\gamma_1^B = \gamma_{1:K,1:M}$, where $\gamma_{i:K,1:M}$ denotes the ith largest best beam SINRs among all K ones. Noting that the largest SINRs of different users

are independent, the PDF of γ_1^B is given by

$$f_{\gamma_1^B}(x) = KF_{\gamma_{i,1:M}}(x)^{K-1} f_{\gamma_{i,1:M}}(x), \tag{3.12}$$

where $F_{\gamma_{i,1:M}}(\cdot)$ and $f_{\gamma_{i,1:M}}(\cdot)$ are the CDF and PDF of the best beam SINR for a particular user, given in (3.5) and (3.6), respectively.

We now consider the SINR of the second beam. Based on the mode of operation, the SINR of the second beam may be the ith largest one among all K best beam SINRs, $i = 2, 3, \cdots, K$, if the previous $i-2$ largest ones are for the first beam. For example, if the second and third largest best beam SINRs are also for the first beam, then the SINR of the second beam will be equal to the fourth largest best beam SINR. Since the user SINRs for different beams are i.i.d., each beam has the same probability to lead to the largest SINR for a particular user. It can be shown that the probability that the second beam is assigned to a user with the ith largest best beam SINRs among all K ones, i.e. $\gamma_2^B = \gamma_{i:K,1:M}, i = 2, 3, \cdots, K$, is given by

$$P_i^2 = \left(\frac{1}{M}\right)^{i-2} \left(1 - \frac{1}{M}\right), \tag{3.13}$$

where $\frac{1}{M}$ gives the probability that the best SINR of a user is for a particular beam. In the worst case, where all K SINRs belong to the first assigned beam, i.e. all users request the same beam, the SINR of the second beam is equal to the SINRs of a randomly chosen user, whose PDF can be shown to be given by

$$f_{\gamma^R}(x) = \frac{1}{M-1} \sum_{j=2}^{M} f_{\gamma_{i,j:M}}(x), \tag{3.14}$$

where $f_{\gamma_{i,j:M}}(x)$ is the PDF of the jth largest beam SINR for a user given in (3.9). The probability that the second beam is assigned to a random user is equal to $(\frac{1}{M})^{K-1}$. Consequently, the PDF of the SINR for the second beam γ_2^B can be shown to be given by

$$f_{\gamma_2^B}(x) = \sum_{i=2}^{K} P_i^2 f_{\gamma_{i:K,1:M}}(x) + \left(\frac{1}{M}\right)^{K-1} f_{\gamma^R}(x), \tag{3.15}$$

where $f_{\gamma_{i:K,1:M}}(x)$ is the PDF of the ith largest best beam SINR among all K ones,

given by

$$f_{\gamma_{i:K,1:M}}(x) = K\binom{K-1}{i-1} F_{\gamma_{i,1:M}}(x)^{(K-i)} \times [1 - F_{\gamma_{i,1:M}}(x)]^{i-1} f_{\gamma_{i,1:M}}(x). \tag{3.16}$$

Similarly, the SINR of the third beam may be the ith largest SINRs among all K ones, $i = 3, 4, \cdots, K$, if one of the previous $i-2$ largest best beam SINR is assigned to the second beam and the remaining $i-3$ largest ones are for either the first or the second beam. It can be shown that the probability that the third beam is assigned to a user with the ith largest best beam SINRs among all K users, i.e. $\gamma_3^B = \gamma_{i:K,1:M}, i = 3, 4, \cdots, K$, is given by

$$P_i^3 = \sum_{j=0}^{i-3} \left(\frac{1}{M}\right)^j \left(1 - \frac{1}{M}\right) \left(\frac{2}{M}\right)^{i-3-j} \left(1 - \frac{2}{M}\right),$$

where $\frac{2}{M}$ gives the probability that the largest SINR for a particular user is for the first and second assigned beams. Note that in the worst case where all K best beam SINRs belong to the first and second beam, whose probability is $\left(\frac{2}{M}\right)^{K-1}$, the SINR of the third assigned beam is equal to the SINRs of a randomly chosen user, whose PDF was given in (5.10). Consequently, the PDF of the SINR for the third beam with BBSI strategy can be shown to be given by

$$f_{\gamma_3^B}(x) = \sum_{i=3}^{K} P_i^3 f_{\gamma_{i:K,1:M}}(x) + \left(\frac{2}{M}\right)^{K-1} f_{\gamma^R}(x). \tag{3.17}$$

In general, the SINR of the mth beam may be the ith largest best beam SINRs, where $i = m, m+1, \cdots, K$. More specifically, $\gamma_m^B = \gamma_{i:K,1:M}$ when a scenario as shown in Table 3.1 occurs. After determining the probability of the scenario in Table 3.1 for a particular vector $\{n_j\}_{j=1}^{m-1}$ and summing over all possible vectors $\{n_j\}_{j=1}^{m-1}$, while noting that $\{n_j\}_{j=1}^{m-1}$ need to satisfy $n_j \in \{0, 1, \cdots, i-m\}$ and $\sum_{j=1}^{m-1} n_j = i - m$, we obtain the probability that the SINR of the mth beam is the ith largest user SINRs

Table 3.1: Sample scenario for the event that the mth beam is assigned to the user with the ith largest best beam SINR among all K users, i.e. $\gamma_m^B = \gamma_{i:K,1:M}$.

Ordered best beam SINRs	Corresponding beams	# of users
1	for the first beam	1
2 to n_1+1	for the first beam	n_1
n_1+2	for the second beam	1
$\vdots$	$\vdots$	$\vdots$
$\sum_{k=1}^{j-1} n_k + j$	for the jth beam	1
$\sum_{k=1}^{j-1} n_k + j + 1$ to $\sum_{k=1}^{j-1} n_k + n_j + j$	for the first j beams	n_j
$\vdots$	$\vdots$	$\vdots$
$\sum_{j=1}^{m-2} n_j + m$ to $\sum_{j=1}^{m-2} n_j + n_{m-1} + m - 1$	for the first $m-1$ beams	n_{m-1}
$i = \sum_{j=1}^{m-1} n_j + l$	for the mth beam	1

as

$$P_i^m = \sum_{\substack{\sum_{j=1}^{m-1} n_j = i-m \\ n_j \in \{0,1,\cdots,i-m\}}} \left[\prod_{j=1}^{m-1} \left(\frac{j}{M}\right)^{n_j} \left(1 - \frac{j}{M}\right) \right] \tag{3.18}$$
$$i = m, m+1, \cdots, K.$$

Consequently, after noting that it is with a probability of $\left(\frac{m-1}{M}\right)^{K-1}$ that the mth beam is assigned to a random selected user, the PDF of the SINR on the mth beam γ_m^B can be shown to be given by

$$f_{\gamma_m^B}(x) = \sum_{i=m}^{K} P_i^m \; f_{\gamma_{i:K,1:M}}(x) + \left(\frac{m-1}{M}\right)^{K-1} f_{\gamma^R}(x). \tag{3.19}$$

Finally, after applying (3.12) and (3.19) in (3.4), the exact sum-rate expression for the RUB scheme under consideration can be calculated as

$$E(R) = \int_0^\infty \log_2(1+x) K F_{\gamma_{i,1:M}}(x)^{K-1} f_{\gamma_{i,1:M}}(x) dx \tag{3.20}$$
$$+ \sum_{m=2}^{M} \sum_{i=m}^{K} \left(P_i^m \int_0^\infty \log_2(1+x) \; f_{\gamma_{i:K,1:M}}(x) dx \right.$$
$$\left. + \left(\frac{m-1}{M}\right)^{K-1} \int_0^\infty \log_2(1+x) f_{\gamma^R}(x) dx \right),$$

where P_i^m, $f_{\gamma_{i:K,1:M}}(x)$ and $f_{\gamma^R}(x)$ are given in (3.18), (3.16) and (3.14), respectively.

3.4 High SNR Approximation

We now consider the approximate sum-rate analysis for high SNR region, where the system becomes interference-limited and the noise effect can be neglected. In this case, (3.3) is simplified to

$$\gamma_{i,j} \approx \frac{|\mathbf{h}_i^T \mathbf{u}_j|^2}{\sum_{m=1,m\neq j}^{M} |\mathbf{h}_i^T \mathbf{u}_m|^2}, \; j = 1, 2, \cdots, M. \tag{3.21}$$

Noting that $|\mathbf{h}_i^T \mathbf{u}_m|^2$, $m = 1, 2, \ldots, M$ in above expression is the norm square of the projection of the channel vector onto the mth beam, (3.21) can be further simplified to

$$\gamma_{i,j} \approx \frac{|\cos(\theta_{ij})|^2 \|\mathbf{h}_i\|^2}{|\sin(\theta_{ij})|^2 \|\mathbf{h}_i\|^2} = |\cot(\theta_{ij})|^2, \tag{3.22}$$

where θ_{ij} is the angle between the channel vector of user i and beamforming vector j. From [19], the random variable $|\cos(\theta)|^2$, where θ is the angle between a random channel vector and a specific beam, follows the Beta distribution parameterized by 1 and $M-1$, with PDF and CDF given by

$$f_{|\cos(\theta)|^2}(x) = (M-1)(1-x)^{M-2}, \; 0 \leq x \leq 1 \tag{3.23}$$

and

$$F_{|\cos(\theta)|^2}(x) = 1 - (1-x)^{M-1}, \; 0 \leq x \leq 1 \tag{3.24}$$

respectively. As a result, $|\cos(\theta_j^*)|^2$, where θ_j^* is the smallest angle between beam j and all user channel vectors, will have the largest value among K Beta distributed random variables. The PDF of $|\cos(\theta_j^*)|^2$ is thus given by

$$f_{|\cos(\theta_j^*)|^2}(x) = K f_{|\cos(\theta)|^2}(x) F^{K-1}_{|\cos(\theta)|^2}(x), \; 0 \leq x \leq 1. \tag{3.25}$$

If we assume that every beam is assigned to the user with the smallest angle from this beam, i.e. θ_j^*, while noting $\log_2(1+|\cot(\theta_{ij})|^2) = -\log_2(1-|\cos(\theta_{ij})|^2)$, we arrive at the following approximate expression for the sum rate over high SNR region

$$E(R) = M \int_0^1 -\log_2(1-x) f_{|\cos(\theta_j^*)|^2}(x) \mathrm{d}x. \tag{3.26}$$

which is actually a tight upper bound as there is a small probability that beams may not be assigned to the closest users.

3.5 Numerical Examples

In this section, we study the effect of the number of transmit antennas and the number of users on the sum-rate performance of multiuser MIMO system with the RUB scheme under consideration. Note that all the numerical results have been verified through Monte Carlo simulation.

In Fig. 3.1, we plot the sum rate of the RUB scheme as function of transmit SNR and its high SNR approximation (upper bound). As we can see, for the fixed number of users and transmit antennas, the sum rate increases more rapidly when SNR is low and saturate to the upper bound when SNR becomes large. This confirms that interference plays an more important role than noise in limiting a user's capacity in high SNR region. When SNR is high, the comparison between the sum rate with $M = 2$ and $M = 4$ shows that using less transmit antennas will introduce less multiuser interference and can enhance the sum rate performance. This observation differs from the observations made in earlier works where the number of users is assumed to be extremely large. Note that we have fixed the number of users to a moderate number.

In Fig. 3.2, we plot the sum rate as function of the number of users and its high SNR bound. It is shown that the sum rate always increases when there are more users in the system. When the SNR is high, the sum rate approaches the upper bound and, at the same time, increase at the same rate as the upper bound when the number of users increases. As the upper bound depends only on the angle between a beam and the channel vector of the user assigned to it, this fact indicates that the sum rate increases because multiuser diversity increases the possibilities for the basestation to select users with smaller angle from the beamforming vectors.

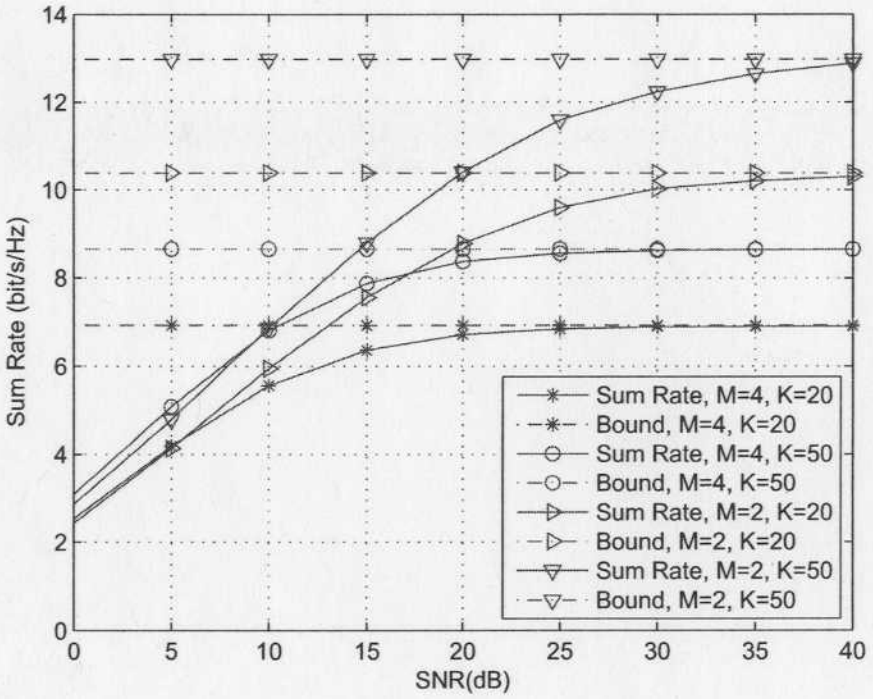

Figure 3.1: The sum rate versus SNR with different number of transmit antennas and users.

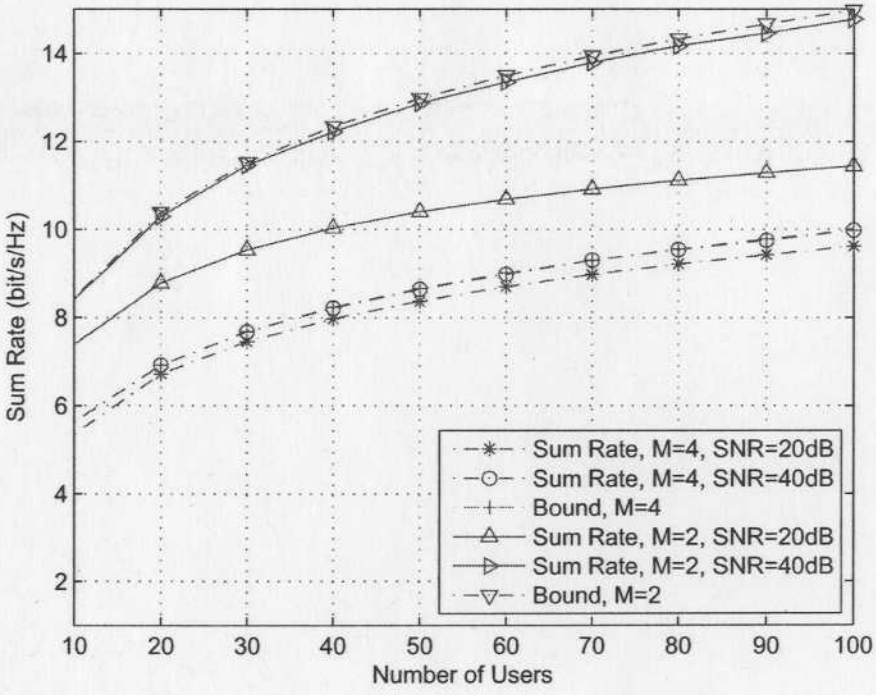

Figure 3.2: The sum rate versus the number of users with different number of transmit antennas and SNR.

Chapter 4

Efficient User Scheduling for Random Unitary Beamforming

In Chapter 3, we analyzed the sum-rate performance of RUB-based multiuser MIMO Systems. It is shown that the sum-rate performance becomes interference-limited at high SNR. Since interference is caused by simultaneous transmission to M users, it is feasible to suppress multiuser interference by reducing the number of users served at the same time.

Based on this idea, we present a user scheduling scheme for multiuser MIMO systems with RUB in this chapter. The new scheme, termed as adaptive beam activation based on conditional best beam index feedback (ABA-CBBI), requires low average feedback load by imposing a feedback threshold on the users' signal to interference plus noise ratio (SINR) and suffers less multiuser interference by only activating those beam requested by at least one user. We derive the exact analytical expression for the sum rate of the resulting multiuser MIMO system, based on which we examine the optimal selection of the feedback threshold in terms of sum rate maximization. We demonstrate through selected numerical examples that the ABA-CBBI scheme with optimal thresholds can achieve better sum-rate performance than existing schemes over the high signal to noise ratio (SNR) region.

This rest of this chapter is organized as follows. Section 4.1 presents the multiuser MIMO system and channel model adopted in this work. In section 4.2, we describe the proposed user scheduling strategy. We perform the exact sum-rate analysis of RUB-based multiuser MIMO systems with proposed scheduling strategy in section 4.3. Several selected numerical examples are discussed in section 4.4.

4.1 System and Channel Model

We consider the downlink transmission in a single-cell wireless system. The basestation is equipped with M antennas and, as such, can generate a set of M random orthonormal beams from an isotropic distribution [28]. Let $\mathcal{U} = \{\mathbf{u}_1, \mathbf{u}_2, \cdots, \mathbf{u}_M\}$ denotes the set of beamforming vectors, known to both the basestation and mobile users. With these M beams, the basestation can serve as many as M users simultaneously with each user being assigned to a different beam. When M_a, $M_a \leq M$, users are being served[1], the transmitted signal vector from M antennas over one symbol period can be written as

$$\mathbf{x} = \sum_{n=1}^{M_a} \mathbf{u}_{\phi(n)} s_n, \tag{4.1}$$

where s_n denotes the information symbol for the nth selected user, $\mathbf{u}_{\phi(n)}$ stands for the beamforming vector for the nth selected user, and $\phi(n) \in [1, 2, \cdots, M]$. The transmitted signal vector $\mathbf{x}$ has an average power constraint of $tr\{\mathbf{E}[\mathbf{x}\mathbf{x}^H]\} \leq P$, where P is the maximum average transmitting power, $\mathbf{E}[\cdot]$ denotes the statistical expectation and $(\cdot)^H$ stands for the Hermitian transpose.

We assume that there are a total of K active users in the system, where $K \geq M$, and each user is equipped with a single antenna. We further assume that with a certain slow power control mechanism, the users experience homogeneous Rayleigh flat fading. In particular, the channel gain from the ith antenna to the kth mobile user, denoted by h_{ik}, is assumed to be an independent zero-mean complex Gaussian random variable with unitary variance, i.e. $h_{ik} \sim \mathcal{CN}(0, 1)$. As such, the instantaneous channel from the basestation to the kth mobile user can be characterized by a zero-mean complex Gaussian channel vector, denoted by $\mathbf{h}_k = \{h_{1k}, h_{2k}, \cdots, h_{Mk}\}^T$. In this work, we assume that each user can accurately estimate its own channel vector using the training pilots.

Based on the signal and channel models, the received symbol of the ith selected user can be written as

$$y_i = \mathbf{h}_i^T \mathbf{x} + n_i = \mathbf{h}_i^T \mathbf{u}_{\phi(i)} s_i + \sum_{n=1, n\neq i}^{M_a} \mathbf{h}_i^T \mathbf{u}_{\phi(n)} s_n + n_i, \tag{4.2}$$

[1]Most previous works assume that all M beams are always active for analytical convenience. In this work, we allow the number of active beams, or equivalently, the number of active users, to be less than M.

where n_i is independent zero mean additive Gaussian noise with unitary variance. Consequently, with equal power allocation among the selected users, the SINR at the ith selected user, assuming that M_a users are being served simultaneously, is given by

$$\gamma_i = \frac{\frac{P}{M_a}|\mathbf{h}_i^T \mathbf{u}_{\phi(i)}|^2}{\frac{P}{M_a}\sum_{n=1,n\neq j}^{M_a}|\mathbf{h}_i^T \mathbf{u}_{\phi(n)}|^2 + 1}, \ i = 1, 2, \cdots, M_a. \tag{4.3}$$

It follows that the instantaneous sum-rate capacity of the system can be calculated as

$$R = \sum_{i=1}^{M_a} \log_2(1 + \gamma_i). \tag{4.4}$$

During each user scheduling period, the basestation will select a proper user subset for simultaneous downlink transmission. Different user scheduling strategies obtain different amount of multiuser diversity gain for sum-rate performance benefit while requiring certain CSI feedback. In this chapter, we present an efficient scheduling scheme with great sum-rate performance and low average feedback load. To facilitate the performance comparison with existing scheduling strategies, we use the average sum rate $\mathbf{E}[R]$ as the performance metric and derive its exact analytical expression in the following sections.

4.2 Adaptive User Scheduling with Limited Feedback

In this section, we present the proposed ABA-CBBI user scheduling strategy for RUB-based multiuser MIMO systems. The ABA-CBBI strategy differs from existing strategies in the literature in at least one of the following three aspects: i) Conditional feedback with thresholding; ii) Best beam index feedback only for user scheduling; and iii) No random user selection for unrequested beams.

4.2.1 Mode of Operation of ABA-CBBI Strategy

At the beginning of each scheduling period, each user will determine the instantaneous SINR on the available beams while assuming that all M beams will be active. Specifically, with the knowledge of beamforming vector set $\mathcal{U}$ and the estimated channel

vector $\mathbf{h}_k$, the SINR of user k on the jth beam can be calculated as

$$\gamma_{k,j} = \frac{\frac{P}{M}|\mathbf{h}_k^T \mathbf{u}_j|^2}{\frac{P}{M}\sum_{m=1,m\neq j}^{M}|\mathbf{h}_k^T \mathbf{u}_m|^2 + 1}, \quad k = 1, 2, \cdots, K, \; j = 1, 2, \cdots, M. \tag{4.5}$$

The users will then perform some comparisons to determine their *best beams* j^*, with which the largest SINR among all beams is achieved, namely $j^* = \arg\max_j(\gamma_{k,j})$. The corresponding SINR, denoted as γ_{k,j^*}, is called the *best beam SINR* of user k. Each user compares its best beam SINR with an SINR threshold, denoted by β. Only when its best beam SINR is greater than β, will the user feed back its best beam index, resulting in feedback load of $\log_2(M)$ bits per feedback user. After collecting the best beam indexes fed back from qualified users, the basestation will assign a beam randomly to a user requesting it. If a beam is not requested by any feedback user, the basestation will simply turn off that beam and redistribute the power to other beams. In this case, the number of active beams (or selected users) M_a will be less than the number of available beams M. Since a beam is randomly assigned to one of the users requesting it, the proposed scheduling strategy has lower operational complexity than the scheme proposed in [15], which ranks the SINR of all users requesting that beam first and then assigns it to the user archiving the maximum SINR on it.

4.2.2 Feedback Load

The feedback load of the proposed ABA-CBBI strategy varies over time as the number of qualified users is changing with the channel condition[2]. We can quantify the average feedback load of this strategy as

$$F = KP_f \log_2 M, \tag{4.6}$$

where P_f is the probability that a user is qualified to feedback. Based on the above-mentioned mode of operation , P_f is equal to the probability that the best beam SINR of a user while assuming all M beams are active, γ_{k,j^*}, is greater than the threshold β, i.e. $P_f = \Pr[\gamma_{k,j^*} > \beta]$. With the homogeneous Rayleigh fading assumption, it

[2]We focus on the feedback load required for user scheduling only in the following analysis. Note that if link adaptive techniques are employed to achieve the sum rate in practical system, we may ask each scheduled user to feedback its best beam SINR value before actual transmission, which leads to an additional feedback load of at most M real numbers.

can be shown that γ_{k,j^*} are identically distributed with common probability density function (PDF) given by [33]

$$f_{\gamma_B^{(M)}}(x) \tag{4.7}$$
$$= \frac{M}{(M-2)!}\int_0^\infty (M/P+z)e^{-x(\frac{M}{P}+z)-z}\times \sum_{j=0}^{M-1}\binom{M-1}{j}$$
$$(-1)^j\big(z-jx(\frac{M}{P}+z)\big)^{M-2}\mathrm{U}\big(z-jx(\frac{M}{P}+z)\big)dz,$$

where $\mathrm{U}(\cdot)$ denotes the unit step function. As such, the average feedback load with the proposed ABA-CBBI strategy is given by[3]

$$F = K\log_2 M\int_\beta^\infty f_{\gamma_B^{(M)}}(x)dx. \tag{4.8}$$

4.2.3 Distribution of the Number of Active Beams

A unique feature of the proposed ABA-CBBI strategy is no random user selection for unrequested beams. As a result, the number of selected users, or equivalently, active beams, M_a, becomes a discrete random variable taking values in $[1, 2, \cdots, M]$. Note that if every user feeds back, the probability of a beam not being requested by any user will be small and even negligible, as long as the number of users is large enough. But with the conditional feedback strategies, this probability becomes larger as the number of feedback users can be small due to the feedback thresholding. In the following, we derive the probability mass function (PMF) of M_a, which will be applied to the sum rate analysis of the proposed scheme in the next section.

With ABA-CBBI strategy, the number of users that are qualified to feed back, denoted by N_f, is random. The probability of $N_f = k$ is given by

$$\Pr[N_f = k] = \binom{K}{k}P_f^k(1-P_f)^{K-k},\ k = 0, 1, \cdots, K. \tag{4.9}$$

Given that k users feed back their best beam indexes, the probability that only one beam is active, i.e. $M_a = 1$ is equal to the probability that all k users feed back the

[3]This result corrects an error in [36, Eq. (13)] as the SINR of a user for different beams are correlated random variables.

same beam index, which can be calculated as

$$\Pr[M_a = 1|N_f = k] = \binom{M}{1}\left(\frac{1}{M}\right)^k. \tag{4.10}$$

The probability of exact two beams are active can be calculated by subtracting from the probability that at most two beams are active, which is given by $\binom{M}{2}\left(\frac{2}{M}\right)^k$, the probability of only one of those two beams is active, which is equal to $\binom{M}{2}\binom{2}{1}\left(\frac{1}{M}\right)^k$. Therefore, we have

$$\Pr[M_a = 2|N_f = k] = \binom{M}{2}\left[\left(\frac{2}{M}\right)^k - \binom{2}{1}\left(\frac{1}{M}\right)^k\right]. \tag{4.11}$$

Similarly, the probability that exact three beams are active can be calculated by subtracting from the probability that at most three beams are active, the probabilities that not all three beams are active. Hence, the probability of $M_a = 3$ is given by

$$\begin{aligned}\Pr[M_a = 3|N_f = k] = \binom{M}{3}\Bigg\{&\left(\frac{3}{M}\right)^k - \binom{3}{2}\cdot \\ &\left[\left(\frac{2}{M}\right)^k - \binom{2}{1}\left(\frac{1}{M}\right)^k\right] - \binom{3}{1}\left(\frac{1}{M}\right)^k\Bigg\}.\end{aligned} \tag{4.12}$$

In general, the probability that exactly m beams out of M available beams are active given that k users feed back their best beam indexes can be recursively calculated as

$$\begin{aligned}\Pr[M_a = m|N_f = k] = \binom{M}{m}\Bigg\{&\left(\frac{m}{M}\right)^k \\ &-\sum_{j=1}^{m-1}\binom{m}{j}\frac{\Pr[M_a = j|N_f = k]}{\binom{M}{j}}\Bigg\},\ m = 1, 2, \cdots, M.\end{aligned} \tag{4.13}$$

In Appendix A, we prove that (4.13) can be simplified to the following compact expression

$$\begin{aligned}\Pr[M_a = m|N_f = k] = \frac{1}{M^k}\binom{M}{m}\cdot \\ \sum_{q=1}^{m}(-1)^{m-q}\binom{m}{q}q^k,\quad m = 1, 2, \cdots, M.\end{aligned} \tag{4.14}$$

Finally, combining (4.9) and (4.14), the probability that exact m beams are active can be obtained by applying the total probability theorem as

$$\begin{aligned} &\Pr[M_a = m] \\ &= \sum_{k=1}^{K} \Pr[N_f = k] \Pr[M_a = m | N_f = k] \\ &= \binom{M}{m} \sum_{q=1}^{m} (-1)^{m+q} \binom{m}{q} \left[\left(1 - \frac{M-q}{M} P_f \right)^K - (1-P_f)^K \right]. \end{aligned} \tag{4.15}$$

4.3 Sum Rate Analysis

In this section, we investigate the performance of the proposed ABA-CBBI strategy by analytically deriving the exact sum-rate expression for the resulting multiuser MIMO systems. Conditioning on the number of active beams, the average sum rate with ABA-CBBI strategy can be calculated as

$$\mathbf{E}[R] = \sum_{m=1}^{M} \Pr[M_a = m] \mathbf{E} \left[\sum_{i=1}^{m} \log_2(1+\gamma_i) \right], \tag{4.16}$$

where $\Pr[M_a = m]$ was given in (4.15) and γ_i, given by (4.3), is the SINR of the ith selected user. Based on the mode of operation of the proposed strategy, the SINR of users on different active beams are identically distributed. As such, we can rewrite the sum rate as

$$\mathbf{E}[R] = \sum_{m=1}^{M} \Pr[M_a = m] m \int_0^{\infty} \log_2(1+x) f_{\gamma_B^{(m)}}(x) dx, \tag{4.17}$$

where $f_{\gamma_B^{(m)}}(\cdot)$ denotes the common PDF of the SINR of the selected users given that exactly m beams are active.

We now proceed to derive the PDF $f_{\gamma_B^{(m)}}(\cdot)$. Based on the mode of operation of the proposed ABA-CBBI strategy, $\gamma_B^{(m)}$ is also the best beam SINR of a feedback user when m beams are active. Meanwhile, the best beam SINR of such a user when assuming all M beams are active, $\gamma_B^{(M)}$, must be greater than the threshold β. Therefore, the SINR distribution for active beams with ABA-CBBI strategy is the conditional distribution of $\gamma_B^{(m)}$ given $\gamma_B^{(M)} > \beta$. It follows that the cumulative distribution function (CDF) of the SINR of the selected users when m beams are

active can be determined as

$$F_{\gamma_B^{(m)}}(x) = \frac{\Pr[\gamma_B^{(m)} < x, \gamma_B^{(M)} > \beta]}{\Pr[\gamma_B^{(M)} > \beta]}. \tag{4.18}$$

To proceed further, we note that a beam becomes the best beam for a particular user if and only if the user's channel vector has the largest projection norm square ($|\mathbf{h}_k^T \mathbf{u}_j|^2$) on that beam direction [33]. Therefore, we can rewrite $\gamma_B^{(m)}$ based on (4.3) as

$$\gamma_B^{(m)} = \begin{cases} \frac{\alpha_{1:M}}{z_{m-1}+m/P}, & 1 < m \leq M, \\ P\alpha_{1:M}, & m = 1, \end{cases} \tag{4.19}$$

where $\alpha_{1:M} = \max\{|\mathbf{h}_i^T \mathbf{u}_j|^2, j = 1, 2, \cdots, M\}$ is the largest projection norm squares onto all M possible beam directions and z_{m-1} is the sum of arbitrary $m-1$ projection norm squares out of the remaining $M-1$ ones. As such, the joint probability in (4.18) can be rewritten as

$$\begin{aligned} &\Pr[\gamma_B^{(m)} < x, \gamma_B^{(M)} > \beta] \\ &= \begin{cases} \Pr[P\alpha_{1:M} < x, \frac{\alpha_{1:M}}{z_{M-1}+M/P} > \beta], & m = 1; \\ \Pr[\frac{\alpha_{1:M}}{z_{m-1}+m/P} < x, \frac{\alpha_{1:M}}{z_{m-1}+z_{M-m}+M/P} > \beta], & 1 < m < M; \\ \Pr[\beta < \frac{\alpha_{1:M}}{z_{M-1}+M/P} < x], & m = M, \end{cases} \end{aligned} \tag{4.20}$$

where we define $z_{M-m} = z_{M-1} - z_{m-1}$ for the case of $1 < m < M$. Consequently, the joint probability of the case of $m = 1$ can be calculated using the joint PDF of $\alpha_{1:M}$ and z_{M-1} as

$$\begin{aligned} &\Pr[\gamma_B^{(m)} < x, \gamma_B^{(M)} > \beta] \\ &= \int_0^{x/P} dy \int_0^{\min\{y/\beta - M/P, (M-1)y\}} dup_{\alpha_{1:M}, z_{M-1}}(y, u), \end{aligned} \tag{4.21}$$

where the joint PDF $p_{\alpha_{1:M}, z_{M-1}}(y, u)$ is given by [33]

$$\begin{aligned} &p_{\alpha_{1:M}, z_{M-1}}(y, u) = p_{\alpha_{1:M}}(y) p_{z_{M-1}|\alpha_{1:M}=y}(u) \\ &= Me^{-y-u} \sum_{j=0}^{M-1} \binom{M-1}{j} \frac{(-1)^j (u - jy)^{M-2}}{(M-2)!} \mathrm{U}(u - jy), \\ &\quad y > 0, u < (M-1)y. \end{aligned} \tag{4.22}$$

The joint probability of the cases of $1 < m < M$ can be calculated using the joint PDF of $\alpha_{1:M}$, z_{m-1}, and z_{M-m} as

$$\Pr[\gamma_B^{(m)} < x, \gamma_B^{(M)} > \beta] = \int_0^\infty dy \int_{y/x-m/P}^{y/\beta-M/P} du \int_0^{y/\beta-u-M/P} dv p_{\alpha_{1:M},z_{m-1},z_{M-m}}(y,u,v). \tag{4.23}$$

The joint PDF of $\alpha_{1:M}$, z_{m-1} and z_{M-m} can be determined by following the Bayesian approach. It has been shown that the unordered projection norm squares $|\mathbf{h}_i^T \mathbf{u}_j|^2$, $j = 1, 2, \cdots, M$, are i.i.d. χ^2 random variables with two degrees of freedom [28]. Due to the ordering process, $\alpha_{1:M}$, z_{m-1} and z_{M-m} are correlated random variables. On the other hand, it can be shown that given $\alpha_{1:M} = y$, z_{m-1} and z_{M-m} are the sum of $m-1$ and $M-m$ i.i.d. random variables with truncated distribution on the right at y [38], respectively, and as such are independent. Specifically, the joint PDF of $\alpha_{1:M}$, z_{m-1} and z_{M-m} can be written as

$$\begin{aligned} & p_{\alpha_{1:M},z_{m-1},z_{M-m}}(y,u,v) \\ &= p_{\alpha_{1:M}}(y) p_{z_{m-1}|\alpha_{1:M}=y}(u) p_{z_{M-m}|\alpha_{1:M}=y}(v) \\ &= p_{\alpha_{1:M}}(y) p_{\sum_{j=1}^{m-1}\alpha_j^-}(u) p_{\sum_{j=m+1}^{M}\alpha_j^-}(v), \end{aligned} \tag{4.24}$$

where α_j^- are i.i.d. random variables with PDF for the Rayleigh fading scenario under consideration given by

$$p_{\alpha_j^-}(x) = \frac{e^{-x}}{1-e^{-y}}, \quad 0 < x < y. \tag{4.25}$$

After some mathematical manipulations, we can obtain the closed-form expression for the joint PDF of $\alpha_{1:M}$, z_{m-1} and z_{M-m} as

$$\begin{aligned} & p_{\alpha_{1:M},z_{m-1},z_{M-m}}(y,u,v) \\ &= M e^{-y-u-v} \sum_{j=0}^{m-1} \binom{m-1}{j} \frac{(-1)^j (u-jy)^{m-2}}{(m-2)!} \mathrm{U}(u-jy) \\ &\times \sum_{k=0}^{M-m} \binom{M-m}{k} \frac{(-1)^k (v-ky)^{M-m-1}}{(M-m-1)!} \mathrm{U}(v-ky), \\ & y > 0, u < (m-1)y, v < (M-m)y. \end{aligned} \tag{4.26}$$

The joint probability for the case of $m = M$ can be calculated using the PDF of $\gamma_B^{(M)}$ given in (4.7) as

$$\Pr[\gamma_B^{(m)} < x, \gamma_B^{(M)} > \beta] = \int_\beta^x f_{\gamma_B^{(M)}}(y)dy. \tag{4.27}$$

After proper substitutions and taking derivative, we obtain the PDF of active beam SINR $\gamma_B^{(m)}$ as

$$f_{\gamma_B^{(m)}}(x) = \frac{1}{P_f}\begin{cases} \int_0^{\frac{x}{P\beta}-\frac{M}{P}} \frac{1}{P} p_{\alpha_{1:M},z_{M-1}}(\frac{x}{P},u)du, & m=1; \\ \int_0^\infty \int_0^{\frac{y}{\beta}-\frac{y}{x}-\frac{M-m}{P}} \frac{y}{x^2} p_{\alpha_{1:M},z_{m-1},z_{M-m}} & \\ \quad (y, \frac{y}{x}-\frac{m}{P}, v)dvdy, & 1<m<M; \\ f_{\gamma_B^{(M)}}(x)\mathrm{U}(x-\beta), & m=M. \end{cases} \tag{4.28}$$

Finally, the exact sum rate expression for RUB-based multiuser MIMO systems with ABA-CBBI strategy can be obtained by substituting (4.15) and (4.28) into (4.17).

$$\begin{aligned} P_f\mathbf{E}[R] = & \binom{M}{1}\left(\frac{1}{M}\right)^k \int_0^\infty \log_2(1+x)\int_0^{\frac{x}{P\beta}-\frac{M}{P}} \frac{1}{P} p_{\alpha_{1:M},z_{M-1}}(\frac{x}{P},u)dudx \\ & + \sum_{m=2}^{M-1}\binom{M}{m}\sum_{q=1}^{m}(-1)^{m+q}\binom{m}{q}\left[\left(1-\frac{M-q}{M}P_f\right)^K - (1-P_f)^K\right]\times \\ & m\int_0^\infty \log_2(1+x)\int_0^\infty \int_0^{\frac{y}{\beta}-\frac{y}{x}-\frac{M-m}{P}} \frac{y}{x^2} p_{\alpha_{1:M},z_{m-1},z_{M-m}}(y,\frac{y}{x}-\frac{m}{P},v)dvdydx \\ & + \sum_{q=1}^{M}(-1)^{M+q}\binom{M}{q}\left[\left(1-\frac{M-q}{M}P_f\right)^K - (1-P_f)^K\right]\times \\ & M\int_0^\infty \log_2(1+x)\frac{M}{(M-2)!}\int_0^\infty (M/P+z)e^{-x(\frac{M}{P}+z)-z}\times \\ & \sum_{j=0}^{M-1}\binom{M-1}{j}(-1)^j\big(z-jx(\frac{M}{P}+z)\big)^{M-2}\mathrm{U}\big(z-jx(\frac{M}{P}+z)\big)dzdx \end{aligned} \tag{4.29}$$

The final expression can be readily evaluated using mathematical softwares such as Maple and Mathematica.

Table 4.1: Features of Different Strategies

	SINR Thresholding	SINR Value Feedback	Random Selection
BBSI [8]	NO	YES	YES
Conventional CBBI [12]	YES	NO	YES
ABA-CBBI	YES	NO	NO
BBI [9]	NO	NO	YES

4.4 Numerical Examples

In this section, based on the analytical results in previous sections, we study the sum-rate performance of the proposed ABA-CBBI scheduling strategy through selected numerical examples. In particular, we compare its performance and complexity with some well-known user scheduling strategies for RUB-based multiuser MIMO systems. The first scheduling strategy for RUB systems, as proposed in [15], requires the feedback of best beam index and the corresponding SINR from each user and is thus termed as BBSI [35] in this thesis. A reduced-feedback strategy was presented in [36], where only the best beam indexes of those users with high enough best beam SINR are fed back. This strategy is termed as conventional CBBI in this thesis. Note that the conventional CBBI scheme differs from the proposed ABA-CBBI scheme in that it applies random user selection for those unrequested beams. By comparison, BBI [33] is a strategy that the best beam index is fed back from every user regardless of its SINR. Table 4.1 summarizes the key features of different user scheduling strategies under consideration. It is worthwhile to point out that besides the largest feedback load, BBSI strategy also has higher operational complexity as the basestation needs to rank the SINR values fed back in order to select a user for each beam. In the following numerical examples, we fix the number of transmit antennas to $M = 4$ and use SNR per transmit antenna, defined as P/M, as a channel quality measure.

Fig. 4.1 illustrates the effects of random user selection for unrequested beams on the sum-rate performance. In particular, we plot the sum rate of ABA-CBBI and conventional CBBI as a function of SNR. As we can see, with the same thresholds, the sum rate of ABA-CBBI is always greater than that of conventional CBBI, which shows that the RUB-based system is not benefiting from random user selection. We also notice from Fig. 4.1 that ABA-CBBI with different thresholds has better sum-rate performance over different SNR ranges. Therefore, to achieve the best sum-rate

performance, we should use the optimal value of the feedback threshold β.

In Fig. 4.2, we plot the sum rate of the proposed ABA-CBBI strategy as a function of the feedback threshold β. For a fixed SNR, there exists an optimal value of β maximizing the sum rate, which is marked in the figure. Intuitively, when β is very small, almost all users will feed back their best beam indexes to the basestation. Since the basestation randomly assigns a beam to one of the users requesting it, that beam may be assigned to a user that does not achieve high SINR, which leads to relatively poorer sum-rate performance. On the other hand, when β is very large, few users will be qualified to feed back and some beams may not be requested. As such, not enough spatial multiplexing gain will be explored, which also causes poorer sum-rate performance.

In Fig. 4.3, we plot optimal values of feedback threshold, denoted by β^*, as function of SNR and the number of users. It is shown that β^* always increases when either SNR or the number users increases. Since the sum-rate performance is primarily limited by multiuser interference at high SNR, the increase of β^* means that the average number of feedback users is reduced and more beams will not be requested and are as a result "turned off", which helps reduce multiuser interference and achieve better sum-rate performance. As the number of users increases, it becomes more likely to select those users achieving relatively larger SINR. This benefit brought by more active users is called multiuser diversity gain. Since a corresponding increase in threshold values provides a certain degree of guarantee for the feedback users' SINR, it is a feasible way to exploit multiuser diversity. In addition, increased threshold values also lead to more feedback load savings.

In Fig. 4.4, we compare the sum-rate performance of the proposed ABA-CBBI strategy with two strategies without thresholding, BBSI and BBI. As we can see, the sum rate of ABA-CBBI with optimal thresholds approaches that of BBSI over low SNR region and considerably outperforms as SNR increases. This somewhat surprising behavior can be explained as follows. While the sum rate of BBSI strategy saturates over high SNR region due to multiuser interference, ABA-CBBI manages to reduce multiuser interference by raising the threshold (as shown in Fig. 4.3) and then selecting less users to serve. As a result, the selected users will experience less multiuser interference, a bottleneck to achieving better sum-rate performance at high SNR for conventional RUB-based user scheduling schemes. By comparison, BBI has the worst performance due to its complete lack of a mechanism to guarantee the high SINR of selected users.

Fig. 4.5 plots the sum rates of ABA-CBBI and BBSI schemes versus the number of users in the systems. The sum rate of ABA-CBBI is obtained using the optimal threshold. As we can see, when the number of users is small or moderate, ABA-CBBI considerably outperforms BBSI, especially for the higher SINR case, i.e. SNR=40 dB. When K increases, the sum rate of BBSI improves and becomes larger than that of ABA-CBBI for the lower SNR case, i.e. SNR=20 dB. But for the case of SNR = 40 dB, the performance of ABA-CBBI with optimal threshold remains better than that of BBSI as long as K is not extremely large. Based on Figs. 4.4 and 4.5, we conclude that ABA-CBBI is an attractive multiuser scheduling strategy for the RUB-based systems from the sum-rate performance perspective.

As a final numerical example, we show the average feedback load of BBI ($\log_2(M)$ bits per user) and ABA-CBBI with optimal thresholds in Fig. 4.6. Since BBSI also requires users to feed back their best beam SINR, it has even greater feedback load than BBI. From Fig. 4.6 we can see, as the number of users increases, the feedback load of ABA-CBBI increases much more slowly than that of BBI. More interestingly, higher SNR leads to a lower average feedback load for ABA-CBBI, which matches the observation of increased values for the optimal feedback threshold at higher SNR in Fig. 4.3.

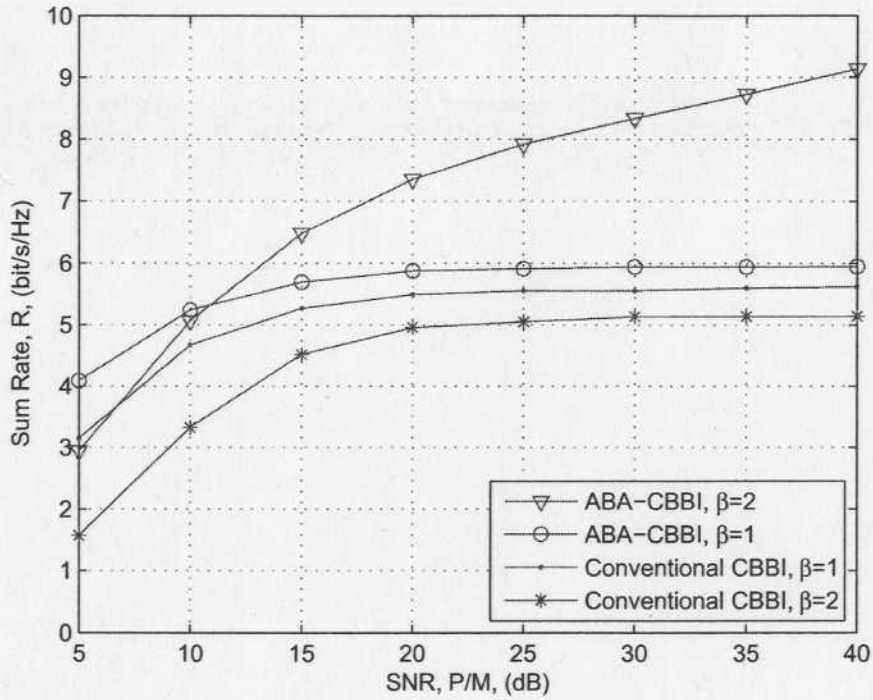

Figure 4.1: Effect of random user selection on sum rate performance ($K = 20$).

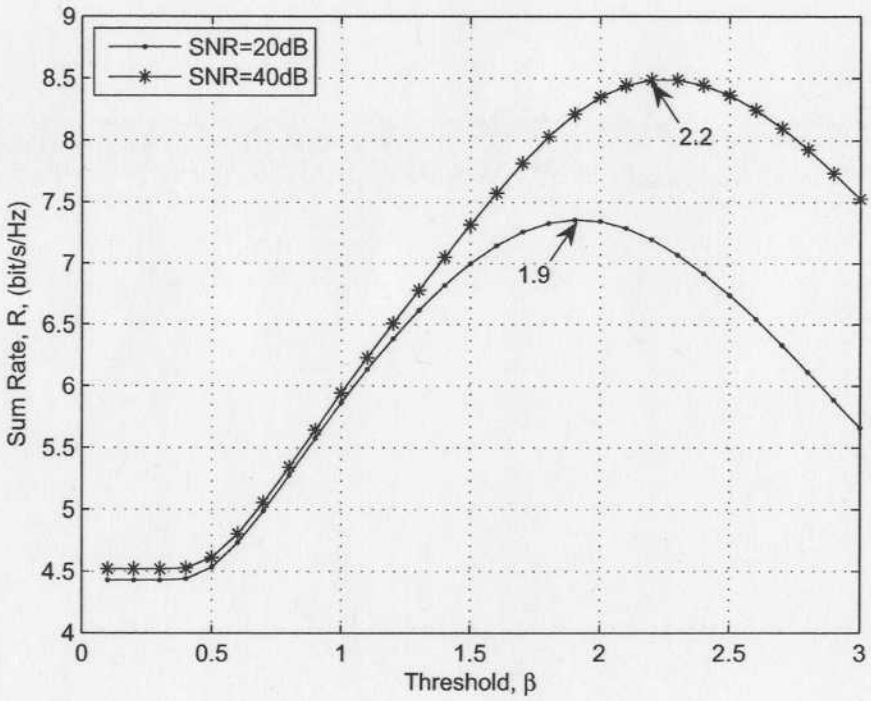

Figure 4.2: Sum rate of ABA-CBBI as function of SINR threshold for different SNR values (K =20).

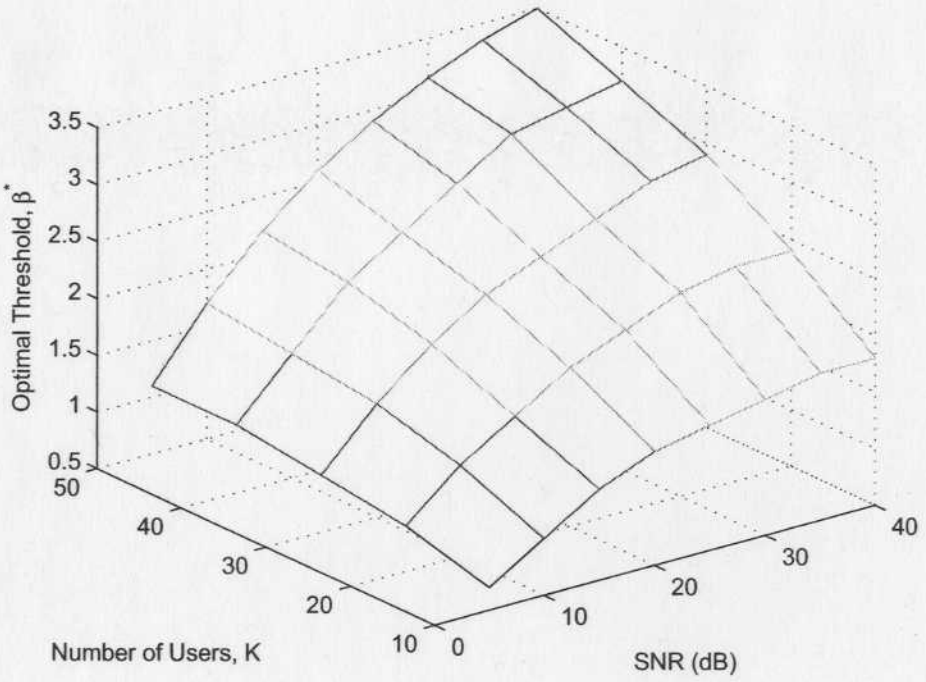

Figure 4.3: Optimal threshold for ABA-CBBI versus SNR and the number of users K.

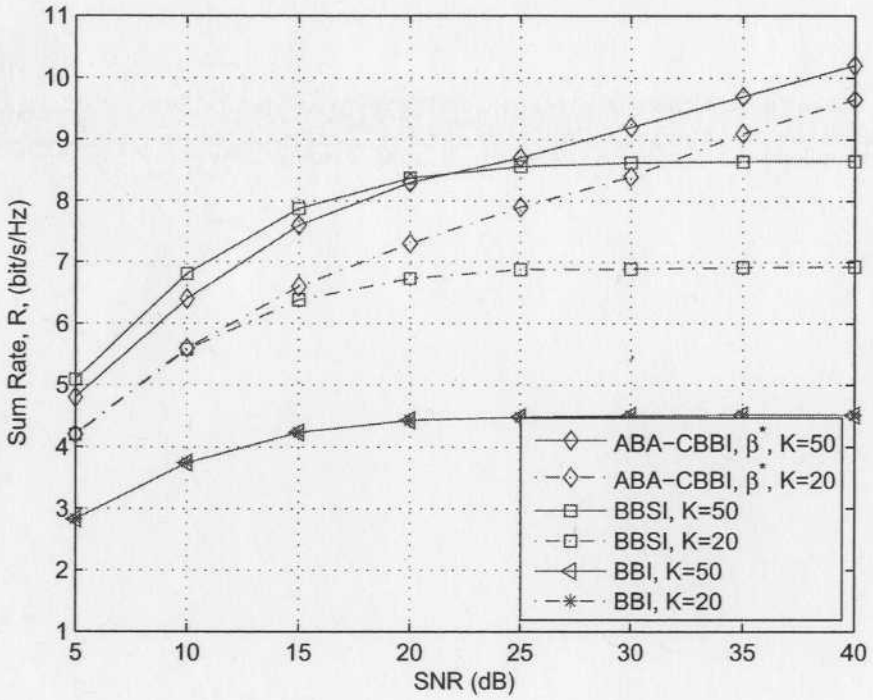

Figure 4.4: Sum rate comparison between ABA-CBBI, BBSI and BBI strategies.

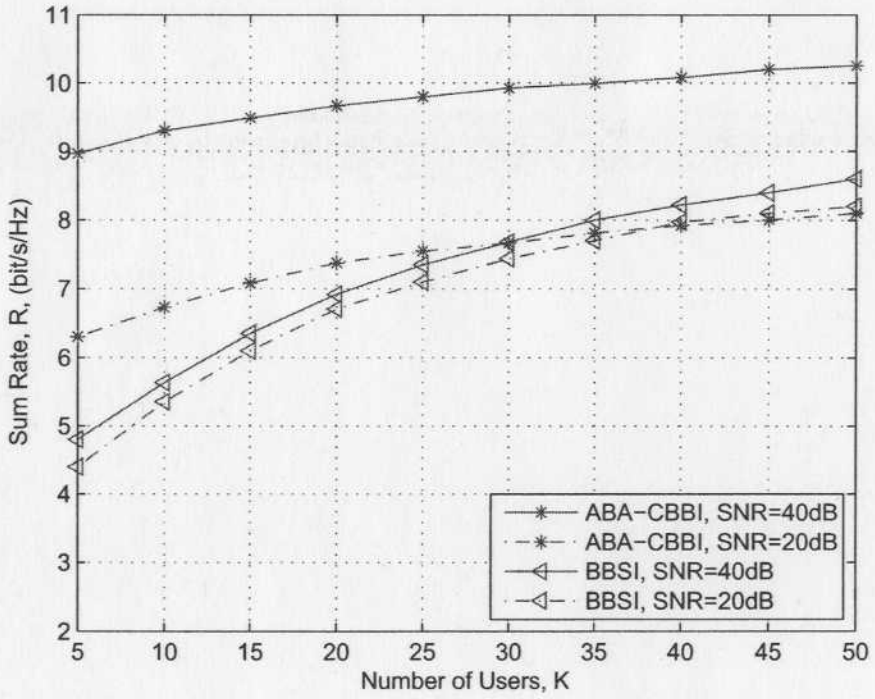

Figure 4.5: Sum rate of ABA-CBBI and BBSI strategies as function of the number of users K.

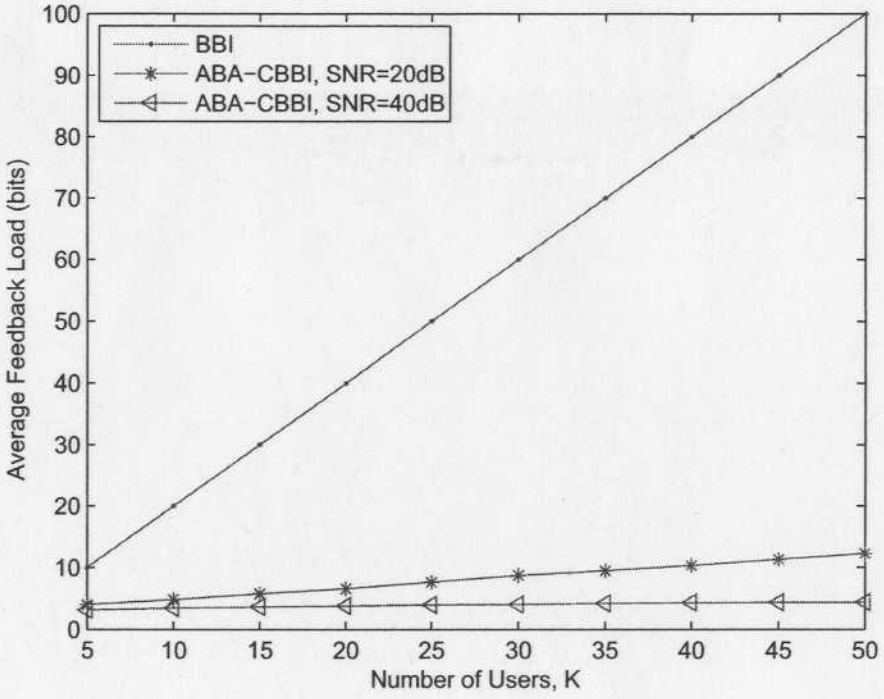

Figure 4.6: Feedback load comparison between ABA-CBBI and BBI strategies.

Chapter 5

Receiver Combining for Random Unitary Beamforming

With Random Unitary Beamforming (RUB), the basestation communicates with M selected users using M predefined random orthonormal beams. For user selection purpose, each user feeds back certain SINR information of available beams. It has been proven in [15] that even if each user just feeds back its maximum beam SINR and the index of the corresponding beam, RUB can achieve the asymptotically optimal sum-rate performance, i.e., the sum rate scales as $M \log \log K$, where K is the total number of single-antenna users in the system. However, such results only hold when the number of users is very large. In practical systems, where the number of users is usually finite and moderate, it is shown in Chapter 3 that the sum rate achieved with RUB quickly becomes interference-limited with the increase of SNR.

In this chapter, we investigate how to enhance the sum-rate performance of the RUB-based MIMO broadcast channels when N ($N > 1$) antennas are used at the mobile terminals. A conventional approach to exploit receive diversity is to treat the N receive antennas independently and let each user feed back the best beam indexes and corresponding SINR values for all its receive antennas [15]. Intuitively, this would improve the sum-rate performance since it is equivalent to increasing the number of single-antenna users in the system to NK. The main disadvantage with this approach is an N times increase of system feedback load. It is highly desirable that we can explore receive diversity while maintaining the same feedback load as the single antenna per user case.

To serve this purpose, we in this chapter apply selection combining (SC) [61] and

optimum combining (OC)[1] [60, 62, 63] schemes to the N receive antennas of mobile users. The operation is as follows. For each of the M beams, a user first calculates the weighting vector that maximizes the output SINR and the resulting SINR. Then, the user selects its best beam among M beams, with which the largest combiner output SINR is achieved. The index of the best beam and its corresponding output SINR are fed back to the basestation. Note that the feedback load with combining techniques is one integer (for best beam index) and one real number (for best beam output SINR) per user, which is the same as single antenna per user case, and each receiver just needs to implement a linear diversity combiner.

Linear combining for the RUB-based multiuser MIMO systems is also considered in [55, 56]. The schemes therein, however, assume that each user feeds back the combiner output SINRs for all M beams, which leads to much higher feedback load. Furthermore, the limiting distribution approach adopted in their work applies only when the number of users is very large. In this chapter, based on the derived statistics of the feedback SINR, we present the exact sum-rate analysis of the SC based scheme. By following a geometric approach, we develop the statistics of the OC output SIR in the high SNR region, which is then used to obtain an upper bound for the sum rate. The upper bound is shown to be tight for the case of a moderate number of users, but the number of users must be at least five times the number of transmit antennas. Numerical examples show that, comparing to the conventional approach, the OC based scheme exhibits much better and the SC based scheme offers similar sum-rate performance, while both requiring less feedback load.

The rest of the chapter is organized as follows. Section 5.1 presents the multiuser MIMO system and channel model adopted in this work. The procedure of user selection and beam assignment based on combined SINR are described in section 5.2. In section 5.3, we analyze the sum-rate performance of the RUB-based multiuser system with SC and OC. Several selected numerical examples are presented in section 5.4 with related discussions.

5.1 System and Channel Model

We consider the downlink transmission of a single-cell wireless system. The basestation is equipped with M antennas and each mobile terminal is equipped with N

[1]We omit the maximum ratio combining (MRC) scheme because MRC is optimal only in the noise limited environment.

antennas, where $N<M$ due to the size and cost limitations of the mobile terminals. We assume that there are a total of K active users in the cell where $K \gg M$. With RUB, the basestation utilizes M random orthonormal vectors generated from an isotropic distribution [28] to transmit to as many as M selected users simultaneously. We denote the orthonormal vector set as $\mathcal{U} = \{\mathbf{u}_1, \mathbf{u}_2, \cdots, \mathbf{u}_M\}$. The transmitted signal vector from the M transmit antennas over one symbol period can be written as

$$\mathbf{x} = \sum_{m=1}^{M} \mathbf{u}_{\phi(m)} s_m, \tag{5.1}$$

where s_m denotes the information symbol and $\mathbf{u}_{\phi(m)} \in \mathcal{U}$ stands for the beam for the mth selected user. The transmitted signal vector $\mathbf{x}$ has an average power constraint of $\mathbf{E}(\mathbf{x}^H\mathbf{x}) \leq P$, where P is the maximum average transmitting power, $\mathbf{E}(\cdot)$ denotes the statistical expectation and $(\cdot)^H$ stands for the Hermitian transpose.

We adopt a homogeneous flat fading channel model for analytical tractability. Specifically, the channel gains from each transmit antenna to each receive antenna of users follow independent and identically distributed (i.i.d.) zero-mean complex Gaussian distribution with unitary variance. The channel gain from the mth transmit antenna to the nth receive antenna of the kth mobile users is denoted by $h_{nm}^{(k)}$. As such, the $N \times M$ channel matrix for the kth user is constructed as

$$\mathbf{H}_k = \begin{pmatrix} h_{11}^{(k)} & \cdots & h_{1M}^{(k)} \\ \vdots & \ddots & \vdots \\ h_{N1}^{(k)} & \cdots & h_{NM}^{(k)} \end{pmatrix} \tag{5.2}$$

with the transpose of the nth row, denoted by $\mathbf{h}_n^{(k)}$, being the MISO channel for the nth receive antenna of user k.

The received signal vector over a symbol period at the ith selected user, when the jth beam is assigned to it, can be written as

$$\mathbf{y}_j^{(i)} = \mathbf{H}_i\mathbf{x} + \mathbf{n}_i = \mathbf{H}_i\mathbf{u}_j s_j + \sum_{m=1, m\neq j}^{M} \mathbf{H}_i\mathbf{u}_m s_m + \mathbf{n}_i, \tag{5.3}$$

where $\mathbf{n}_i$ is the $N \times 1$ additive Gaussian noise vector, whose entries follow independent complex Gaussian distribution with zero mean and variance σ_n^2. Note that $\mathbf{H}_i\mathbf{u}_j s_j$ is the desired signal for user i while $\sum_{m=1,m\neq j}^{M} \mathbf{H}_i\mathbf{u}_m s_m$ acts as interference.

5.2 User Selection and Beam Assignment

The mobile receivers apply linear diversity combining techniques, such as SC and OC, to combine the signal received from the N different receive antennas. When beam j is assigned to user i, the combined signal at user i can be written as

$$z_j^{(i)} = \mathbf{w}_{ij}^H \mathbf{y}_j^{(i)} = \mathbf{w}_{ij}^H \mathbf{H}_i \mathbf{u}_j s_j + \mathbf{w}_{ij}^H \sum_{m=1, m\neq j}^{M} \mathbf{H}_i \mathbf{u}_m s_m + \mathbf{w}_{ij}^H \mathbf{n}_i, \tag{5.4}$$

where $\mathbf{w}_{ij}$ denotes the weighting vector of user i for the jth beam. Assuming that the transmit power is equally allocated among the M selected users, the SINR of the combined signal at user i is given by

$$\gamma_j^{(i)} = \frac{|\mathbf{w}_{ij}^H \mathbf{H}_i \mathbf{u}_j|^2}{\sum_{m=1, m\neq j}^{M} |\mathbf{w}_{ij}^H \mathbf{H}_i \mathbf{u}_m|^2 + \frac{1}{\rho}\|\mathbf{w}_{ij}\|^2}, \tag{5.5}$$

where $\rho = \frac{P}{M\sigma_n^2}$ is the normalized transmit SNR.

We assume that mobile receivers obtain the perfect knowledge of their downlink channel matrix through channel estimation. Applying (5.5), user i calculates the SINRs after beam-specific combining for all M available beams, $\gamma_j^{(i)}, j = 1, 2, \cdots, M$, and determines its best beam. Let b_i denote the index of the best beam for user i. Mathematically, b_i is given by $b_i = \arg\max_j \gamma_j^{(i)}$. For user selection purpose, all users in the system feed back their best beam indexes and the corresponding combiner output SINRs to the basestation. As a result, the proposed RUB schemes with receive diversity combining enjoy the same low feedback load of one integer and one real number per user as the single antenna per user case.

The basestation assigns a beam to the user that feeds back the largest SINR value among all users requesting for that beam. Specifically, let $\mathcal{K}_m$ denote the set containing all users who feed back beam index m, i.e. $b_k = m$ if and only if $k \in \mathcal{K}_m$. If $\gamma_m^{(\hat{k})}$ is the largest one among all $\gamma_m^{(k)}$, $k \in \mathcal{K}_m$, then the mth beam will be assigned to user $\hat{k}$ and the SINR of the mth beam γ_m^B will be equal to $\gamma_m^{(\hat{k})}$. If a particular beam is not requested by any user, i.e. the set $\mathcal{K}_m$ is empty for such a beam, then the basestation knows that this beam is not the best one for any user and will allocate it to a randomly chosen user. The selected user will then apply proper weights to combine the signal from different antennas.

5.3 Performance Improvement with Receiver Combining

5.3.1 Selection Combining

With SC scheme, the combiner output SINR at user i for the jth beam is equal to the largest SINR among N ones corresponding to different receive antennas for this beam. Specifically, the SINR on user i's nth receive antenna, while assuming beam j is assigned to it, can be written as

$$\gamma_{n,j}^{(i)} = \frac{|(\mathbf{h}_n^{(i)})^T \mathbf{u}_j|^2}{\sum_{m=1,m\neq j}^{M} |(\mathbf{h}_n^{(i)})^T \mathbf{u}_m|^2 + \frac{1}{\rho}}, \; 1 \leq n \leq N, \; 1 \leq j \leq M, \tag{5.6}$$

where $\mathbf{h}_n^{(i)}$ is the $M \times 1$ channel vector from M transmit antennas to the n-th receive antenna of user i. The combined SINR for the jth beam is then mathematically given by $\gamma_j^{(i)} = \max\{\gamma_{1,j}^{(i)}, \gamma_{2,j}^{(i)}, \cdots, \gamma_{N,j}^{(i)}\}$. If a user is selected for data reception on a certain beam, the user will use only the best receive antenna for this beam, which constitutes the main complexity advantage of the SC scheme.

The sum-rate performance of the resulting multiuser MIMO system can be analyzed by following a similar approach taken in [59] while treating each user as a single antenna receiver. On the other hand, due to antenna selection, the statistics of the feedback SINR will be different from the single antenna per user case. In particular, $\gamma_{b_i}^{(i)}$ is the largest one of M i.i.d. combined SINRs, i.e. $\gamma_{b_i}^{(i)} = \max\{\gamma_1^{(i)}, \gamma_2^{(i)}, \cdots, \gamma_M^{(i)}\}$. Equivalently, the feedback SINR $\gamma_{b_i}^{(i)}$ can be viewed as the largest one among N best beam SINRs, i.e. $\gamma_{b_i}^{(i)} = \max\{\gamma_{1,j^*}^{(i)}, \gamma_{2,j^*}^{(i)}, \cdots, \gamma_{N,j^*}^{(i)}\}$, where $\gamma_{n,j^*}^{(i)} = \max\{\gamma_{n,1}^{(i)}, \gamma_{n,2}^{(i)}, \cdots, \gamma_{n,M}^{(i)}\}$ denotes the best beam SINR for the nth antenna at user i, whose probability density function (PDF) was obtained in [59] as

$$f_{\gamma_{n,j^*}^{(i)}}(x) = \sum_{j=0}^{M-1} \frac{(-1)^j M(M-1)}{(M-j-1)!j!} \int_0^\infty (\rho + z) \times \tag{5.7}$$
$$\big((1-jx)z - jx\rho\big)^{M-2} e^{-(1+x)z - x\rho} U\big((1-jx)z - jx\rho\big) dz.$$

Therefore, the common PDF of the feedback SINRs $\gamma_{b_i}^{(i)}$ can be obtained as

$$f_{\gamma_{b_i}^{(i)}}(x) = N F_{\gamma_{n,j^*}^{(i)}}(x)^{N-1} f_{\gamma_{n,j^*}^{(i)}}(x), \tag{5.8}$$

where $F_{\gamma_{n,j^*}^{(i)}}(x) = \int_0^x f_{\gamma_{n,j^*}^{(i)}}(z)dz$ is the cumulative distribution function (CDF) of $\gamma_{n,j^*}^{(i)}$.

Based on the mode of operation for user selection detailed in the previous section, a beam might be assigned to a randomly selected user if no user feeds back the index of this beam. In this case, the user will choose the best antenna, i.e. the receive antenna that leads to the largest SINR on this beam, for data reception. As such, the beam SINR for such a beam will be equal to the largest SINR among N i.i.d. ones, whose PDF is given by

$$f_{\gamma^R}(x) = N\big(F_{\gamma_{n,j}^{(i)}}(x)\big)^{N-1} f_{\gamma_{n,j}^{(i)}}(x), \tag{5.9}$$

where $f_{\gamma_{n,j}^{(i)}}(x)$ and $F_{\gamma_{n,j}^{(i)}}(x)$ denote the PDF and CDF of $\gamma_{n,j}^{(i)}$ in (5.6), respectively. The closed-form expression of $f_{\gamma_{n,j}^{(i)}}(x)$ is given by [15, Eq. (14)].

$$f_{\gamma_{n,j}^{(i)}}(x) = \frac{e^{-x/\rho}}{(1+x)^M}\left(\frac{x+1}{\rho} + M - 1\right). \tag{5.10}$$

Finally, following a similar analytical approach applied in [59] and noting that the PDFs of the user feedback SINR and randomly assigned beam SINR have been given by (5.7) and (5.10) respectively, the sum rate of the RUB based systems with SC at receivers can be calculated as

$$\begin{aligned} R^{SC} = &\int_0^\infty \log_2(1+x) f_{\gamma_{b_i}^{(1:K)}}(x)dx \\ &+ \sum_{m=2}^{M}\sum_{k=m}^{K}\Bigg(P_k^m \int_0^\infty \log_2(1+x)\ f_{\gamma_{b_i}^{(k:K)}}(x)dx + \\ &\left(\frac{m-1}{M}\right)^{K-1} \int_0^\infty \log_2(1+x) f_{\gamma^R}(x)dx\Bigg), \end{aligned} \tag{5.11}$$

where P_k^m denotes the probability that the mth beam is assigned to the user with the kth largest feedback SINR, i.e. $\gamma_m^B = \gamma_{b_i}^{(k:K)}, i = m, m+1, \cdots, K$, which is given by [59]

$$P_k^m = \sum_{\substack{\sum_{j=1}^{m-1} n_j = k-m \\ n_j \in \{0,1,\cdots,k-m\}}} \left[\prod_{j=1}^{m-1}\left(\frac{j}{M}\right)^{n_j}\left(1-\frac{j}{M}\right)\right],\ k = m, m+1, \cdots, K, \tag{5.12}$$

and $f_{\gamma_{b_i}^{(k:K)}}(x)$ represents the PDF of the kth largest feedback SINR, given in terms of $f_{\gamma_{b_i}^{(i)}}(x)$ as

$$f_{\gamma_{b_i}^{(k:K)}}(x) = \frac{K!}{(K-k)!(k-1)!} F_{\gamma_{b_i}^{(i)}}(x)^{K-k}[1 - F_{\gamma_{b_i}^{(i)}}(x)^M]^{k-1} f_{\gamma_{b_i}^{(i)}}(x). \tag{5.13}$$

5.3.2 Optimum Combining

With OC scheme [60, 61], it can be shown that the optimal weighting vector of user i for the jth beam is given by

$$\mathbf{w}_{ij}^* = \left(\sum_{m=1, m\neq j}^{M} \mathbf{H}_i \mathbf{u}_m (\mathbf{H}_i \mathbf{u}_m)^H + \frac{1}{\rho}\mathbf{I} \right)^{-1} \mathbf{H}_i \mathbf{u}_j, \tag{5.14}$$

and the corresponding maximum combiner output SINR is given by

$$\gamma_j^{(i)} = (\mathbf{H}_i \mathbf{u}_j)^H \mathbf{w}_{ij}^* = (\mathbf{H}_i \mathbf{u}_j)^H \left(\sum_{m=1, m\neq j}^{M} \mathbf{H}_i \mathbf{u}_m (\mathbf{H}_i \mathbf{u}_m)^H + \frac{1}{\rho}\mathbf{I} \right)^{-1} \mathbf{H}_i \mathbf{u}_j, \tag{5.15}$$

where $\mathbf{I}$ denotes the identity matrix. User i will feed back its best beam index, b_i, and the corresponding SINR, $\gamma_{b_i}^{(i)}$, to the basestation for user selection. If user i is selected by the basestation for data reception on the b_ith beam, it will combine the signals from N receive antennas using the weights $\mathbf{w}_{ib_i}^*$ given by (5.14) for data detection.

After some mathematical manipulation, the optimal weight vector and corresponding output SINR are simplified to

$$\mathbf{w}_{ij}^* = \frac{(\mathbf{H}_i \mathbf{H}_i^H + \frac{1}{\rho}\mathbf{I})^{-1} \mathbf{H}_i \mathbf{u}_j}{1 - (\mathbf{H}_i \mathbf{u}_j)^H (\mathbf{H}_i \mathbf{H}_i^H + \frac{1}{\rho}\mathbf{I})^{-1} \mathbf{H}_i \mathbf{u}_j}, \tag{5.16}$$

and

$$\gamma_j^{(i)} = \frac{(\mathbf{H}_i \mathbf{u}_j)^H (\mathbf{H}_i \mathbf{H}_i^H + \frac{1}{\rho}\mathbf{I})^{-1} \mathbf{H}_i \mathbf{u}_j}{1 - (\mathbf{H}_i \mathbf{u}_j)^H (\mathbf{H}_i \mathbf{H}_i^H + \frac{1}{\rho}\mathbf{I})^{-1} \mathbf{H}_i \mathbf{u}_j}, \tag{5.17}$$

respectively. Note that each user needs only to calculate the inversion of one matrix $(\mathbf{H}_i \mathbf{H}_i^H + \frac{1}{\rho}\mathbf{I})$. Although the statistics of the output SINR for a random beam can be obtained [56, 65], because of the dependence between the SINRs for different beams, it is very difficult, if not impossible, to derive the statistics of the feedback SINR with OC scheme. Therefore, we focus on the sum rate upper bound analysis over the high

SNR region in what follows.

When the SNR is very high, the system will become interference limited. After setting ρ in (5.16) to infinity, the optimal weighting vector can be approximated by

$$\mathbf{w}_{ij}^{*} = \frac{(\mathbf{H}_i\mathbf{H}_i^H)^{-1}\mathbf{H}_i\mathbf{u}_j}{1-(\mathbf{H}_i\mathbf{u}_j)^H(\mathbf{H}_i\mathbf{H}_i^H)^{-1}\mathbf{H}_i\mathbf{u}_j}. \tag{5.18}$$

It follows that $\mathbf{w}_{ij}^{*}$ is proportional to the least square solution of $\mathbf{H}_i^H\mathbf{w} = \mathbf{u}_j$ [65,66]. Therefore, with the optimal weighting vector, the angle between $\mathbf{H}_i^H\mathbf{w}_{ij}^{*}$, the effective MISO channel for user i, and $\mathbf{u}_j$ is minimized. The resulting minimum angel will be equal to the angle between $\mathbf{u}_j$ and the range space of $\mathbf{H}_i^H$ denoted as $\mathcal{R}(\mathbf{H}_i^H)$.

Lemma 1. *Over the high SNR region, the output SINR at user i after performing optimal combining with respect to the jth beam is given by*

$$\gamma_{i,j}^{*} = |\cot(\theta_{ij})|^2, \tag{5.19}$$

where θ_{ij} is the angle between $\mathbf{u}_j$ and $\mathcal{R}(\mathbf{H}_i^H)$.

Proof. Letting ρ in (5.17) go to infinity, the OC output SINR at user i becomes

$$\gamma_{i,j}^{*} = \frac{(\mathbf{H}_i\mathbf{u}_j)^H(\mathbf{H}_i\mathbf{H}_i^H)^{-1}\mathbf{H}_i\mathbf{u}_j}{1-(\mathbf{H}_i\mathbf{u}_j)^H(\mathbf{H}_i\mathbf{H}_i^H)^{-1}\mathbf{H}_i\mathbf{u}_j}. \tag{5.20}$$

Since $\mathbf{H}_i^H(\mathbf{H}_i\mathbf{H}_i^H)^{-1}\mathbf{H}_i$ is the projection matrix onto $\mathcal{R}(\mathbf{H}_i^H)$, we have

$$|\cos(\theta_{ij})|^2 = (\mathbf{H}_i\mathbf{u}_j)^H(\mathbf{H}_i\mathbf{H}_i^H)^{-1}\mathbf{H}_i\mathbf{u}_j. \tag{5.21}$$

The lemma is proved after substituting (5.21) into (5.20). □

Remark 1. *Since* $\cot(\cdot)$ *is a monotonically decreasing function, each user will feed back the index and SINR value of the beam that forms the smallest angle with $\mathcal{R}(\mathbf{H}_i^H)$.*

It can be shown that the random variable $|\cos(\theta_{ij})|^2$, where θ_{ij} is the angle between an M-dimensional complex vector and a space spanned by N complex random vectors of the same dimension, follows the Beta distribution parameterized by N and $M-N$, with the PDF and CDF given by [19]

$$f_{|\cos(\theta)|^2}(x) = (M-N)\binom{M-1}{N-1}x^{N-1}(1-x)^{M-N-1}, \quad 0 \leq x \leq 1 \tag{5.22}$$

and

$$F_{|\cos(\theta)|^2}(x) = \mathrm{I}(x; N, M),\ 0 \leq x \leq 1 \tag{5.23}$$

respectively, where $\mathrm{I}(\cdot)$ is the regularized Beta function. To derive an upper bound of the system sum rate, we assume that every beam of the base station is requested by at least one user. In this case, since a user can only be assigned to one beam, the SINR of the jth assigned beam will be equal to the largest one among $K-j+1$ combiner output SINRs on that beam for the remaining $K-j+1$ users ($j-1$ users have been assigned before). Mathematically speaking, the SINR of the jth assigned beam is equal to $|\cot(\theta_j^*)|^2$, where θ_j^* is the smallest angle among $K-j+1$ ones. Correspondingly, $|\cos(\theta_j^*)|^2$ will be the largest one among $K-j+1$ independent beta-distributed random variables. The PDF of $|\cos(\theta_j^*)|^2$ is thus given by [53]

$$f_{|\cos(\theta_j^*)|^2}(x) = (K-j+1)\big(F_{|\cos(\theta)|^2}(x)\big)^{K-j} f_{|\cos(\theta)|^2}(x), \quad 0 \leq x \leq 1. \tag{5.24}$$

Noting that $\log_2(1+|\cot(\theta_j^*)|^2) = -\log_2(1-|\cos(\theta_j^*)|^2)$, we obtain a sum-rate upper bound for the proposed scheme over the high SNR region as

$$R^{OC} = \sum_{j=1}^{M} -(K-j+1)\int_0^1 \log_2(1-x)\big(F_{|\cos(\theta)|^2}(x)\big)^{K-j} f_{|\cos(\theta)|^2}(x)\mathrm{d}x. \tag{5.25}$$

Remark 2. *As this upper bound is derived based on the assumption that all beam are requested, it will be tight as long as the probability of all beam being requested is close to 1. In chapter 4, we showed that the probability that each of the M available beam is requested by at least one user is given by*

$$\Pr[\textit{every beam requested}] = \sum_{q=1}^{M}(-1)^{M-q}\binom{M}{q}\left(\frac{q}{M}\right)^K. \tag{5.26}$$

This probability is plotted as a function of the number of users K and the number of beams M in Fig. 5.1. As we can see, when K is more than five times of M, which is usually the case in practice, every beam will be requested with probability very close to 1.

5.4 Numerical Examples

In this section, we examine the sum-rate performance of the SC and OC based multiuser MIMO systems through selected numerical examples. The values $M = 4$ and $N = 2$ are used.

In Fig. 5.2, we plot the sum rate of the SC based systems as a function of SNR for a different number of users. For comparison, the sum rate achieved with the conventional approach is also plotted, which treats a user's receive antennas independently. Though requiring only $1/N$ of the feedback load of the conventional approach, SC is shown to achieve nearly the same sum-rate performance. In Fig. 5.2, we also compare our analytical results given by (5.12) to simulation results. The perfect match verifies the analytical approach adopted in this work.

In Fig. 5.3, the sum rate of the OC based systems is plotted as a function of SNR for a different number of users. The sum rate of the conventional approach, M beam feedback (the scheme considered in [55, 56]), and the analytical upper bound given by (5.25) are also plotted. As expected, the analytical upper bound developed for the OC based systems is shown to be tight over the high SNR region. Comparing to the conventional approach, OC achieves noticeably better sum-rate performance while requiring less feedback load. It is worthwhile to mention that the advantages of OC scheme come at the cost of additional processing complexity of channel matrix inversion when calculating the combining weights and output SINR. We further observe that the proposed OC scheme offers nearly the same performance as the M beam feedback scheme in [55,56], which mandates M real numbers per user feedback load.

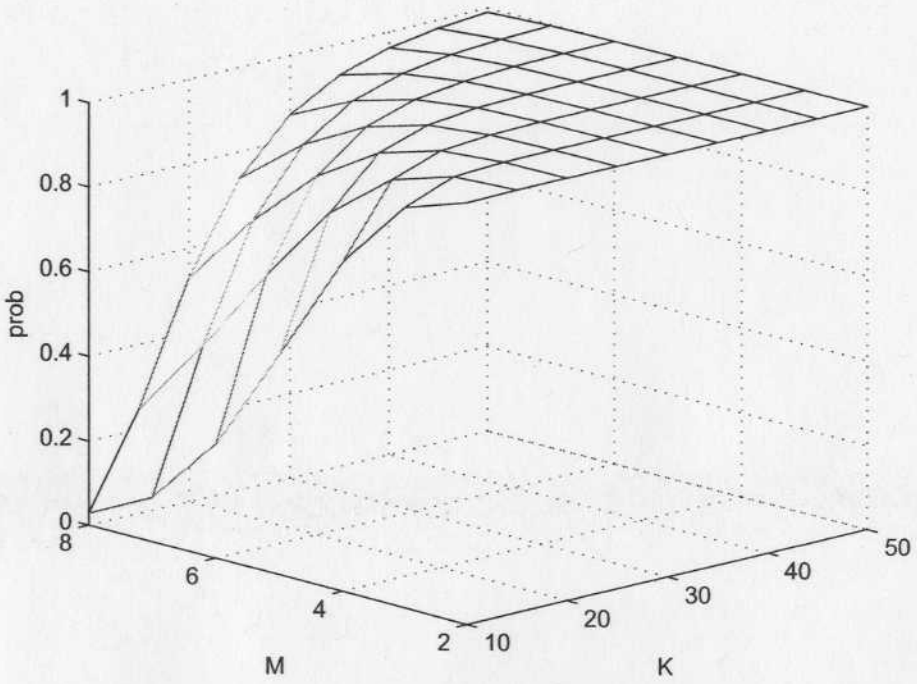

Figure 5.1: Probability of all beams being requested.

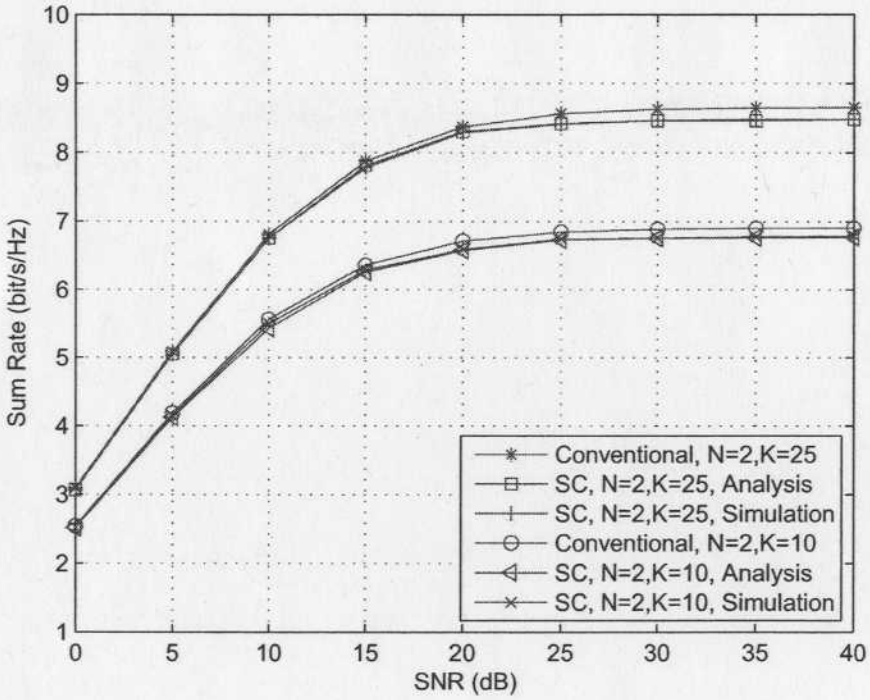

Figure 5.2: Sum-rate performance of RUB systems with SC scheme ($M = 4$).

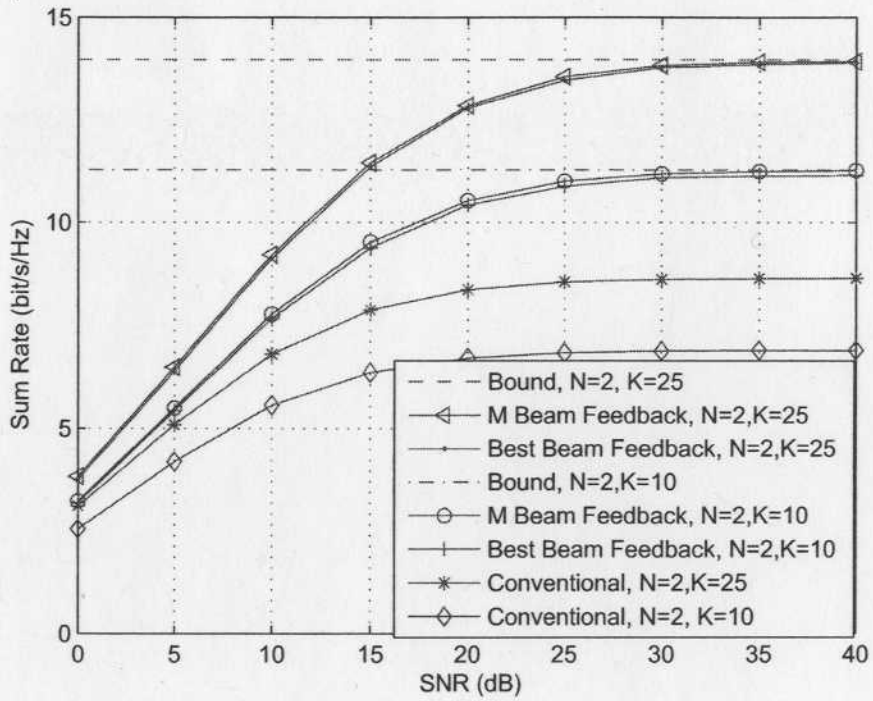

Figure 5.3: Sum-rate performance of RUB systems with OC scheme ($M = 4$).

Chapter 6

Vector Perturbation Precoding with Quantized Channel Feedback

To circumvent the problem of high computational complexity associated with DPC, many sub-optimal precoding techniques are proposed to mitigate multiuser interference. These techniques are categorized into two types: linear and non-linear precoding. In previous chapters, we focus on two popular linear precoding techniques, zero forcing beamforming and random unitary beamforming. In addition, with the knowledge of receiver noise variance, linear precoding based on minimum mean square error (MMSE) criterion is proposed in [70]. While sum-rate performance is an important criterion to evaluate a precoding scheme, symbol error error (SER) performance for a given modulation scheme is also of great interest and practical importance. With lower computational complexity, linear techniques generally suffer from a performance loss in terms of SER comparing to non-linear techniques including BLAST [67], vector perturbation (VP) precoding [72], Tomlinson-Harashima (TH) precoding [69, 71] and lattice-basis reduction precoding [73, 74]. Especially, it is proven in [74] that full diversity order equal to the number of transmit antennas is achieved by lattice-basis reduction and VP precoding.

In this chapter, we focus on the SER performance of VP precoding technique. With VP precoding, the transmitter reshapes the data vector with a perturbation vector (Tomlinson-Harashima coding [75, 76]) and generates the transmit vector by multiplying the perturbed data vector with a precoding matrix. By appropriately designing precoding matrix and perturbation vector, this technique can cancel mutual interference and reduce transmit power. In [72], with zero-forcing and regularized

zero-forcing precoding matrix, the authors propose to use the perturbation vector which minimizes the transmit power. In [77–79], joint optimal perturbation vector and precoding matrix under MMSE criterion are given.

Previous studies of VP precoding usually assume perfect CSI is available at the basestation, which is unrealistic in practice due to limited bandwidth of feedback channel. In this chapter, we study the effects of imperfect CSI on the SER performance of VP precoding. We assume that the imperfectness of CSI results from the channel quantization procedure, which is modeled following rate-distortion theory. A robust VP precoding scheme is proposed for quantized channel feedback. We establish equivalent relations in terms of MMSE and SER between VP precoding with quantized and perfect channel feedback. Based on the relations, we investigate how feedback load affects the SER performance of VP precoding.

The rest of the chapter is organized as follows. Section 6.1 consists of system model and introduction to VP precoding. In section 6.2, we describe channel quantization model and VP precoding based on MMSE criterion with quantized channel imformation. In section 6.3, we establish equivalent relations between VP precoding with quantized and perfect channel feedback. Some numerical examples and remarks are presented in section 6.4.

6.1 System Overview

6.1.1 Multiuser MIMO Transmission

We assume N_t antennas are used at the basestation in an multiuser MIMO system. The basestation transmits information to N_r non-cooperative single-antenna receivers simultaneously, where $N_r \leq N_t$. We denote the channel vector of receiver i as $\mathbf{h}_i = [h_{i1}, \ldots, h_{iN_t}]^T \in \mathbb{C}^{N_t}$, where h_{ij} indicates the channel gain between the jth transmit antenna and receiver i. The channel gain is assumed to be independent and identically distributed (i.i.d.) complex Gaussian random variables with zero mean and unitary variance.

Given a transmit vector $\mathbf{x} = [x_1, \ldots, x_{N_t}] \in \mathbb{C}^{N_t}$ over a time slot, the discrete-time complex baseband symbol received by user i is given by

$$y_i = \mathbf{h}_i^T \mathbf{x} + n_i, \tag{6.1}$$

where n_i is the zero-mean complex Gaussian noise with variance σ_n^2. With unit transmit power, the SNR is defined as

$$\rho_n = \frac{1}{\sigma_n^2}. \tag{6.2}$$

We denote the concatenation of the channel vectors by $H = [\mathbf{h}_1, \ldots, \mathbf{h}_{N_r}]^T$, i.e., $H \in \mathcal{C}^{N_r \times N_t}$, with the ith row being receiver i's channel vector. The N_r-dimensional received vector $\mathbf{y}$ is formed by stacking the received signals of all N_r receivers, i.e., $\mathbf{y} = [y_1, \ldots, y_{Nr}]^T$. Following from (6.1), the received vector can be expressed as

$$\mathbf{y} = H\mathbf{x} + \mathbf{n}, \tag{6.3}$$

where $\mathbf{n} = [n_1, \ldots, n_{N_r}]^T \in \mathbb{C}^{N_r}$ is the additive noise vector. Though (6.3) shares the same form as a point-to-point MIMO system, each receiver only has the knowledge of its own channel vector.

6.1.2 Vector Perturbation Precoding

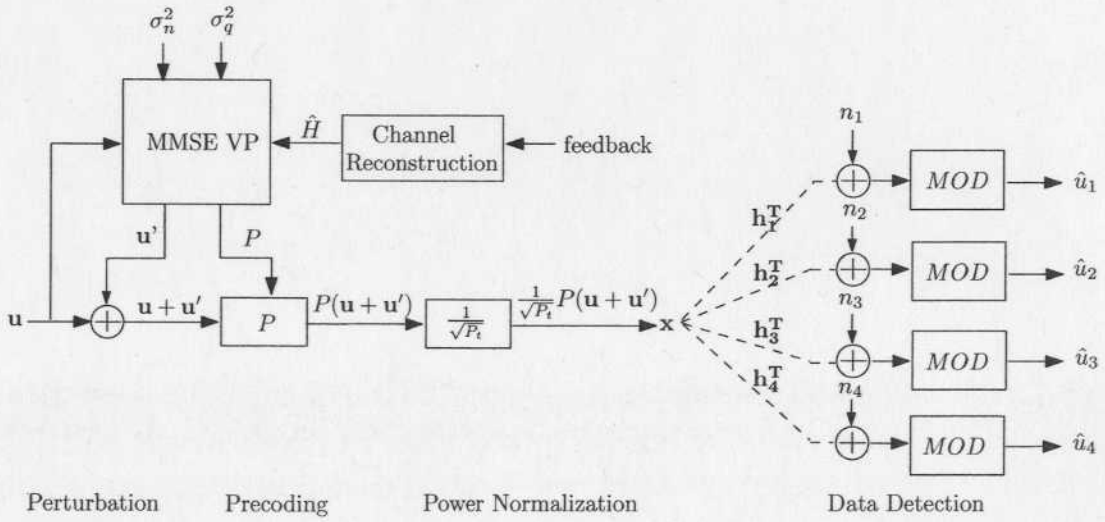

Figure 6.1: System Model of Vector Perturbation Precoding

The procedures of VP precoding are illustrated in Fig. 6.1. The *data vector* $\mathbf{u} = [u_1, \ldots, u_{N_r}]^T$ consists of data symbols to be transmitted to the N_r receivers. The data symbol u_i is for user i and is chosen from an M-ary square quadrature amplitude modulation (QAM) constellation $\mathcal{A}$, where the coordinates of the signal

points are odd numbers, i.e., $\mathcal{A} = \{a_I + a_Q | a_I, a_Q \in \pm 1, \pm 3, \ldots, \pm(\sqrt{M} - 1)\}$. The constellation is bounded by the square region of width $2\sqrt{M}$. To reduce the power of transmit vector, a *perturbation vector* $\mathbf{u}' \in \mathbb{C}^{N_r}$ is added to the data vector, resulting in a *perturbed data vector* as $\mathbf{u} + \mathbf{u}'$. Both real and imaginary parts of each element of $\mathbf{u}' = [u'_1, \ldots, u'_{N_r}]^T$ are integer times of a constant value τ, which is set as $\tau = 2\sqrt{M}$ in this work. For illustration purpose, the perturbation of a data symbol is shown in Fig. 6.2, where $M = 4$, $\tau = 4$, $u_i = (+1, +1)$, and $u'_i = (+4, +4)$ result in a perturbed symbol as (+5, +5).

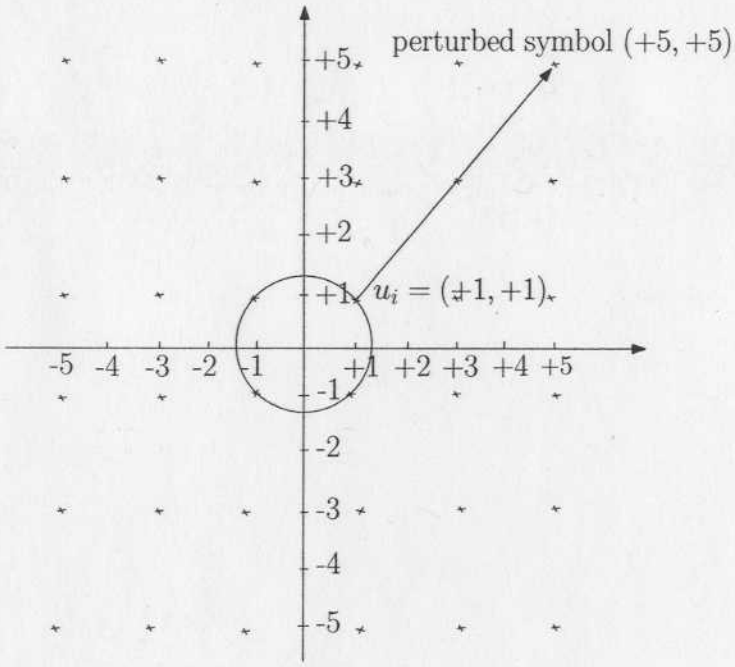

Figure 6.2: Data Symbol Perturbation

The *transmit vector* $\mathbf{x}$ is formed by multiplying perturbed data vector $\mathbf{u} + \mathbf{u}'$ with a $N_t \times N_r$ precoding matrix P and then being normalized to unit transmit power as

$$\mathbf{x} = \frac{1}{\sqrt{P_t}} P(\mathbf{u} + \mathbf{u}'), \tag{6.4}$$

where $P_t = \|P(\mathbf{u} + \mathbf{u}')\|^2$. Here, $\|\cdot\|$ stands for Euclidean norm. Substituting (6.4) into (6.3), the received vector can be written as

$$\mathbf{y} = \frac{1}{\sqrt{P_t}} HP(\mathbf{u} + \mathbf{u}') + \mathbf{n}. \tag{6.5}$$

Assuming that receivers know the scalar $\sqrt{P_t}$, receiver i estimates its data symbol u_i by performing a modulo operation on the scaled received symbol $\sqrt{P_t}y_i$. This operation translates $\sqrt{P_t}y_i$ into the range of original constellation $\mathcal{A}$ by adding a integer times of τ to its real and imaginary parts separately, which is expressed as

$$\hat{u}_i = \sqrt{P_t}y_i - \lfloor \frac{\mathrm{Re}(\sqrt{P_t}y_i)}{\tau} + \frac{1}{2} \rfloor \tau - j \lfloor \frac{\mathrm{Im}(\sqrt{P_t}y_i)}{\tau} + \frac{1}{2} \rfloor \tau, \tag{6.6}$$

where $\lfloor \cdot \rfloor$ means rounding to the nearest smaller integer. The transmitted symbol is then detected as the constellation point in $\mathcal{A}$ with nearest Euclidean distance.

6.1.3 Optimal Design with MMSE

From (6.5), we define a *deviation vector*, which measures the distortion of the scaled received vector $\sqrt{P_t}\mathbf{y}$ from perturbed data vector $\mathbf{u} + \mathbf{u}'$, as

$$\mathbf{d} = \sqrt{P_t}\mathbf{y} - (\mathbf{u} + \mathbf{u}') = (HP - I_{N_r})(\mathbf{u} + \mathbf{u}') + \sqrt{P_t}\mathbf{n}, \tag{6.7}$$

where I_{N_r} is a identity matrix of size $N_r \times N_r$. Given data vector $\mathbf{u}$ and channel realization H, the MSE as a function of $\mathbf{u}'$ and P is expressed as

$$\begin{aligned} e(\mathbf{u}', P) &= \mathbb{E}_{\mathbf{n}}(\|\mathbf{d}\|^2 | H, \mathbf{u}) \\ &= \|(HP - I_{N_r})(\mathbf{u} + \mathbf{u}')\|^2 + N_r P_t \sigma_n^2, \end{aligned} \tag{6.8}$$

where $\mathbb{E}_{\mathbf{n}}(\cdot)$ means taking the expectation over $\mathbf{n}$. The optimal precoding matrix that minimizes (6.8) is found to be [78]

$$P_{o,\ mmse} = H^H \left(HH^H + N_r \sigma_n^2 I_{N_r}\right)^{-1}. \tag{6.9}$$

The optimal perturbation vector can be obtained as

$$\mathbf{u}'_{o,\ mmse} = \arg_{\mathbf{u}'} \min N_r \sigma_n^2 (\mathbf{u} + \mathbf{u}')^H \left(HH^H + N_r \sigma_n^2 I_{N_r}\right)^{-1} (\mathbf{u} + \mathbf{u}'), \tag{6.10}$$

and the achieved MMSE with $\mathbf{u}' = \mathbf{u}'_{o,\ mmse}$ is equal to

$$e_{o,\ mmse} = N_r \sigma_n^2 (\mathbf{u} + \mathbf{u}'_{o,\ mmse})^H \left(HH^H + N_r \sigma_n^2 I_{N_r}\right)^{-1} (\mathbf{u} + \mathbf{u}'_{o,\ mmse}). \tag{6.11}$$

6.2 Vector Perturbation with Quantized Channel Feedback

6.2.1 Channel Quantization Model

In practical systems, receiver i can only feed back limited amount of information on its channel vector to the basestation, based on which the basestation tries to reconstruct $\mathbf{h}_i$. The reconstructed channel vector at the basestation is called *quantized channel vector* and is denoted as $\hat{\mathbf{h}}_i = [\hat{h}_{i1}, \ldots, \hat{h}_{iN_t}] \in \mathbb{C}^{N_t}$. The average squared-error distortion between $\mathbf{h}_i$ and $\hat{\mathbf{h}}_i$ is defined as

$$D = \mathbb{E}_{\hat{\mathbf{h}}_i, \mathbf{h}_i}(\|\hat{\mathbf{h}}_i - \mathbf{h}_i\|^2) \tag{6.12}$$

Since feedback information aims at reducing the uncertainty of $\mathbf{h}_i$ at the basestation, we define *feedback load* as the amount of reduced uncertainty of $\mathbf{h}_i$ when using $\hat{\mathbf{h}}_i$ to represent it, which is equal to $\mathcal{I}(\mathbf{h}_i, \hat{\mathbf{h}}_i)$, the mutual information between $\mathbf{h}_i$ and $\hat{\mathbf{h}}_i$.

Given a constraint D on the average distortion, the lower bound of feedback load, denoted as $R(D)$, can be expressed as

$$R(D) = \min_{f_{\hat{\mathbf{h}}_i|\mathbf{h}_i}(\hat{\mathbf{h}}_i|\mathbf{h}_i):\ \mathbb{E}_{\hat{\mathbf{h}}_i, \mathbf{h}_i}(\|\hat{\mathbf{h}}_i - \mathbf{h}_i\|^2) \leq D} \mathcal{I}(\mathbf{h}_i, \hat{\mathbf{h}}_i) \tag{6.13}$$

where $f_{\hat{\mathbf{h}}_i|\mathbf{h}_i}(\hat{\mathbf{h}}_i|\mathbf{h}_i)$ denotes the conditional PDF of $\hat{\mathbf{h}}_i$ given $\mathbf{h}_i$. Following the rate distortion theory, $R(D)$ is given by [3]. This bound can only be approached in practice and vector quantization may be employed to reduce the feedback load.

$$R(D) = N_t \log_2 \frac{N_t}{D}, \quad D \leq N_t. \tag{6.14}$$

Equality is achieved only when the following two conditions are met:

1. N_t elements of $\mathbf{h}_i$ are quantized independently with each element having a distortion constraint of D/N_t. For convenience, we let $\sigma_q^2 = D/N_t$ and term it as *quantization noise power*.

2. $\hat{h}_{ij}$ and $\Delta h_{ij} = h_{ij} - \hat{h}_{ij}$ are independent random variables following independent zero-mean complex Gaussian distribution with variance $1 - \sigma_q^2$ and σ_q^2, respectively.

Since receivers quantize their channel vectors separately, the quantized channel vectors and quantization noise vectors of different receivers are independent. The *quantized channel matrix* $\hat{H} \in \mathbb{C}^{N_r \times N_t}$ is formed as $\hat{H} = [\hat{\mathbf{h}}_1, \ldots, \hat{\mathbf{h}}_{N_r}]^T$. The *quantization noise matrix* $\Delta H \in \mathbb{C}^{N_r \times N_t}$ is defined as the difference between H and $\hat{H}$

$$\Delta H = H - \hat{H}. \tag{6.15}$$

With the same quantization noise power constraints for all receivers, the *signal to quantization noise power ratio* (SQR) is equal to

$$\rho_q = \frac{1}{\sigma_q^2}. \tag{6.16}$$

6.2.2 MMSE-based Design

Assuming the basestation has the following partial CSI: quantized channel matrix $\hat{H}$, quantization noise power σ_q^2, and additive noise power σ_n^2, we consider the joint design of precoding matrix and perturbation vector associated with VP precoding based on MMSE criterion.

With arbitrary precoding matrix $\hat{P}$ and perturbation vector $\hat{\mathbf{u}}'$, the received signal vector can be written as

$$\mathbf{y} = \frac{1}{\sqrt{\hat{P}_t}} H\hat{P}(\mathbf{u} + \hat{\mathbf{u}}') + \mathbf{n}, \tag{6.17}$$

where $\hat{P}_t = \|\hat{P}(\mathbf{u} + \hat{\mathbf{u}}'\|^2$. Substituting (6.15) into (6.17) , we have

$$\mathbf{y} = \frac{1}{\sqrt{\hat{P}_t}}\big((\mathbf{u} + \hat{\mathbf{u}}') + (\hat{H}\hat{P} - I_{N_r})(\mathbf{u} + \hat{\mathbf{u}}') + \Delta H\hat{P}(\mathbf{u} + \hat{\mathbf{u}}')\big) + \mathbf{n}. \tag{6.18}$$

The deviation vector is obtained as

$$\begin{aligned} \mathbf{d} &= \sqrt{\hat{P}_t}\mathbf{y} - (\mathbf{u} + \hat{\mathbf{u}}') \\ &= (\hat{H}\hat{P} - I_{N_r})(\mathbf{u} + \hat{\mathbf{u}}') + \Delta H\hat{P}(\mathbf{u} + \hat{\mathbf{u}}') + \sqrt{\hat{P}_t}\mathbf{n}. \end{aligned} \tag{6.19}$$

Given data vector $\mathbf{u}$ and quantized channel matrix $\hat{H}$, the MSE as a function of $\hat{P}$

and $\hat{\mathbf{u}}'$ is obtained by taking expectation taken over $\mathbf{n}$ and ΔH as

$$\begin{aligned} & e(\hat{P}, \hat{\mathbf{u}}') \\ &= \mathbb{E}_{\mathbf{n},\Delta H}(\|\mathbf{d}\|^2 | \mathbf{u}, \hat{H}) \\ &= \|(\hat{H}\hat{P} - I_{N_r})(\mathbf{u} + \hat{\mathbf{u}}')\|^2 + N_r \hat{P}_t(\sigma_q^2 + \sigma_n^2). \end{aligned} \tag{6.20}$$

A comparison between (6.8) and (6.20) shows that optimization problems of MMSE VP precoding with quantized and perfect channel feedback share a similar form. It follows that the optimal precoding matrix is given by

$$\hat{P}_{o,\ mmse} = \hat{H}^H \big(\hat{H}\hat{H}^H + N_r(\sigma_q^2 + \sigma_n^2) I_{N_r}\big)^{-1}. \tag{6.21}$$

The optimal perturbation vector can be found with

$$\begin{aligned} \hat{\mathbf{u}}'_{o,\ mmse} = \arg_{\hat{\mathbf{u}}'} \min\, & N_r(\sigma_q^2 + \sigma_n^2)(\mathbf{u} + \hat{\mathbf{u}}')^H \times \\ & \big(\hat{H}\hat{H}^H + N_r(\sigma_q^2 + \sigma_n^2) I_{N_r}\big)^{-1} (\mathbf{u} + \hat{\mathbf{u}}'). \end{aligned} \tag{6.22}$$

Substituting $\hat{\mathbf{u}}'_{o,\ mmse}$ and $\hat{P}_{o,\ mmse}$ into (6.20) leads to the MMSE as

$$\begin{aligned} \hat{e}_{o,mmse} = & N_r(\sigma_q^2 + \sigma_n^2)(\mathbf{u} + \hat{\mathbf{u}}'_{o,\ mmse})^H \times \\ & \big(\hat{H}\hat{H}^H + N_r(\sigma_q^2 + \sigma_n^2) I_{N_r}\big)^{-1} (\mathbf{u} + \hat{\mathbf{u}}'_{o,\ mmse}). \end{aligned} \tag{6.23}$$

It is worthwhile to make some remarks on the results we have derived for VP with quantized channel feedback.

1. Based on MMSE criterion, the precoding matrix and perturbation vector depend only on partial CSI, i.e., $\hat{H}$, σ_q^2 and σ_n^2.

2. (6.23) shows that quantization error always deteriorates MMSE performance and appropriately selected perturbation vector and precoding matrix result in a simultaneous reduction of MSE incurred by both quantization and additive noise.

3. The search of optimal perturbation vector $\mathbf{u}'_o$ using (6.10) and (6.22) is a well-known $2K$-dimensional closest-lattice-point search problem. It can be performed with sphere decoding algorithm [85, 86], which achieves the the maximum likelihood solution. Many sub-optimal algorithms like lattice-basis re-

duction [87–89] may also be used to find approximation solutions with lower complexity.

6.3 Analysis

In this section, we first establish equivalent relations between quantized and perfect channel feedback cases in terms of MMSE and SER. Based on the equivalent relations, we then develop a feedback scaling rule to ensure full diversity order for VP precoding with quantized channel feedback.

6.3.1 MMSE Equivalence between Quantized and Perfect Channel Feedback Cases

Lemma 2. *The MMSE of VP precoding with quantized channel feedback with quantization noise power σ_q^2 and additive noise power σ_n^2 is equal to that of perfect channel feedback with additive noise power $\frac{\sigma_n^2+\sigma_q^2}{1-\sigma_q^2}$.*

Proof. From channel quantization model, we know that $\hat{H}$ has the same distribution as H except its elements having a reduced variance of $1-\sigma_q^2$. Define a new random matrix as

$$\tilde{H} = \frac{1}{\sqrt{1-\sigma_q^2}}\hat{H}, \tag{6.24}$$

which has the same distribution as H. Eq. (6.22) can be rewritten in terms of $\tilde{H}$ as

$$\hat{\mathbf{u}}'_{o,\ mmse} = \arg_{\hat{\mathbf{u}}'} \min N_r \frac{\sigma_q^2+\sigma_n^2}{1-\sigma_q^2}(\mathbf{u}+\hat{\mathbf{u}}')^H \times \left(\tilde{H}\tilde{H}^H + N_r\frac{\sigma_q^2+\sigma_n^2}{1-\sigma_q^2}I_{N_r}\right)^{-1}(\mathbf{u}+\hat{\mathbf{u}}'). \tag{6.25}$$

Solution of Eq. (6.25) is the same as that of perfect channel feedback with channel matrix $\tilde{H}$, data vector $\mathbf{u}$ and additive noise power $\frac{\sigma_q^2+\sigma_n^2}{1-\sigma_q^2}$, which in turn leads to an identical MMSE. □

6.3.2 SER Equivalence between Quantized and Perfect Feedback

Treating all receivers equally, the SER of a multiuser MIMO system is defined as the average SER of all receivers. Let $e(\sigma_n^2, \sigma_q^2)$ denote the SER of VP precoding with quantization noise power σ_q^2 and additive noise power σ_n^2. Note that $\sigma_q^2 = 0$ corresponds to the SER with perfect channel feedback.

Lemma 3. *The SER of VP precoding with quantized channel feedback with quantization noise power σ_q^2 and additive noise power σ_n^2 is equal to that of perfect channel feedback with additive noise power $\frac{\sigma_n^2+\sigma_q^2}{1-\sigma_q^2}$, namely*

$$e(\sigma_n^2, \sigma_q^2) = e\left(\frac{\sigma_n^2 + \sigma_q^2}{1 - \sigma_q^2}, 0\right). \tag{6.26}$$

Proof. Firstly, given $\hat{H}$ and $\mathbf{u}$, we show that deviation vectors of the following two cases follow the same distribution. The first case is quantized channel feedback with quantization noise power σ_q^2 and additive noise power σ_n^2. The second case is perfect channel feedback with channel matrix $\tilde{H}$ and additive noise power $\frac{\sigma_q^2+\sigma_n^2}{1-\sigma_q^2}$. Here, $\tilde{H}$ is related to $\hat{H}$ as given by (6.24).

For case 1, the deviation vector can be obtained from (6.19) by replacing $\hat{P}$ with the optimal precoding matrix $\hat{P}_{o,\ mmse} = \hat{H}^H\left(\hat{H}\hat{H}^H + N_r(\sigma_q^2 + \sigma_n^2)I_{N_r}\right)^{-1}$ as

$$\begin{aligned}\mathbf{d}_1 = &\underbrace{(\hat{H}\hat{P}_{o,\ mmse} - I_{N_r})(\mathbf{u} + \hat{\mathbf{u}}')}_{\text{part 1}} \\ &+ \underbrace{\Delta H \hat{P}_{o,\ mmse}(\mathbf{u} + \hat{\mathbf{u}}') + \|\hat{P}_{o,\ mmse}(\mathbf{u} + \hat{\mathbf{u}}')\|\mathbf{n}_1}_{\text{part 2}}.\end{aligned} \tag{6.27}$$

Since Case 2 uses (6.25) to search for the perturbation vector, the result remains the same as that of Case 1 and is still denoted as $\hat{\mathbf{u}}'$. Substituting $P_{o,\ mmse} = \tilde{H}^H\left(\tilde{H}\tilde{H}^H + N_r\frac{\sigma_q^2+\sigma_n^2}{1-\sigma_q^2}I_{N_r}\right)^{-1}$ into (6.7) yields the deviation vector of case 2 as

$$\mathbf{d}_2 = \underbrace{(\tilde{H}P_{o,\ mmse} - I_{N_r})(\mathbf{u} + \mathbf{u}')}_{\text{part 1}} + \underbrace{\|P_{o,\ mmse}(\mathbf{u} + \mathbf{u}')\|\mathbf{n}_2}_{\text{part 2}}. \tag{6.28}$$

Using (6.24), we have $\hat{P}_{o,\ mmse} = \frac{1}{\sqrt{1-\sigma_q^2}}P_{o,\ mmse}$. It follows that Part 1 of (6.27) and (6.28) are equal.

For convenience, we let $c = \|\hat{P}_{o,\ mmse}(\mathbf{u}+\mathbf{u}')\|^2 = \frac{1}{1-\sigma_q^2}\|P_{o,\ mmse}(\mathbf{u}+\mathbf{u}')\|^2$. Since elements of ΔH and $\mathbf{n}_1$ are i.i.d. Gaussian random variables with variance σ_q^2 and σ_n^2, respectively, it can be shown that elements of part 2 of (6.27) are i.i.d. Gaussian random variables with variance $c(\sigma_n^2+\sigma_q^2)$. Similarly, noting that elements of $\mathbf{n}_2$ has variance $\frac{\sigma_n^2+\sigma_q^2}{1-\sigma_q^2}$, part 2 of (6.28) can be proven to have the same distribution as that of (6.27).

Since deviation vector determines the number of wrongly detected symbols, case 1 and case 2 achieve the same SER. Furthermore, because the mapping between $\hat{H}$ and $\tilde{H}$ is one to one, the achieved SER after averaging over the distribution of $\hat{H}$ and $\tilde{H}$ will also be equal. □

Table 6.1: SER for different SNR and SQR with VP precoding ($Nt = Nr = M = 4, 10^5$ simulations)

SQR\SNR	5 dB	10 dB	20 dB
5 dB	0.3707 (0.3712)	0.3055 (0.3049)	0.2654 (0.2656)
10 dB	0.2615 (0.2620)	0.1436 (0.1437)	0.0662 (0.0666)
20 dB	0.2056 (0.2059)	0.0586 (0.0584)	4.6e-4 (4.6e-4)

Table 6.1 gives the simulation results of the SER performance of VP precoding with quantized channel feedback and its equivalent perfect channel feedback, whose data is in the parenthesis. The close match between the two sets of data verifies the equivalent relation given by (6.26).

6.3.3 Feedback Load and SER Performance

As an application of the equivalent relations, we investigate the tradeoff between feedback load and SER performance. For VP precoding with perfect channel feedback, it is proved in [74] that full diversity order of N_t is achieved, namely

$$\lim_{\rho_n\to\infty} \frac{-\log(e\,(\sigma_n^2,0))}{\log(\rho_n)} = \lim_{\sigma_n^2\to 0} \frac{\log(e\,(\sigma_n^2,0))}{\log(\sigma_n^2)} = N_t. \tag{6.29}$$

With quantized channel feedback, how much feedback load is required to obtain the same precoding diversity order is of particular interest. The following lemma answers this question.

Lemma 4. *In order to achieve the same diversity order as perfect channel feedback, VP precoding with quantized channel feedback has to increase each user's feedback load by at least $3.32N_t$ bits for every 10 dB increase in SNR.*

Proof. Let the feedback load increase with SNR at a rate such that

$$\sigma_q^2 = k(\sigma_n^2)^\alpha + o(\sigma_n^2), \tag{6.30}$$

where k is a constant and $\alpha \in \mathbb{R}$ is the lowest power within the polynomial, namely

$$\lim_{\sigma_n^2 \to 0} \frac{o(\sigma_n^2)}{(\sigma_n^2)^\alpha} = 0. \tag{6.31}$$

From (6.29), we can express the SER with perfect channel feedback as

$$\log\left(e(\sigma_n^2, 0)\right) = N_t \log(\sigma_n^2) + o(\log\left(\sigma_n^2\right)), \tag{6.32}$$

where

$$\lim_{\sigma_n^2 \to 0} \frac{o(\log\left(\sigma_n^2\right))}{\log(\sigma_n^2)} = 0. \tag{6.33}$$

Using (6.26), (6.32), and (6.30), we have

$$\log\left(e(\sigma_n^2, \sigma_q^2)\right) = N_t \log\left(\frac{\sigma_n^2 + k(\sigma_n^2)^\alpha + o(\sigma_n^2)}{1 - k(\sigma_n^2)^\alpha - o(\sigma_n^2)}\right) + o\left(\log\left(\frac{\sigma_n^2 + k(\sigma_n^2)^\alpha + o(\sigma_n^2)}{1 - k(\sigma_n^2)^\alpha - o(\sigma_n^2)}\right)\right)$$

The diversity order can be determined as

$$\lim_{\sigma_n^2 \to 0} \frac{\log e(\sigma_n^2, \sigma_q^2)}{\log(\sigma_n^2)} = \begin{cases} N_t & \alpha \geq 1 \\ \alpha N_t & 0 \leq \alpha < 1 \end{cases} \tag{6.34}$$

Therefore, we have to keep $\sigma_q^2 = k(\sigma_n^2)$ in order to achieve full diversity order. Combined with (6.14), we obtain a simple relation between feedback load and SNR

$$R(D) = N_t \left(\log_2(\rho) - \log_2(k)\right), \tag{6.35}$$

which reveals that we need an extra $3.32N_t$ bits per user for every 10 dB increase in SNR to achieve full diversity order. □

6.4 Numerical Examples

In this section, we present some simulation results on the SER performance of VP precoding with quantized channel feedback. We use $N_t = N_r = 4$, $M = 4$ in the simulations.

Fig. 6.3 shows the SER performance of different precoding schemes with SQR=15 dB. Comparing to linear precoding schemes (ZF and MMSE), VP can achieve much better performance. This is because perturbation vector reduces the transmit power and mean square error simultaneously. In addition, with the knowledge of both quantization and additive noise power, MMSE VP has a better SER performance than that of the regularized MMSE, which is designed assuming basestation only has the knowledge of additive noise power and arbitrarily setting $\sigma_q^2 = 0$ regardless of its true value. ZF VP, which requires neither quantization nor additive noise power is shown to be suboptimal than MMSE VP and regularized MMSE. Therefore, with VP, the more knowledge we have about quantization and additive noise power, the better SER performance we can achieve. With a fixed SQR, there exists lower bounds for all precoding schemes. However, the bounds are different, which illustrate the capability of different schemes combatting quantization noise. Again, the best lower bound is shown to be achieved with MMSE VP.

In Fig. 6.4, we plot the SER of VP precoding as a function of SNR for different feedback schemes. With a fixed feedback load corresponding to SQR=17 dB, the SER performance becomes quantization-noise-limited at high SNR region. Moreover, its SER floor is shown to be approximately the SER of perfect channel feedback with SNR=17 dB. When the feedback load is adjusted in a way such that $\sigma_q^2 = \sigma_n^2$, SER is shown to decrease at the same rate as perfect channel feedback at high SNR region. Therefore, full diversity order is achieved with this feedback scheme. As expected, the performance gap between quantized channel feedback with $\sigma_q^2 = \sigma_n^2$ and perfect channel feedback is about 3 dB at high SNR. On the other hand, SER performance of feedback schemes, whose quantization noise power decrease at rates $(\sigma_n^2)^{\frac{2}{3}}$ and $(\sigma_n^2)^{\frac{1}{2}}$, can not achieve the same diversity order.

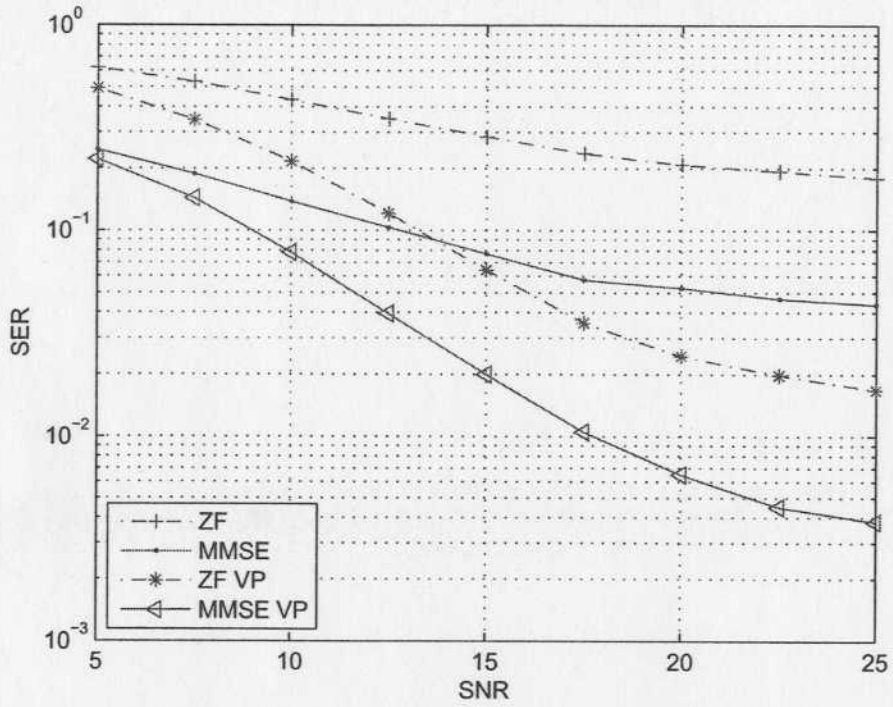

Figure 6.3: SER versus SNR with SQR=15 dB.

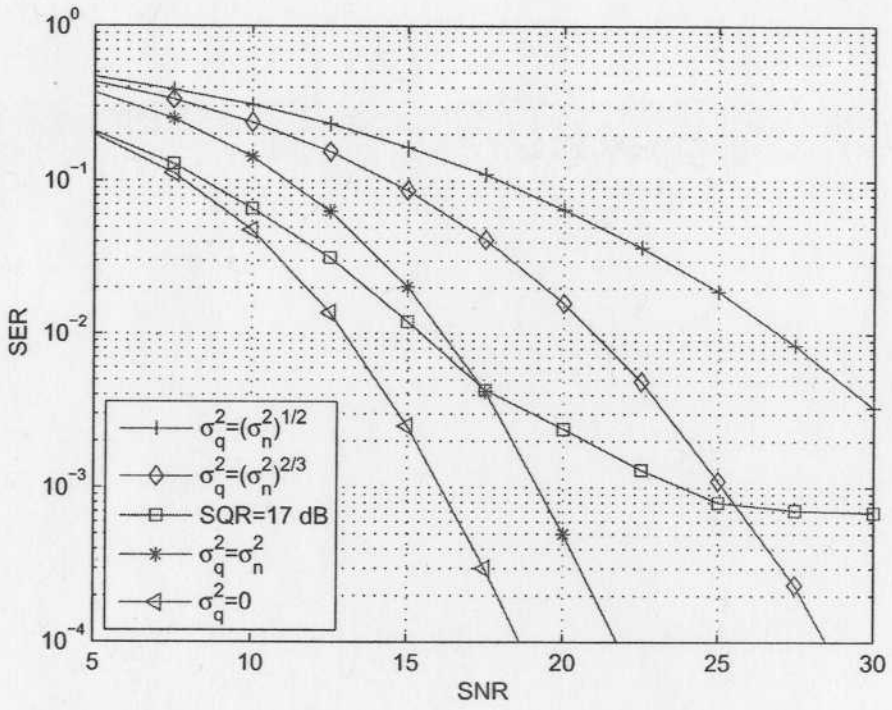

Figure 6.4: SER versus SNR with different feedback load.

Chapter 7

Conclusions

7.1 Summary

In this work, we focused on performance evaluation and enhancement of multiuser MIMO systems while assuming channel gain follows Rayleigh flat fading.

In Chapter 2, we analyzed the sum-rate performance of multiuser MIMO systems with ZFBF for dual-transmit-antenna single-receive-antenna case. Two low-complexity user selection schemes, GWC-ZFBF and SUP-ZFBF, are considered. With the analytical expressions developed, we studied the effects of directional constraint used in user selection process on system sum rate. Through selected numerical examples, we demonstrate that the sum rate of SUP-ZFBF is not sensitive to λ_d unless it is close to one and that GWC-ZFBF with optimal λ_d approaches the performance of SUP-ZFBF with lower computational complexity.

In Chapter 3, we presented an exact analysis of the sum rate of multiuser MIMO systems with RUB. Using the derived analytical expressions, we studied the effects of several system parameters on sum rate. Although noise power is the main factor that affects the sum rate when SNR is low, its effects become negligible at high SNR region, where the data rate on a beamforming direction is determined primarily by the angle between the beamforming vector and the channel vector of the user assigned to it. The interference-limited sum rate can be improved by either increasing the number of users in the system or reducing the number of transmit antennas.

In Chapter 4, we proposed a new user scheduling strategy for the RUB-based multiuser MIMO systems, namely the ABA-CBBI scheme. With the ABA-CBBI scheme, the system imposes a threshold on user's best beam SINR and only activates

those beams that are requested by feedback users. With these two simple but effective mechanisms, the resulting multiuser MIMO systems will not only entail low average feedback load requirement, but also suffer less multiuser interference over high SNR region. We carried accurate statistical analysis on the resulting systems and developed the exact analytical expression for the system sum-rate capacity. We show through selected numerical examples that, with the optimal thresholds, ABA-CBBI strategy can achieve better sum-rate performance than existing strategies, such as BBSI [15] and CBBI [36], over high SNR region while maintaining low average feedback load. We further notice that the double benefits of better performance and low feedback load of the ABA-CBBI scheme come at the costs of determining the optimal feedback thresholds and serving less users simultaneously over high SNR region.

In Chapter 5, we studied the sum-rate performance improvement for RUB-based multiuser MIMO systems with SC and OC diversity combining schemes at the receivers. The resulting systems have the same low feedback load as single-antenna-per-user case. We derived an accurate analytical expression of the sum rate for SC scheme and obtained upper bounds over high SNR region for OC scheme. These analytical results are applied to the tradeoff analysis between different system parameters. We observe, through selected numerical examples, that the OC scheme effectively explores the receive diversity and considerably improve the sum-rate performance with no requirement of additional feedback load.

In Chapter 6, we studied the VP precoding with quantized channel feedback. Based on the MMSE criterion, we considered a joint optimal design of precoding matrix and perturbation vector. We modeled channel vector quantization following the rate-distortion theory, based on which we established an equivalent relation between the SER of VP precoding with quantized and perfect channel feedback. This equivalent relation can be conveniently used to evaluate the SER performance of VP precoding with quantized channel feedback relative to that of perfect channel feedback. Applying the equivalent relation, we investigated the tradeoff between SER performance and feedback load. We show that feedback load per user should scale at $N_t \log_2(\rho)$ to achieve full diversity order.

7.2 Future Directions

With imperfect CSI, the sum-rate and SER performance of MIMO broadcast channels deteriorate due to extra multiuser interference caused by uncertainty of channel

conditions at the basestation. Consequently, there is a great interest in interference suppression techniques. Previous methods to mitigate the multiuser interference include reducing channel quantization error by increasing feedback load [80], exploiting multiuser diversity [15] and/or receive diversity [55,81,82] and designing robust precoding schemes [83,84]. Through this study, we identify the following possible future research directions.

7.2.1 Relation between Feedback Load and QoS Requirements

Progressive refinement of channel feedback is proposed in [92]. The basic idea is to refine the CSI at basestation by feeding back the CSI incrementally. Yet, in practical communications systems, feedback will decrease the spectral efficiency and thus data throughput. At high SNR, while progressive refinement helps improve the QoS performance including SER and throughput, it is not required any more once a certain target SINR is reached. This is because each user usually only needs to meet the minimum QoS requirement determined by its type of service (voice, data, video, etc.). On the other hand, progressive refinement may not contribute at low SNR since noise is the bottleneck to QoS performance improvement. Therefore, we are interested in how to minimize the feedback load when targeting at a certain QoS requirement.

7.2.2 BER Based Multimode Transmission

In Chapter 4, we proposed to adaptively turn off beams to increase the sum rate for MIMO broadcast channels with RUB. For both RUB and ZFBF with quantized channel feedback, imperfect CSI at the basestation causes multiuser interference and degrades BER performance. Since BER is another criterion commonly used for performance evaluation, we hope to study how to change the number of served users so that BER requirements can be met. We will apply the same idea as described in Chapter 4. When BER requirements can not be met, we propose to reduce the number of served users at a time. In this way, multiuser interference shall be reduced and thus BER performance of remaining served users can be improved.

7.2.3 Antenna Combining for MIMO Broadcast Channel with Limited Feedback

Practical partial CSI models including shape feedback and limited feedback are proposed for MIMO broadcast channels in [91]. For those precoding schemes like zero-forcing beamforming, Jindal in [81] propose to align a user's effective channel vector to the codevector when it is employed with more than one antenna. For VP precoding, however, not only channel direction but also magnitude has a impact on the performance. Therefore, we plan to adopt limited feedback model and study the antenna combining criterion for such a case under the constraint of feedback load.

7.2.4 Effects of Doppler Spread on User Scheduling

In mobile communications systems, the speed of mobile users vary from one to another. Therefore, with the same feedback delay, it is expected that channel deviation between the feedback and instantaneous channel will also differ among users. If we group high- and low-mobility users together and apply ZFBF, the big channel deviation of the high mobility users will deteriorate the performance of the low mobility users. It is therefore of interest to study 1) how to schedule users when taking their Doppler spread into account, and 2) how to handle large channel deviation of high-mobility users.

Appendix A

Proof of (4.13) being equal to (4.14)

We prove by induction. It is easy to verify it is true for $i = 1$. Assume that it is true for all $1 \leq i \leq m-1$, then we have

$$\Pr[M_a = i | N_f = k] = \frac{1}{M^k}\binom{M}{i} \cdot \sum_{q=1}^{i}(-1)^{i-q}\binom{i}{q}q^k, \; i = 1, 2, \cdots, m-1. \tag{A.1}$$

We now consider $i = m$. From (4.13), we have

$$\Pr[M_a = m | N_f = k] = \binom{M}{m}\left\{\left(\frac{m}{M}\right)^k - \sum_{j=1}^{m-1}\binom{m}{j}\frac{\Pr[M_a = j | N_f = k]}{\binom{M}{j}}\right\}. \tag{A.2}$$

Substituting $(A.1)$ into $(A.2)$, we have

$$
\begin{aligned}
&\Pr[M_a = m | N_f = k] \\
&= \frac{1}{M^k}\binom{M}{m}\left\{m^k - \sum_{j=1}^{m-1}\binom{m}{j}\sum_{q=1}^{j}(-1)^{j-q}\binom{j}{q}q^k\right\} \\
&\overset{(a)}{=} \frac{1}{M^k}\binom{M}{m}\left\{m^k - \sum_{q=1}^{m-1}\left\{\sum_{j=q}^{m-1}(-1)^j\binom{m}{j}\binom{j}{q}\right\}(-1)^q q^k\right\} \\
&\overset{(b)}{=} \frac{1}{M^k}\binom{M}{m}\left\{m^k - \sum_{q=1}^{m-1}\left\{\sum_{j=q}^{m-1}(-1)^j\binom{m-q}{j-q}\right\}(-1)^q\binom{m}{q}q^k\right\} \\
&\overset{(c)}{=} \frac{1}{M^k}\binom{M}{m}\left\{m^k - \sum_{q=1}^{m-1}\left\{\sum_{j=0}^{m-q-1}(-1)^j\binom{m-q}{j}\right\}\binom{m}{q}q^k\right\} \\
&\overset{(d)}{=} \frac{1}{M^k}\binom{M}{m}\left\{m^k + \sum_{q=1}^{m-1}(-1)^{m-q}\binom{m}{q}q^k\right\} \\
&= \frac{1}{M^k}\binom{M}{m}\left\{\sum_{q=1}^{m}(-1)^{m-q}\binom{m}{q}q^k\right\}
\end{aligned}
$$

where

(a) follows by change order of summation.

(b) follows since $\binom{m}{j}\binom{j}{q} = \binom{m}{q}\binom{m-q}{j-q}$, which can be proven by direct calculation.

(c) follows by the change of variable.

(d) follows from the formula $\sum_{j=0}^{m}(-1)^j\binom{m}{j} = 0$, which results from the binomial expansion of $(1-1)^m$.

Therefore, for the case of $i = m$, the claim is also true and thus the proof is complete.

Bibliography

[1] E. Telatar, "Capacity of multi-antenna Gaussian channels," *Eur. Trans. Telecommun.*, vol. 10, pp. 585–598, Nov. 1999.

[2] G. J. Foschini and M. J. Gans, "On limits of wireless communications in a fading environment when using multiple antennas," *Wireless Pers. Commun.*, vol. 6, pp. 311–335, Mar. 1998.

[3] T. Cover, "Broadcast channels," *IEEE Trans. Inform. Theory*, vol. IT-18, no.1, pp.2–14, Jan. 1972.

[4] P. Bergman, "Random coding theorem for broadcast channels with degraded components", *IEEE Trans. Inform. Theory*, vol. IT-19, no.3, pp.197–207, Mar. 1973.

[5] G. Caire and S. Shamai, "On the achievable throughput of a multiantenna Gaussian broadcast channel", *IEEE Trans. Inf. Theory*, vol. 49, no. 7, pp. 1691–1706, Jul. 2003.

[6] H. Sato, "An outer bound to the capacity region of broadcast channels," *IEEE Trans. Inf. Theory*, vol. IT-24, pp. 374–377, May 1978.

[7] N. Jindal and A. Goldsmith, "Dirty paper coding vs. TDMA for MIMO broadcast channels," *Proc. IEEE Int. Conf. Commun.* (ICC'2004), Paris, France, vol. 2, pp. 682–686, Jun. 2004.

[8] M. Sharif and B. Hassibi, "A comparison of time-sharing, DPC, and bemforming for MIMO broadcast channels with many users," *IEEE Trans. Commun.*, vol. 55, no. 1, pp. 11–15, Jan. 2007.

[9] M. Costa, "Writing on dirty paper," *IEEE Trans. Inf. Theory*, vol. 29, pp. 439–441, May 1983.

[10] U. Erez, S. Shamai, and R. Zamir, "Capacity and lattice strategies for canceling known inteference," *IEEE Trans. Inf. Theory*, vol. 51, no. 11, pp. 3820–3833, Nov. 2005.

[11] H. Weingarten, Y. Steinberg, and S. Shamai, "The capacity region of the Gaussian MIMO broadcast channel", in *Proc. IEEE ISIT* (ISIT'04), Jul. 2004, p. 174.

[12] P. Viswanath and D. N. Tse,"Sum capacity of the vector Gaussian broadcast channel and downlink-uplink duality", *IEEE Trans. Inf. Theory*, vol. 49, no. 8, pp. 1912–1921, Aug. 2003.

[13] W. Yu and J. Cioffi, "Sum capacity of Gaussian vector broadcast channels", *IEEE Trans. Inf. Theory*, vol. 52, no. 2, pp. 754–759, Feb. 2006.

[14] S. Vishwanath, N. Jindal and A. Goldsmith, "Duality, achievable rate and sum-rate capacity of Gaussian MIMO broadcast channels", *IEEE Trans. Inform. Theory*, vol. 49, no. 10, pp. 2659–2668, Oct. 2003.

[15] M. Sharif, and B. Hassibi, "On the capacity of MIMO broadcast channels with partial side information", *IEEE Trans. Inform. Theory*, Vol. 51, no. 2, pp. 506–522, February 2005.

[16] W. Rhee, W. Yu, and J. M. Cioffi, "The optimality of beamforming in uplink multiuser wireless systems," *IEEE Trans. Wireless Commun.*, vol. 3, no. 1, pp. 86–96, Jan. 2004.

[17] P. Viswanath, D. N. C. Tse, and R. Laroia, "Opportunistic beamforming using dumb antennas," *IEEE Trans. Inform. Theory*, vol. 48, no. 6, pp. 1277 – 1294, Jun. 2002.

[18] Q. H. Spencer, A. L. Swindlehurst, and M. Haardt, "Zero-forcing methods for downlink spatial multiplexing in multiuser MIMO channels," *IEEE Trans. Sig. Proc.*, vol. 52, pp. 461-471, Feb. 2004.

[19] T. Yoo and A. Goldsmith, "On the optimality of multiantenna broadcast scheduling using zero-forcing beamforming," *IEEE Journal on Selected Areas in Commun.*, vol. 24, no. 3, pp. 528–541, Mar. 2006.

[20] T. Yoo and A. Goldsmith, "Sum-rate optimal multi-antenna downlink beamforming strategy based on clique search," *Proc. IEEE Global Telecomm. Conf.* (Globecom' 2005), St. Louis, Missouri, vol. 3, pp. 1510–1514, Dec. 2005.

[21] J. Kim, S. Park, J. H. Lee, J. Lee and H. Jung, "A scheduling algorithm combined with zero-forcing beamforming for a multiuser MIMO wireless system," *Proc. IEEE Semiannual Veh. Tech. Conf.* (VTC' 2005), Dallas, Texas, vol. 1, pp. 211–215, Sep. 2005

[22] A. M. Toukebri, S. Aissa, M. Maier, "Resource allocation and scheduling for multiuser MIMO systems: a beamforming-based strategy," *Proc. IEEE Global Telecomm. Conf.* (Globecom' 2006), San Francisco, California, Nov. 2006.

[23] G. Dimic and N. D. Sidiropoulos, "On downlink beamforming with greedy user selection: performance analysis and a simple new algorithm," *IEEE Trans. Sig. Pro.*, vol. 53, no. 10, pp. 3857–3868, Oct. 2005.

[24] M. Trivellato, F. Boccardi and F. Tosato, "User selection schemes for MIMO broadcast channels with limited feedback," in *Proc. IEEE Semiannual Veh. Tech. Conf.* (VTC' 2007), Dublin, Ireland, Apr. 2007.

[25] H. A. David, *Order Statistics*, John Wieley and Sons, Inc, New York, second edition, 1980.

[26] A. Bletsas, A. Khisti, D. P. Reed, and A. Lippman, "A simple cooperative diversity method based on network path selection," *IEEE Journal on Selected Areas in Commun.*, vol. 52, no. 3, pp. 659–672, Mar. 2006.

[27] N. Jindal, "MIMO broadcast channels with finite feedback," in *Proc. of IEEE Global Telecomm.* Conf. (Globecom'2005), St. Louis, MO, November 2005.

[28] B. Hassibi and T. L. Marzetta, "Multiple-antennas and isotropically random unitary inputs: the received signal density in closed form", *IEEE Trans. Inform. Theory*, vol. 48, no. 6, pp. 1473–1484, June 2002.

[29] K. K. J. Chung, C.-S. Hwang and Y. K. Kim, "A random beamforming technique in mimo systems exploiting multiuser diversity," *IEEE J. Select. Areas Commun.*, vol. 21, no. 5, pp. 848–855, June 2003.

[30] H. Wang, A. B. Gershman, and T. Kirubarajan, "Random unitary beamforming with partial feedback for multi-antenna downlink transmission using multiuser diversity," in *Proc. of IEEE Veh. Technol. Conf.* (VTC'Spring 2005), Stockholm, Sweden, June 2005.

[31] K. Zhang, and Z. Niu, "Random beamforming with multibeam selection for MIMO broadcast channels," in *Proc. of IEEE Intl. Conf. Commun.* (ICC'2006), Istanbul, Turkey, pp. 4191 – 4195, June 2006.

[32] Y.-C. Ko, H.-C. Yang, S.-S. Eom and M.-S. Alouini, "Adaptive modulation with diversity combining based on output-threshold MRC," *IEEE Trans. Wireless Commun.*, Vol. 6, no. 10, pp. 3728 – 3737, October 2007.

[33] H.-C. Yang, P. Lu, H.-K. Sung and Y.-C. Ko, "Exact sum-rate analysis of MIMO broadcast channels with random unitary beamforming based on quantized SINR feedback," submitted to *IEEE Int. Conf. Commun.* (ICC'2008), Beijing, China, May 2008.

[34] J. Diaz, O. Simeone, O. Somekh, and Y. bar-Ness, "Scaling law of the sum-rate for multiantenna broadcast channels with deterministic or selective binary feedback," in *Proc. of Inform. Theory Workshop* (ITW'2006), Punta del Este, Uruguay, March 2006, pp. 298 – 301.

[35] P. Lu, H.-C. Yang and Y.-C. Ko, "Sum-rate analysis of MIMO broadcast channel with random unitary beamforming", *Proc. of IEEE Wireless Commun. and Networking Conf. (WCNC'2008)*, Las Vegas, Nevada, March, 2008.

[36] J. Diaz, O. Simeone, O. Somekh, and Y. Bar-Ness, "Scaling law of the sum-rate for multi-antenna broadcast channels with deterministic or selective binary feedback," in *IEEE Infor. Theory Workshop* (ITW'06), Punta del Este, Uruguay, pp. 298–301, March, 2006.

[37] J. Diaz, O. Simeone, and Y. bar-Ness, "Sum-rate of MIMO broadcast channels with one bit feedback," in *Proc. of Int. Symp. Inform. Theory* (ISIT'2006), Seattle, Washington, July 2006, pp. 1944 – 1948.

[38] Y.-C. Ko, H.-C. Yang, S.-S. Eom and M.-S. Alouini, " Adaptive modulation with diversity combining based on output-threshold MRC," *IEEE Trans. Wireless Commun.*, Vol. TWC-6, no. 10, pp. 3728–3737, October 2007.

[39] P. Lu, H. C. Yang, and Y. C. Ko, "Sum-rate analysis of MIMO broadcast channel with random unitary beamforming," *Proc. of IEEE Wireless Commun. and Networking Conf.* (WCNC'2008), Las Vegas, Nevada, Mar. 2008.

[40] J. H. Winters, "Optimum combining in digital mobile radio with cochannel interference," *IEEE Trans. Veh. Tech.*, vol.33, no.3, pp. 144–155, Aug. 1984.

[41] M. K. Simon and M. S. Alouini, *Digital communication over fading channels*, second edition, New Jersey, John Wieley & Sons, Inc, 2004.

[42] A. Shah and A. M. Haimovich, "Performance analysis of optimum combining in wireless communications with Rayleigh fading and cochannel interference," *IEEE Trans. Commun.*, vol. 46, no. 4, pp. 47–C479, Apr. 1998.

[43] M. Chiani, M. Z. Win, A. Zanella, R. K. Mallik, and J. H. Winters, "Bounds and approximations for optimum combining of signals in the presence of multiple cochannel interferers and thermal noise," *IEEE Trans. Commun.*, vol.51, no.2, pp. 296–307, Feb. 2003.

[44] E. villier, "Performance analysis of optimum combining with multiple interferers in flat Rayleigh fading," *IEEE Trans. Commun.*, vol.47, no.10, pp. 1503–1510, Oct. 1999.

[45] P. Lu, H. C. Yang and Y. C. Ko, "Performance enhancement with optimum combining for random unitary beamforming based multiuser MIMO systems", *Submitted to IEEE International Symposium on Information Theory* (ISIT'08), Toronto, Canada, July, 2008.

[46] N. Jindal, "MIMO broadcast channels with finite feedback," in *IEEE Trans. Inform. Theory*, vol. IT-52, no. 11, pp. 5045–5059, November 2006, See also *Proc. of IEEE Global Telecomm. Conf. (Globecom'2005), St. Louis, MO*, November 2005.

[47] D. Gesbert and M.-S. Alouini, "How much feedback is multi-user diversity really worth?" in *Proc. of IEEE Int. Conf. on Commun. (ICC'2004), Paris, France*, June 2004, pp. 234 – 238.

[48] P. Lu, H. C. Yang, and Y. C. Ko, "Sum-rate analysis of MIMO broadcast channel with random unitary beamforming," *Proc. of IEEE Wireless Commun. and*

Networking Conf. (WCNC'2008), Las Vegas, Nevada, pp. 533–537, Mar. 2008. Full paper submitted to *IEEE Trans. Wireless Commun.*.

[49] J. H. Winters, "Optimum combining in digital mobile radio with cochannel interference," *IEEE Trans. Veh. Tech.*, vol.33, no.3, pp. 144–155, Aug. 1984.

[50] M. K. Simon and M. S. Alouini, *Digital communication over fading channels*, 2nd edition, New Jersey, John Wiley & Sons, Inc, 2004.

[51] A. Shah and A. M. Haimovich, "Performance analysis of optimum combining in wireless communications with Rayleigh fading and cochannel interference," *IEEE Trans. Commun.*, vol. 46, no. 4, pp. 473–479, Apr. 1998.

[52] M. Chiani, M. Z. Win, A. Zanella, R. K. Mallik, and J. H. Winters, "Bounds and approximations for optimum combining of signals in the presence of multiple cochannel interferers and thermal noise," *IEEE Trans. Commun.*, vol.51, no.2, pp. 296–307, Feb. 2003.

[53] H. A. David, *Order Statistics*, 2nd edition, New York, NY: John Wiley & Sons, Inc., 1981.

[54] H. S. Wilf, "Matrix inversion by the annihilation of rank," *J. Soc. Indust. Appl. Math.*, vol. 7, no. 2, pp. 149–151, Jun., 1959.

[55] M. O. Pun, V. Koivunen and H. V. Poor, "SINR analysis of opportunistic MIMO-SDMA downlink systems with linear combining," *Proc. of IEEE Int. Conf. Commun.* (ICC'2008), Beijing, China, May 2008.

[56] M. O. Pun, V. Koivunen and H. V. Poor, "Opportunistic scheduling and beamforming for MIMO-SDMA downlink systems with linear combining," *Proc. of Int. Symp. Personal, Indoor and Mobile Radio Commun.* (PIMRC' 2007), Athens, Greece, Sep., 2007.

[57] H. S. Gao, P. J. Smith and M. V. Clark, "Theoretical reliability of MMSE linear diversity combining in Rayleigh-fading additive interference channels," *IEEE Trans. Commun.*, vol. 46, no. 5, pp. 666–672, May 1998.

[58] S. Haykin, "Adaptive filter theory," *Information and System Sciences*, Englewood Cliffs, NJ: Prentice Hall, 1986.

[59] P. Lu, H. C. Yang, and Y. C. Ko, "Sum-rate analysis of MIMO broadcast channel with random unitary beamforming," *Proc. of IEEE Wireless Commun. and Networking Conf.* (WCNC'2008), Las Vegas, Nevada, pp. 533–537, Mar. 2008. Full paper submitted to *IEEE Trans. Wireless Commun.*.

[60] J. H. Winters, "Optimum combining in digital mobile radio with cochannel interference," *IEEE Trans. Veh. Tech.*, vol.33, no.3, pp. 144–155, Aug. 1984.

[61] M. K. Simon and M. S. Alouini, *Digital communication over fading channels*, 2nd edition, New Jersey, John Wiley & Sons, Inc, 2004.

[62] A. Shah and A. M. Haimovich, "Performance analysis of optimum combining in wireless communications with Rayleigh fading and cochannel interference," *IEEE Trans. Commun.*, vol. 46, no. 4, pp. 473–479, Apr. 1998.

[63] M. Chiani, M. Z. Win, A. Zanella, R. K. Mallik, and J. H. Winters, "Bounds and approximations for optimum combining of signals in the presence of multiple cochannel interferers and thermal noise," *IEEE Trans. Commun.*, vol.51, no.2, pp. 296–307, Feb. 2003.

[64] H. S. Wilf, "Matrix inversion by the annihilation of rank," *J. Soc. Indust. Appl. Math.*, vol. 7, no. 2, pp. 149–151, Jun., 1959.

[65] H. S. Gao, P. J. Smith and M. V. Clark, "Theoretical reliability of MMSE linear diversity combining in Rayleigh-fading additive interference channels," *IEEE Trans. Commun.*, vol. 46, no. 5, pp. 666–672, May 1998.

[66] S. Haykin, "Adaptive filter theory," *Information and System Sciences*, Englewood Cliffs, NJ: Prentice Hall, 1986.

[67] G. J. Foschini, "Layered space-time architecture for wireless communication in a fading environment when using multiple antennas," *Bell Laboratories Tech. J.*, pp. 41-59, Autumn 1996.

[68] C. B. Peel, B. M. Hochwald, and A. L. Swindlehurst, "A vector perturbation technique for near-capacity multiantenna multiuser communication-part I: channel inversion and regularization," *IEEE Trans. Commun.*, vol. 53, no. 1, pp. 195-202, Jan. 2005.

[69] C. Windpassinger, R. F. H. Fischer, T. Vencel, and J. B. Huber, "Precoding in miltiantenna and multiuser communications," *IEEE Trans. Wireless Commun.*, vol. 3, no. 4, pp. 1305-1316, Jul. 2004.

[70] M. Joham, K. Kusume, M. H. Gzara, and W. Utschick, "Transmit wiener filter for the downlink of TDD DS-CDMA systems," in *Proc. IEEE 7th Symp. Spread-spectrum Tech. Appl.*, Prague, Czech Republic, Sept. 2002, pp. 9-13.

[71] M. Joham, J. Brehmer, and W. Utschick, "MMSE approaches to multiuser spatio-temporal Tomlinson-Harashima precoding," in *Proc. ITG Conf. Source Channel Coding* (ITG SCC'04), Jan. 2004, pp. 387-394.

[72] B. M. Hochwald, C. B. Peel, and A. L. Swindlehurst, "A vector perturbation technique for near-capacity multiantenna multiuser communication - part II: perturbation," *IEEE Trans. Commun.*, vol. 53, pp. 537-544, Mar. 2005.

[73] C. Windpassinger, R. F. H. Fischer, and J. B. Huber, "Lattice-reduction-aided broadcast precoding," *IEEE Trans. Commun.*, vol. 52, pp. 2057- 2060, Dec. 2004.

[74] M. Taherzadeh, A. Mobasher, and A. K. Khandani, "Communications over MIMO broadcast channels using lattice-basis reduction," *IEEE Trans. Info. Theory*, vol. 53, No. 12, pp. 4567-4582, Dec. 2007.

[75] M. Tomlinson, "New automatic equaliser employing modulo arithmetic," *Electronics Letters*, vol.7, no. 5/6, pp. 138-139, Mar. 1971.

[76] H. Harashima and H. Miyakawa, "Matched-transmission technique for channels with intersymbol interference," *IEEE Trans. Commun.*, vol. 20, no. 4, pp. 774-780, Aug. 1972.

[77] D. Schmidt, M. Joham, and W. Utschick, "Minimum mean square error vector precoding," in *Proc. Personal, Indoor and Mobile Radio Communications*, Berlin, Germany, vol. l, pp .107-111, Sept. 2005.

[78] D. A. Schmidt, M. Joham, and W. Utschick, "Minimum mean square error vector precoding," *Eur. Trans. Telecommun.*, vol. 19, no. 3, pp. 219-231, Apr. 2008.

[79] Eun Yong Kim and Joohwan Chun, "Optimum vector perturbation minimizing total MSE in multiuser MIMO downlink," in *Proc. Int. Conf. Commun.* (ICC'06), pp. 4242-4247, 2006.

[80] N. Jindal, "MIMO broadcast channels with finite-rate feedback," *IEEE Trans. Inf. Theory*, vol. 52, no. 11, pp. 5045-5060, Nov. 2006.

[81] N. Jindal, "Antenna combining for the MIMO downlink channel," *IEEE Trans. Wireless Commun.*, vol. 7, no. 10, pp. 3834-3844, Oct. 2008.

[82] P. Lu and H. C. Yang, "Performance enhancement with optimum combining for random unitary beamforming based multiuser MIMO Systems," in *Proc. IEEE Global Commun.* (Globecom'08), New Orleans, Louisiana, Dec. 2008.

[83] K. J. Kim and C. Zhang, "Jointly optimized MIMO multiuser precoding system with channel mismatch," in *Proc. Fortieth Asilomar Conference on Signals, Systems and Computers*, pp. 384-387, Nov. 2006.

[84] F. A. Dietrich, P. Breun, and W. Utschick, "Robust Tomlinson-Harashima precoding for the wireless broadcast channel," *IEEE Trans. Sig. Pro.*, vol. 55, no. 2, pp. 631-644, Feb. 2007.

[85] U. Fincke and M. Pohst, "Improced methods for calculating vectors of short lengths in a lattice, including a complexity analysis," *Math. Computat.*, vol. 44, pp. 463-471, Apr. 1985.

[86] M. O. Damen, A. Chkeif, and J. C. Belfiore, "Lattice code decoder for space-time codes," *IEEE Commun. Lett*, vol. 4, pp. 161-163, May 2000.

[87] A. L. Lenstra, H. W. Lenstra, and L. Lovasz, "Factoring polynomials with rational coefficients," *Math. Ann.*, vol. 261, pp. 515- 534, 1982.

[88] L. Babai, "On Lovasz's lattice reduction and the nearest lattice point problem," *Combinatorica*, vol. 6, pp. 1-13, Jan. 1986.

[89] H. Yao and G. W. Wornell, "Lattice-reduction-aided detectors for MIMO communication systems," in *Proc. IEEE Globecom* (Golobecom'02), Taiper, Taiwan, pp. 424-428, Nov. 2002.

[90] T. M. Cover, "Elements of information theory," John Wiley and Sons, 2006.

[91] P. Ding, D. J. Love, and M. D. Zoltowski, "Multiple antenna broadcast channels with shape feedback and limited feedback," *IEEE Trans. Sig. Pro.*, vol. 55, no. 7, pp. 3417-3428, Jul. 2007.

[92] R. W. Heath Jr, T. Wu, and A. C. K. Soong, "Progressive refinement of beamforming vectors for high-resolution limited feedback," *EURASIP Journal on Advances in Signal Processing*, no. 6, pp. 743-747, Feb. 2009.